



**RÉPONSES FONCTIONNELLES ET STRUCTURELLES  
DES ASSOCIATIONS PHYTOPLANCTONIQUES FACE A  
UNE PERTURBATION ANTHROPIQUE : UN SCÉNARIO  
DE DÉVERSEMENT D'HYDROCARBURES**

Mémoire présenté  
dans le cadre du programme de maîtrise en  
océanographie en vue de l'obtention du grade de  
maître ès sciences

PAR  
© ANDREANA MACKENNA CADAILLON

**septembre 2018**



**Composition du jury :**

**Michel Gosselin, président du jury, Institut des sciences de la mer de Rimouski/Université du Québec à Rimouski**

**Gustavo Ferreyra, directeur de recherche, Institut des sciences de la mer de Rimouski/Université du Québec à Rimouski. Présentement au Centre Austral des Recherches Scientifiques (CADIC) (Argentina)**

**Michel Starr, codirecteur de recherche, Institut Maurice-Lamontagne**

**Irene Schloss, codirectrice de recherche, Centre Austral des Recherches Scientifiques (CADIC) et Institut Antarctique Argentine (Argentina)**

**Behzad MOSTAJIR, examinateur externe, Université de Montpellier, Ifremer, MARBEC (France)**

Dépôt initial le 11 avril 2018

Dépôt final le 10 septembre 2018



UNIVERSITÉ DU QUÉBEC À RIMOUSKI  
Service de la bibliothèque

Avertissement

La diffusion de ce mémoire ou de cette thèse se fait dans le respect des droits de son auteur, qui a signé le formulaire « *Autorisation de reproduire et de diffuser un rapport, un mémoire ou une thèse* ». En signant ce formulaire, l'auteur concède à l'Université du Québec à Rimouski une licence non exclusive d'utilisation et de publication de la totalité ou d'une partie importante de son travail de recherche pour des fins pédagogiques et non commerciales. Plus précisément, l'auteur autorise l'Université du Québec à Rimouski à reproduire, diffuser, prêter, distribuer ou vendre des copies de son travail de recherche à des fins non commerciales sur quelque support que ce soit, y compris l'Internet. Cette licence et cette autorisation n'entraînent pas une renonciation de la part de l'auteur à ses droits moraux ni à ses droits de propriété intellectuelle. Sauf entente contraire, l'auteur conserve la liberté de diffuser et de commercialiser ou non ce travail dont il possède un exemplaire.



À mon grand-père Toto qui m'a toujours encouragé. Je sais que tu serais très fier de moi, et tu me le dirais en buvant un mate... une larme s'échappe. Je t'aime. Tu es dans mon cœur pour toujours.



## **REMERCIEMENTS**

Je remercie les institutions qui ont rendu ce projet possible et qui m'ont soutenu financièrement : Bec.Ar, MinCyT, CONICET, UQAR et ISMER au Canada, ainsi que le Service aux étudiants de l'UQAR et Québec-Océan. Je remercie aussi mes collègues et les institutions qui ont financé ce projet de maîtrise à savoir, l'ISMER, le MPO et de deux institutions de recherche mexicaines : le Colegio de la Frontera Sur - Unidad Campeche et le Centro de Investigación y de Estudios Avanzados et l'Unidad Merida.

Je remercie énormément les personnes qui m'ont soutenue et accompagnée tout au long de mes études de maîtrise. Merci tout d'abord à tous ceux et celles avec qui j'ai eu le plaisir de travailler et qui m'ont accompagnée avec gentillesse, loyauté, confiance, sincérité et générosité.

Je tiens à remercier mon directeur, Gustavo Ferreyra, et mes codirecteurs, Michel Starr et Irene Schloss. Vos grandes qualités humaines, comme votre compréhension, votre humour exceptionnel, votre détermination, vos précieux conseils et votre foi en moi, m'ont apporté un soutien extraordinaire à chaque étape de ce cheminement. Merci, Gus, pour ta patience, pour m'apprendre à réfléchir, à travailler en équipe, pour partager avec moi tes connaissances et me motiver constamment. Merci Ire pour avoir toujours été là, pour ton temps, ton soutien moral et tout ce que tu m'a appris dans chaque moment. Merci, Michel, pour tous tes apports et ta gentillesse. Je remercie le professeur Richard St- Louis pour ses précieux commentaires et apports dans l'écriture de ce mémoire. Merci à l'équipe technique de l'ISMER, Pascal Rioux, Dominique Lavallé et Mélanie Simard avec qui j'ai passé beaucoup de temps durant mes différentes analyses et pour leur aide lors de ces diverses techniques.

Je tiens également à remercier Francesca Vidussi et Behzad Mostajir de m'avoir accueilli dans le centre de recherche MARBEC à l'Université de Montpellier (France). Merci, Francesca, pour tout ce que tu m'a appris concernant les pigments, cela a été une expérience exceptionnelle pour ma formation professionnelle et académique. Je tiens également à remercier Michel Gosselin d'avoir accepté d'être président du jury. Je remercie également tous les membres du jury d'avoir accepté de lire ce travail.

Un grand merci à Martine Belzile pour ta patience, ta gentillesse et ton amour depuis le début. Ensuite, je souhaite remercier toute la communauté de l'ISMER. Merci aux autorités et à tout le personnel de soutien : Ariane Plourde, Karine Lemarchand, Brigitte Dubé, Marielle Lepage et Nancy Lavergne. Merci à tous les professeurs des cours que j'ai suivis. Parmi eux, j'aimerais spécialement remercier Alain Caron pour ses conseils-statistiques et sa disponibilité. Merci aux copains NEMO ! Merci aux collègues des laboratoires du phytoplancton, pour les blagues, les heures, les aides et les musiques partagées.

Un merci plus que spécial à mes parents “mamá y papá” —y me atrevo a escribir en español porque es para ustedes, por vuestro amor incodicional, por sostenerme siempre, por cada palabra de aliento, por tener fe en mí y darmel alas para volar y acompañarme en ese camino. Si llego hoy a la meta es porque siempre han estado allí a pesar de la distancia, Amarlos es poco—. Merci à toute ma famille mes sœurs, mes grand mères, mes tantes, mes cousins. Merci infiniment à ma petite cousine Émilie, le bonheur que tu donnes, tu ne le comprends pas encore, mais tu as été un important soutien pendant mes derniers mois de rédaction en Argentine.

Merci à mes belles amies argentines pour partager avec moi cette aventure de réaliser une maîtrise à Rimouski: Magalí, Mariana, Belen. Las quiero tanto mis paisas!! Merci, Gonzalo pour ton bonheur, tes blagues et ton aide précieuse avec les problèmes techniques du dernier moment. Merci à la gang argentine de Rimouski spécialement à Jesi et sa famille. Merci aux filles argentines Eloisa, Maité, Ximena, Julieta, pour tout votre aide depuis le début et pour votre amitié. Je vous adore! Merci aussi aux formidables amis de

maîtrise et de l'ISMER, avec qui j'ai partagé plein de beaux moments : Claudie, Fred, Pascal, Maude, Antoine, Grégoire, Jean, Elsa, Valentin, Efflam, Helene, Camille, Francis, Éric, Clémence. Ma belle amie Inès, merci de me remonter le moral aux moments clés, de m'encourager à continuer malgré tout. Merci pour toutes les danses et chansons latines partagées dans les soirées et les couloirs de l'ISMER.

Merci à mes professeures de français Nathalie et Odile. Un gros merci aux colocs (Léo, Francis, Camille, Peter, Antoine, Laoul, Kloé) pour cette expérience de vie commune très agréable, pleine de bonheur, de sourires, de blagues, d'accompagnement, des soirées. Je vous adore ! Merci à ma famille d'accueil, Martin et Julia. Merci à Valérie et ses enfants qui j'adore.

Finalement, un gros merci Léo « bonito » pour ton soutien émotionnel, ton bonheur, ton amour et ta patience. Je t'aime. Merci, Adri, ma sœur du cœur, mi amiga latina. Gracias por tanto! te quiero mucho.



## RÉSUMÉ

Le phytoplancton joue un rôle clé dans l'écologie des écosystèmes marins étant à la base des réseaux trophiques avec un rôle majeur dans la modulation des flux entre l'atmosphère et l'océan. Cependant, cette dynamique peut être affectée négativement par des événements de contamination anthropique dans le milieu marin. Afin de valider cette hypothèse générale, l'objectif principal de cette recherche était d'étudier les réponses naturelles du phytoplancton exposées à un scénario de faible pollution par hydrocarbures raffinés, en utilisant une approche expérimentale en mésocosmes. Deux types d'expositions ont été simulées, l'une « aiguë » et l'autre « chronique ». Les objectifs spécifiques étaient d'évaluer l'effet des ajouts du diesel sur des attributs structurels (1) et fonctionnels clés (2) du phytoplancton. Les hypothèses testées étaient : après les ajouts du diesel, il y aura une diminution de la biomasse et la densité totales des associations phytoplanctoniques avec une réponse différentielle des divers groupes taxonomiques ainsi qu'une diminution de l'efficacité photosynthétique du phytoplancton. La plupart des effets étaient détectés lors de la période de postfloraison de la succession phytoplanctonique. Les concentrations de Chlorophylle *a* étaient réduites ainsi que les densités et biomasses de carbone totales des principaux composants des groupes fonctionnels identifiés (c-à-d pico-, nano et microeucaryotes). Cela implique un impact potentiel important en matière du flux de carbone contrôlé par le phytoplancton dans la pompe biologique. Les associations dominées par des diatomées en début de l'expérience étaient progressivement remplacées par des pico et nanoflagellées et des nanocyanobactéries, étant plus marqué dans les traitements contaminés le deuxième jour expérimental. Ainsi, en présence du diesel un réseau trophique herbivore pourrait évoluer vers un réseau trophique microbien plus rapide et intensément, avec un recyclage relativement plus rapide du carbone, une sédimentation plus lente de la matière organique et, par conséquent, une diminution de l'efficacité de la pompe biologique, ce qui contribuera à l'augmentation du dégazage de CO<sub>2</sub> vers l'atmosphère. Concernant le deuxième objectif, l'efficacité photosynthétique a diminué lors de l'addition de diesel. Ces résultats suggèrent que l'écosystème estuaire du Saint Laurent demeure un environnement qui pourrait être fragilisé par l'augmentation du transport global de produits pétroliers.

Mots clés : diesel, phytoplancton, biomasse de carbone, pigments, efficacité photosynthétique, groupes fonctionnels, *Skeletonema costatum*.



## **ABSTRACT**

Phytoplankton plays a key role in the ecology of marine ecosystems being at the base of food webs with a major role in the modulation of the fluxes between the atmosphere and the ocean. This dynamic can be negatively affected by anthropogenic contamination events in the marine environment. In order to validate this general hypothesis, the main objective of this research was to study the responses of natural phytoplankton assemblages exposed to a low oil pollution scenario, using an experimental mesocosms approach. Two kinds of exposures were simulated, one “chronic” and the other one “acute”. The specific objectives were to evaluate the effects of diesel additions on the structural (1) and functional attributes of phytoplankton assemblages (2). The hypothesis tested were: after diesel inputs total biomass and cell density of phytoplankton assemblages will decline with a different response among phytoplankton taxonomic groups and a diminution of the photosynthetic capacity of phytoplankton. Most of the effects were detected in the post bloom of the phytoplankton succession. Chl *a* concentration declined as well as densities and carbon biomasses of the main components of all functional groups identified (pico-, nano and, microeukaryotes). This implies an important potential impact in terms of carbon flux regulated by phytoplankton in the biological pump. Diatom-dominated phytoplankton assemblages at the beginning of the experiment were gradually replaced by pico-nano-flagellates and nano-cyanobacteria, being more marked in the contaminated treatments after the 12<sup>th</sup> experiment day. Therefore, in the presence of diesel an herbivorous food web could evolve to a microbial food web faster and intensely, with a relatively faster carbon cycling, slower organic matter export and a decrease in the efficiency of the biological pump, which could limit the capacity of the ocean as an atmospheric CO<sub>2</sub> sink. Regarding the second objective, our results showed that photosynthesis efficiency declined after the oil addition. Data obtained through this study suggest that Saint Lawrence estuarine ecosystem remains a fragile environment which would be strongly impacted by the increase in global transportation of oil products.

*Keywords:* diesel, phytoplankton, carbon biomass, pigments, photosynthesis efficiency, functional groups, *Skeletonema costatum*.



## TABLE DES MATIÈRES

REMERCIEMENTS .....	ix
RÉSUMÉ .....	xiii
ABSTRACT.....	xv
TABLE DES MATIÈRES .....	xvii
LISTE DES TABLEAUX .....	xix
LISTE DES FIGURES .....	xxi
LISTE DES ABRÉVIATIONS, DES SIGLES ET DES ACRONYMES .....	xxiv
INTRODUCTION GÉNÉRALE .....	1
CHAPITRE 1 FUNCTIONAL AND STRUCTURAL RESPONSES OF NATURAL PHYTOPLANKTON ASSEMBLAGES TO ANTHROPOIC PERTURBATIONS: THE CASE OF A LOW CONCENTRATION OIL SPILL SCENARIO.....	9
1.1    INTRODUCTION.....	10
1.2    MATERIALS AND METHODS.....	13
1.2.1 Set-up.....	13
1.2.2 Inorganic nutrients .....	15
1.2.3 Chlorophyll <i>a</i> .....	15
1.2.4 Pigments analysis.....	16
1.2.5 Flow cytometry (FCM) analysis .....	19
1.2.6 Light microscopy (LM) analysis .....	20
1.2.7 Image analysis (FlowCAM) .....	20
1.2.8 Fluorescence induction analysis .....	21
1.2.9 Statistical analysis.....	22

1.3      RESULTS .....	22
1.3.1 Inorganic nutrients .....	22
1.3.2 Chlorophyll <i>a</i> concentration evolution.....	25
1.3.3 Nano- and pico-phytoplankton densities and carbon estimations (FCM).....	26
1.3.4 Microphytoplankton densities and carbon estimations (FlowCAM) .....	32
1.3.5 Pigments analyses (HPLC) .....	33
1.3.6 Light microscopy (LM).....	39
1.3.7 Flow cytometry (FCM) versus - HPLC results .....	43
1.3.8 Physiological status of phytoplankton - Fluorescence Induction.....	45
1.4      DISCUSSION.....	46
1.4.1 Chlorophyll <i>a</i> and nutrients' concentrations .....	46
1.4.2 Pico-, nano- and microphytoplankton density and phytoplankton carbon estimations.....	48
1.4.3 Pigments (HPLC) - Light microscopy (LM).....	51
1.4.4 Physiological status of phytoplankton - fluorescence induction.....	57
1.4.5 Time of exposure - Ecological succession .....	58
1.4.6 Synergy effects - Trophic interactions .....	59
1.5      CONCLUSIONS .....	61
CONCLUSION GÉNÉRALE .....	62
RÉFÉRENCES BIBLIOGRAPHIQUES .....	73
ANNEXES .....	86

## **LISTE DES TABLEAUX**

**Table 1:** Pigments identified in the present study and their taxonomic group and/or significance.....16



## LISTE DES FIGURES

Figure 1: Simple Linear Regression between Chl <i>a</i> obtained by flourometry and HPLC methods.....	18
Figure 2: Temporal patterns for mean ( $\pm$ SD) nutrient concentrations: a-b) Nitrate + Nitrite, c-d) Silicate, e-f) Phosphate.....	24
Figure 3: Temporal patterns for mean ( $\pm$ SD) total Chl <i>a</i> concentration measured by fluorimeter for the (a) chronic and (b) acute treatments.....	25
Figure 4: Temporal patterns for mean ( $\pm$ SD) phytoplankton densities measured by Flow Cytometry: a-b) Total phytoplankton ( $<20 \mu\text{m}$ ), c-d) Nano-eukaryotes, e-f) Pico-eukaryotes.....	27
Figure 5: Temporal patterns for average ( $\pm$ SD) cyanobacteria densities measured by Flow Cytometry: a-b) Nano-PE, c-d) Pico-PE, e-f) Nano-PC, g-h) Pico-PC.....	29
Figure 6: Temporal patterns for mean ( $\pm$ SD) phytoplankton carbon biomass estimated from volume (ESD). a-b) Total phytoplankton $<20 \mu\text{m}$ , c-d) Nano-eukaryotes, e-f) Pico-eukaryotes.....	30
Figure 7: Net carbon accumulation for nano- (a) and pico-eukaryotes (b) estimated from day 10 on for all treatments.....	31
Figure 8: Temporal patterns for mean ( $\pm$ SD) microphytoplankton densities (a-b) and carbon biomass (c-d) estimated from the biovolume.....	32
Figure 9: Net carbon accumulation for microphytoplankton estimated day 6 on for all treatments.....	33
Figure 10: Temporal patterns for average ( $\pm$ SD) Chl <i>a</i> (a-b) and accessory pigment concentrations ( $\mu\text{g L}^{-1}$ ) with a similar trends than Chl <i>a</i> : c-d) fucoxanthin, e-f) Chl <i>b</i> , g-h) Chl <i>c1</i> , i-j) Chl <i>c2</i> , k-l) neoxanthin, m-n) violaxanthin, o-p) MgDVP .....	37
Figure 11: Temporal patterns for average ( $\pm$ SD) accessory pigment concentrations ( $\mu\text{g L}^{-1}$ ) with a different trends than those of Chl <i>a</i> : a-b) alloxanthin, c-d) prasinoxanthin, e-f) zeaxanthin.....	38

Figure 12: Total densities of phytoplankton determined by microscopic analyses during the experiments.....	39
Figure 13: Percentage of the main phytoplankton groups in the control and contaminated treatments.....	40
Figure 14: Percentage of different species for Bacillariophyta in control and contaminated treatments .....	41
Figure 15: FlowCAM images showing <i>S. costatum</i> cells mostly forming chains in the control (upper) and aggregated in the chronic treatment (middle) on day 12. Detail of aggregations (lower) .....	42
Figure 16: Simple linear regression between total phytoplankton <20 µm density (cells mL <sup>-1</sup> ) and Chl <i>a</i> concentration obtained by HPLC (left) and between Picoeukaryotes density (cells mL <sup>-1</sup> ) and Chl <i>b</i> concentration (right).....	44
Figure 17: Simple linear regression between nanoeukaryotes density (cells mL <sup>-1</sup> ) and fucoxanthin concentration (µg L <sup>-1</sup> ).....	44
Figure 18: Temporal changes (mean ±SD) in photochemical quantum yield of PSII ( $F_v/F_m = (F_m - F_0)/F_m$ ) as measured by FRRF during the experiment.....	45
Figure 19: Résultats principaux de cette étude concernant la composition, la biomasse et les flux de carbone (C) dans deux scénarios différents: non contaminé (supérieure) et contaminé par HCs (inférieure). Cyano: cyanobactéries, Nano-flag : nanoflagellées, Pico-flag : picoflagellées. Micro: microphytoplancton, Nano: nanophytoplancton, Pico: picophytoplancton, RTH and RTM (Legendre & Rassoulzadegan 1996, Azam et al. 1983, Laws et al. 2000) .....	67



## LISTE DES ABRÉVIATIONS, DES SIGLES ET DES ACRONYMES

### Anglais

<b>B-Fucox</b>	19'-butanoyloxyfucoxanthin
<b>Chl</b>	Chlorophyll
<b>df</b>	Degree of liberty
<b>ESD</b>	Estimated Spherical Diameter
<b>FCM</b>	Flow cytometry
<b>F</b>	Fisher
<b>FRRF</b>	Fast repetition rate fluorometry
<b>F<sub>m</sub></b>	Maximal fluorescence
<b>F<sub>v</sub></b>	Variable fluorescence
<b>F<sub>0</sub></b>	Initial fluorescence
<b>HCs</b>	Hydrocarbons
<b>HNA bacteria</b>	High-nucleic-acid bacteria
<b>HPLC</b>	High performance liquid chromatography
<b>LM</b>	Light microscopy
<b>LSLE</b>	Lower St. Lawrence Estuary
<b>MgDVP</b>	Mg-2,4-divinyl pheoporphyrin a5 monomethyl ester
<b>PAHs</b>	Polycyclic aromatic hydrocarbons
<b>PAR</b>	Photosynthetically active radiation
<b>RM-ANOVA</b>	Repeated Measures Analysis of Variance
<b>Sq</b>	Sum of squares

<b>UV</b>	Ultraviolet Light
<b>WAF</b>	Water accommodated fraction
<b>WSF</b>	Water soluble fraction

### **Français**

<b>BTEX</b>	Benzène, toluène, éthylbenzène et xylène
<b>CO<sub>2</sub></b>	Dioxyde de carbone
<b>EMSL</b>	Estuaire maritime du Saint-Laurent
<b>HAPs</b>	Hydrocarbures aromatiques polycycliques
<b>HCs</b>	Hydrocarbures
<b>UCMs</b>	Mélanges complexes non résolus par chromatogrammes



## **INTRODUCTION GÉNÉRALE**

Les environnements marins sont fréquemment exposés aux déversements d'hydrocarbures (HCs) résultants des opérations de transport, de forage ou par l'utilisation de carburant. Les grands déversements (7–700 et >700 tonnes) provenant des accidents catastrophiques, tels que la plus récente explosion Deepwater Horizon en 2010, le Exxon Valdez en 1989 ou le Prestige en 2002, ont été largement étudiés ainsi que ses effets aigus immédiats et à long terme sur les organismes marins, les zones côtières, les pêcheries, l'aquaculture, les ressources naturelles et le tourisme (Camilli et al. 2010, Bælum et al. 2012, Incardona et al. 2014, Yin et al. 2015). Cependant, les petits déversements ayant un volume inférieur à sept tonnes, représentent actuellement 80% du total des déversements enregistrés à l'échelle du globe (Lee et al. 2015, Brussaard et al. 2016). Les déversements d'hydrocarbures dans les eaux des zones maritimes font partie des conditions inhérentes à la navigation marchande. La Convention internationale pour la prévention de la pollution par les navires reconnaît l'existence des rejets routiniers liés à la marine marchande en imposant une limite de rejets d'eaux huileuses de 30 L/mille marin. Au-delà des rejets routiniers, la navigation marchande représente inévitablement un risque constant de déversements accidentels d'HCs (Institut Maritime du Québec, 2014). Puisque les déversements mineurs ne sont pas spectaculaires, ils sont moins sujets à l'attention de l'opinion publique. Ils peuvent ainsi entraîner une contamination chronique, pouvant représenter une menace potentielle pour les organismes marins qui sont exposés d'une façon répétées à des faibles concentrations d'HCs sur une longue période de temps.

Le diesel, un produit raffiné du pétrole brut, constitue l'un des HC le plus grandement utilisé à l'heure actuelle. La consommation globale du diesel a augmenté de 23% au cours de

la période 2000-2008, tandis que l'augmentation pour l'essence n'a été que de 7% pour la même période (IEA, 2008). Les demandes d'essence et de diesel prévues entre 2012 et 2035 sont supérieures à 2 et 5 millions de barils par jour, respectivement (IEA, 2013). Cette augmentation de la consommation globale de l'essence et du diesel a un impact environnemental direct, et notamment sur les écosystèmes aquatiques, lorsqu'il y a des fuites depuis les lieux de stockage.

Le Canada est l'un des principaux producteurs de pétrole au monde, avec des réserves estimées à 27,5 milliards de m<sup>3</sup> (la plupart provenant des gisements de sables bitumineux de l'Alberta) et un volume d'exportation par voie maritime très important (10 millions de m<sup>3</sup> en 2013; Dupuis et Ucan-Marin, 2015). De 2007 à 2009, plus de 500 déversements sont enregistrés à chaque année au Canada dont quelques 150 à 200 dans le système laurentien (Institut Maritime du Québec 2014). Plus de 80% de ces accidents impliquent des volumes inférieurs à 1 tonne (Villeneuve 2001) et seulement le 2% des déversements accidentels canadiens seraient liés à des pétroliers. Sur la portion québécoise du Saint-

Laurent, la quantité totale d'HCs en transit annuellement est estimée à environ 20 mégatonnes avec quelques 3890 mouvements de navire-citerne (Institut Maritime du Québec 2014). Il existe un vaste réseau de transport d'HCs associé à la distribution de produits provenant de l'Alberta vers les raffineries situées à l'Est et les différents points d'exportation internationaux. Plusieurs projets de transport vers l'Ouest par oléoducs/pipelines (projets *Northern Gateway* et *Trans Mountain*, vers le Pacifique) et vers l'Est (projet *Énergie Est*, vers l'Atlantique) ont été proposés. Ces projets, même s'ils n'ont pas la faveur de la population, s'ils sont réalisés, viendront augmenter sensiblement le transport des HC par voie maritime. D'ailleurs, la majorité du pétrole consommé actuellement au Québec provient principalement de l'importation d'outre-mer, comme l'Afrique ou l'Europe du Nord.

Les grands déversements en raison des accidents des navires ont été rares dans des eaux marines canadiennes. Le plus important est survenu le 4 février 1970 au large des côtes de la Nouvelle-Écosse où le pétrolier Arrow a déversé 200 000 m<sup>3</sup> de mazout de type Bunker C, avec la formation d'une émulsion pétrole-eau, laquelle a affecté 300 km de littoral et a entraîné

la mortalité aiguë de la faune exposée. Des études réalisées six ans après ce déversement ont révélé une vaste mortalité des mollusques et d'herbes de marais salé, ainsi que des algues *Fucus* sp. attachées sur des rivages rocheux. La diversité d'espèces a été réduite dans les sites contaminés (Lee et al. 2015). De plus, il a été observé une persistance à long terme de résidus de pétrole (résidus de goudron altérés par l'environnement), restant sur et dans des sédiments des plages 20 ans après l'accident (Vandermeulen et Singh 1994).

Dernièrement, les petits déversements de diesel et d'essence ayant un volume entre 10-100 m<sup>3</sup> ont été rapportés comme les plus courants avec une fréquence annuelle de 0,6 et 1,9 respectivement (Lee et al. 2015). Par exemple, plus de 107 000 litres de diesel et 2 240 litres de lubrifiants ont été déversés dans l'océan Pacifique suite au naufrage du bateau-remorqueur Nathan E. Steward près de Bella Bella (Colombie Britannique) le 13 octobre 2016. Dans les Îles de la Madeleine, en septembre 2014, un pipeline d'Hydro-Québec, servant à l'alimentation de la centrale électrique, a provoqué un déversement de 100 000 litres de diesel. Le pipeline en cause transporte chaque année 40 millions de litres de diesel vers la centrale, à partir du port de Cap-aux-Meules. Selon l'Institut Maritime du Québec (2014), le transport maritime de produits pétroliers va continuer à croître au cours des 20 prochaines années, impliquant alors des risques d'incidents/accidents maritimes provoquant des déversements accidentels. Dans de tels cas, les conséquences pourraient être substantielles sur les écosystèmes fluviaux, estuariens et marins du bassin du Saint-Laurent (Institut Maritime du Québec 2014).

Le pétrole brut est un mélange complexe d'hydrocarbures (incluant des alcanes, des cyclo alcanes et des hydrocarbures aromatiques) et non-hydrocarbures (incluant la résine et l'asphalte). Il existe différents types de pétrole brut et raffiné qui se distinguent par leur composition et leur solubilité, généralement inférieure à  $200 \times 10^{-6}$  mg L<sup>-1</sup> (Wang et Fingas 2006). Ces pétroles se différencient également par la composition de la fraction soluble du pétrole « Water Accommodated Fraction » (WAF). La WAF est principalement constituée par le BTEX (benzène, toluène, éthylbenzène et xylène), l'alkylation des homologues du benzène, des hydrocarbures aromatiques polycycliques (HAPs), des hydrocarbures pétroliers et

quelques mélanges complexes non résolus par les chromatogrammes (UCMs) (Faksness et al. 2008). Les principales substances toxiques sont les hydrocarbures aromatiques comme le BTEX et les HAPs (Jiang et al. 2010). Les hydrocarbures aromatiques solubles du diesel sont aussi les principaux responsables de la toxicité de ce pétrole raffiné.

Lors de son déversement dans l'eau le pétrole change progressivement son empreinte chimique par des processus physiques, chimiques et biologiques qui sont communément connus sous le terme anglais « weathering ». Ce phénomène comprend différents processus tels que le mélange, l'évaporation, la dissolution, la dispersion, l'émulsification, la photooxydation, la biodégradation et la sédimentation. Ces processus se produisent à des fréquences différentes et avec des temps de début différents, entraînant des changements progressifs dans la composition du pétrole et de son comportement après le déversement.

Quelques processus comme l'évaporation commencent immédiatement, étant significatifs dans le court terme (heures à jours). D'autres processus ont des effets à plus long terme et se produisent avec un décalage par rapport au déversement ou plus lentement (des mois ou même des années) : c'est le cas de la biodégradation. Pour cette raison certains facteurs environnementaux tels que la température, le phénomène des marées, la lumière, les sédiments en suspension dans la colonne d'eau et l'activité microbienne sont des facteurs clés concernant les taux de dégradation et d'altération du pétrole (Lee et al. 2015).

Lors d'un déversement de pétrole, la fraction soluble est rapidement libérée dans la colonne d'eau (González et al. 2006, 2009). Cette fraction, qui contient une grande proportion d'HAPs, devient la source primaire de toxicité persistante (Neff et al. 2000, Boehm et Page 2007), particulièrement pour les organismes planctoniques qui peuvent l'accumuler en raison de leurs grandes propriétés lipophiles (Jiang et al. 2010).

Étant donné que le phytoplancton fait partie des niveaux inférieurs des réseaux trophiques marins, l'étude des impacts des HCs sur le phytoplancton marin s'avère essentiel. Typiquement, la composante planctonique des réseaux trophique marin peut comprendre divers groupes d'organismes de différentes tailles, allant des virus (0.02 – 0.2 µm,

femtoplankton), jusqu'aux larves des poissons. Ces différentes catégories de taille représentent aussi différents groupes fonctionnels, incluant des organismes autotrophes et hétérotrophes. La structure et le fonctionnement de ces réseaux trophiques dépendent essentiellement de l'énergie et de la matière produite par la photosynthèse du phytoplancton. En plus, le phytoplancton joue un rôle essentiel dans le cycle de carbone marin et le climat global, en faisant partie de la pompe biologique, l'ensemble des processus par lesquels le CO<sub>2</sub> atmosphérique est séquestré dans les sédiments marins (Volk et Hoffert 1985, Turner 2002). Cela commence avec l'incorporation d'une partie du CO<sub>2</sub> dissous dans la colonne d'eau par le phytoplancton lors de la photosynthèse et la formation de matière organique dans la zone euphotique.

L'export du carbone en profondeur est contrôlé par des organismes d'ordre supérieur via le broutage et le relâchement de pelotes fécales (Richardson et Jackson 2007), par la sédimentation de la matière organique particulaire (cellules vivantes et mortes du phytoplancton, pelotes fécales, etc.), et par le mélange de la fraction organique dissoute. Les caractéristiques éco-physiologiques de différentes espèces composant le phytoplancton, déterminent la qualité et la quantité de carbone que sera transférée dans le réseau trophique et exportée vers l'océan profond (Finkel et al. 2010).

Au cours des dernières décennies, il y a eu des études examinant les effets du pétrole brut (Kusk 1978, Østgaard et al. 1984), du diesel (Chan et Chiu 1985) et de certaines HAPs sur des cultures mono-spécifiques (Dunstan et al. 1975, Pérez et al. 2010 b) et sur des assemblages phytoplanctoniques naturels (Thomas et al. 1981, Kelly et al. 1999, Marwood et al. 1999, Hjorth et al. 2007). Les effets de la WAF sur des assemblages naturels de phytoplancton ont été également évalués (Kelly et al. 1999, Sargian et al. 2005, González et al. 2009, Pérez et al. 2010a). Cependant, la plupart de ces études ont été conduites avec de petits volumes d'eau (microcosmes) et en conditions de laboratoire. Certaines investigations *in situ* ont suivi les réponses des organismes phytoplanctoniques dans des régions naturelles qui ont été affectées par des déversements accidentels de pétrole (Linden et al. 1979, Ramachandran et al. 2004, Salas et al. 2006, Varela et al. 2006, Díez et al. 2009).

Différentes études ont révélé une réponse de type espèce-spécifique qui varie selon la composition et la concentration d'HCs. Des effets négatifs (Ostgaard et al. 1984, Sargian et al. 2005) et positifs (Oviatt et al. 1982, Vargo et al. 1982) sur la biomasse phytoplanctonique et la photosynthèse ont été rapportés. Également, des modifications cellulaires au niveau génétique (Bopp et Lettieri 2007) et protéique (Wolfe et al. 1999) ont été démontrés, de même que des effets négatifs sur la division cellulaire, le taux de croissance, l'activité photosynthétique (effets principalement associés à l'interférence de la chaîne de transport électronique à niveau des photosystèmes I et II), les membranes cellulaires, les équilibres ioniques, la pression intracellulaire et les concentrations de chlorophylle et de phycoérythrine (Jiang et al. 2010, Perhar et Arhonditsis 2014, Ozhan et al. 2014).

Des différents niveaux de sensibilité aux HAPs entre espèces et groupes taxonomiques ont été aussi proposés, mais les résultats sont variables, parfois contradictoires, selon l'approche méthodologique utilisée (Jiang et al. 2010, Perhar et Arhonditsis 2014). Des études *in situ* après le déversement du navire Tasman Spirit au Pakistan ont montré une diminution de la diversité autour de la zone de pollution. Les diatomées ont été les organismes les plus affectées avec une réduction de 50% de leur richesse spécifique (Gao et al. 2007). Plusieurs études ont suggéré que les espèces de plus petite taille auraient une sensibilité accrue aux HAPs relativement à celles de grande taille (Fan et Reinfelder 2003, González et al. 2009, Echeveste et al. 2010a).

L'exposition au pétrole peut aussi induire des changements dans la structure et la fonction des associations phytoplanctoniques (Shaw 1992), entraînant des effets directs et indirects sur la communauté planctonique entière. Ils ont été décrits aussi des changements significatifs lors de la succession temporelle des espèces en raison de l'exposition aux HCs : les espèces les moins tolérantes diminueront progressivement, voire disparaîtront, tandis que les espèces les plus tolérantes deviendront progressivement dominantes (Jiang et al. 2010). Les brouteurs peuvent être affectés, ce qui atténuerait la pression de prédation sur certaines espèces de phytoplancton plutôt que d'autres (González et al. 2009). En raison de l'importance de la dégradation microbienne du pétrole brut, la relation étroite entre phototrophes et hétérotrophes

peut également jouer un rôle prépondérant au sein de l'environnement marin lors des déversements de pétrole (Ozhan et al. 2014).

À notre connaissance, les études évaluant les réponses structurelles et fonctionnelles des associations phytoplanctoniques sous le stress dû à la pollution par les HCs, en tenant en compte les interrelations avec la communauté planctonique en entier (c'est-à-dire le bactérioplancton et le microzooplancton) ne sont pas nombreuses. D'autre part, les études en utilisant des microcosmes semblent être limitées pour comprendre les effets potentiels de l'exposition au pétrole dans les écosystèmes, car les interactions entre les facteurs biotiques et abiotiques dans l'environnement naturel sont très complexes et, par conséquent, difficiles de reproduire dans des petits volumes. D'ailleurs, les études *in situ* ne permettent pas d'étudier les effets à court terme à cause des délais entre les déversements accidentels et les échantillonnages. De plus, ils représentent des défis logistiques considérables ainsi que des frais/coûts élevés et plus particulièrement pour répondre au besoin des travaux à long-terme. Les expériences en mésocosmes représentent donc une approche utile pour surmonter ces obstacles (Jung et al. 2012), car elles permettent d'utiliser un grand volume d'eau de mer contenant l'ensemble de la communauté planctonique tout en permettant de simuler les conditions physiques de l'environnement naturel (Kemp et al. 2001, Petersen et al. 2003, González et al. 2013).

Le présent projet vise à étudier les réponses structurelles et fonctionnelles des associations phytoplanctoniques face à une perturbation anthropique telle que la contamination par les HCs en utilisant l'approche expérimentale des mésocosmes et le diesel maritime comme source de contamination.

## OBJECTIFS ET HYPOTHESES

**Objectif général :** Pour chacun des scénarios de faible contamination (chronique et aiguë), étudier les effets des HCs sur la structure et la fonction des associations de phytoplancton de l'estuaire maritime du Saint-Laurent (EMSL).

**Objectif spécifique #1 : *Déterminer comment les ajouts d'HCs affectent les attributs structurels (biomasse, densité, composition) des associations phytoplanctoniques.***

**Hypothèse #1a :** La biomasse et la densité totale des associations phytoplanctoniques diminueront après les ajouts d'HCs.

**Hypothèse #1b :** Les divers groupes taxonomiques répondront de façon différentielle à l'exposition par HC.

**Objectif spécifique #2 : *Évaluer l'effet des ajouts d'HCs sur la physiologie des associations phytoplanctoniques.***

**Hypothèse #2 :** Les ajouts d'HCs diminueront l'efficacité photosynthétique du phytoplancton.

## CADRE DU PROJET

Le présent projet de maîtrise a été développé dans le cadre d'une collaboration internationale avec le Mexique, avec la participation de l'ISMER, le Ministère de pêches et océans et de deux institutions de recherche mexicaines : le Colegio de la Frontera Sur - Unidad Campeche et le Centro de Investigación y de Estudios Avanzados et l'Unidad Mérida. Mon sujet d'étude a été l'analyse des perturbations sur le phytoplancton, et les autres membres de l'équipe ont étudié le reste des composants de la communauté planctonique, la chimie des HC et la photochimie. La partie centrale de ce mémoire de maîtrise est présentée dans un chapitre rédigé en anglais sous forme d'article scientifique (Cadaillon et al. in prep).

**CHAPITRE 1**

**FUNCTIONAL AND STRUCTURAL RESPONSES OF NATURAL**

**PHYTOPLANKTON ASSEMBLAGES TO ANTHROPOIC PERTURBATIONS: THE**

**CASE OF A LOW CONCENTRATION OIL SPILL SCENARIO**

## 1.1 INTRODUCTION

Maritime oil transportation is a widely used way to transport oil, therefore threatening marine ecosystems with chronic contamination and spills. The global frequency of large spills (>700 tonnes) from oil tankers has decreased significantly in the past four decades and, fortunately, large spills due to tanker incidents in Canadian marine waters have been rare. In circumstances where the frequency and/or volumes of shipments are increasing (Lee et al. 2015), continued efforts to reduce catastrophic tanker spills have been made. However attention should also focus on the small spills (< 7 tonnes), which are usually chronic and often occur in sensitive ecosystems. Data from the ITOPF (International Tanker Owners Pollution Federation) on oil tanker spills show that for nearly 10 000 incidents, 81% consisted of releases of < 7 tonnes (Lee et al. 2015).

A previous study about the annual frequency of oil spills in Canada has revealed that refined and fuel vessel spills between 10 and 100 m<sup>3</sup> are the most frequent, decreasing with increasing spill size (Ross Environmental Research, 2014, Lee et al. 2015). On October 13, 2016, more than 107 000 litres of diesel and 2 240 litres of lubricants were released into the Pacific Ocean from a 30 meters vessel near Bella Bella, B.C. ([http://www.huffingtonpost.ca/2017/12/04/bella-bella-b-c-oil-spill-likely-caused-by-sleeping-crew-on-tugboat-report\\_a\\_23297031](http://www.huffingtonpost.ca/2017/12/04/bella-bella-b-c-oil-spill-likely-caused-by-sleeping-crew-on-tugboat-report_a_23297031)). In Quebec's Magdalen Islands, one pipeline of Hydro-Québec, that contributed to supplying the electric power plant, transporting 40 million L of diesel annually, spilled 100 000 liters in September 2014

(<http://www.ledevoir.com/societe/environnement/467916/iles-de-la-madeleine-hydroquebec-severement-critiquee-pour-un-deversement-de-diesel>).

Diesel, a refined product from crude oil, is actually one of the most extensively used petroleum hydrocarbons. Global consumption of diesel has a direct impact on environmental contamination when leaked from storage mostly into the aquatic ecosystems. Crude oil and its refined products such as diesel contain an important proportion of the highly toxic polycyclic aromatic hydrocarbons (PAHs), which soluble fraction is rapidly released into the water

column following the spill (González et al. 2006, 2009) and it can be accumulated in plankton due to their great lipophilic capacities (Jiang et al. 2010).

Phytoplankton assemblages play a key role in the ecology of the marine ecosystem, and in the regulation of the amount of carbon in the atmosphere (Ozhan et al. 2014). Considering its basic status and function in marine food web and the role of primary productivity in dynamics of material and energy fluxes, studying the impact of oil pollution on marine phytoplankton is imperative. Research about the responses of the phytoplankton community to oil pollution stress is rare. Over the last decades, effects of crude oil (Kusk 1978, Østgaard et al. 1984), diesel (Chan & Chiu 1985), certain PAHs, and the oil wateraccommodated fraction (WAF) on monospecific cultures (Dunstan et al. 1975, Pérez et al. 2010b) and natural assemblages of phytoplankton (Thomas et al. 1981, Kelly et al. 1999, Marwood et al. 1999, Sargian et al. 2005, Hjorth et al. 2007, González et al. 2009, Pérez et al. 2010a) have been studied. However, most of these studies have been carried out with little volumes (microcosms) or in laboratory conditions. Some other studies have reported change in phytoplankton composition and abundance within natural areas affected by oil spills (Linden et al. 1979, Salas et al. 2006, Varela et al. 2006, Díez et al. 2009). Noteworthy, the potential impacts of diesel has been understudied, comparatively to other kinds of oil.

The interactions between oil pollution and phytoplankton are complex, varying among oil compounds, concentrations, and phytoplankton species (Tukaj 1987, González et al 2009, Pérez et al. 2010, Ozhan et al. 2014, Perhar & Arhonditsis 2014). While some investigations reported negative effects on phytoplankton (Østgaard et al. 1984, Sargian et al., 2005), others found stimulatory effects (Oviatt et al. 1982) on the biomass and the photosynthesis. In both laboratory cultures and natural phytoplankton assemblages, exposure to high concentrations of petroleum water-soluble fraction (WSF) has been observed to be toxic, while stimulatory effects have been reported at lower concentrations (Siron et al. 1991, El-Sheekh et al. 2000, Parab et al. 2008, Pérez et al. 2010). As concentrations increase, regardless of oil chemical profile, the toxic impacts become apparent in the forms of increased cell diameter and reduced cell division, lower chlorophyll-*a* concentrations, and reduced photosynthetic activity resulting

from electrons chain transport interference in PSI and PSII (Aksmann & Tukaj 2008, Perhar & Arhonditsis 2014). Differences in the sensitivity of taxonomic groups have also been reported (Vargo et al. 1982, Harrison et al. 1986, González et al. 2009, Gilde & Pinckney 2012). Several studies suggest cell size as an important factor in PAH toxicity (Fan & Reinfelder 2003, González et al. 2009, Echeveste et al. 2010a).

Phytoplankton assemblages' responses are difficult to predict, because they are in part based on the relative tolerances of the different phytoplankton groups and species present at the time the community was exposed to the crude oil (González et al. 2013). In addition, grazers such as micro- and mesozooplankton may also be affected by oil, which relieves grazing pressures on some phytoplankton species but not on others (González et al. 2009). Microbial degradation of crude oil can also play a prominent role in the marine environment during and after oil spills (Ozhan et al. 2014). Because of the close coupling between phototrophs and heterotrophs, the resultant imbalances may result in phytoplankton assemblage shifts in response to the spill.

In the present study, we attempted to partially overcome some of the limitations associated with study of the effects of oil on plankton. For instance, microcosm studies, in which small water volumes are not hardly representative of the natural environment. Similarly, when studying an *in situ* oil spill situation, sampling usually start after a long time has elapsed between the spills, and consequently important information concerning the short-term effects are lost. In addition, interactions between biotic and abiotic factors in natural environments are very complex. Furthermore, the investigation of oil spills in natural ecosystems poses enormous logistical challenges, which include high costs and the need for long-term study. Experiments using mesocosms allow the use of large volumes of seawater containing whole communities of plankton with significant control over the environmental conditions (Kemp et al. 2001, Petersen et al. 2003), thus partially simulating the physical conditions of the natural environment (González et al. 2013).

The present work aimed to study effects of low HCs concentrations on the structure (1) and function (2) of the phytoplankton assemblages of the Lower St. Lawrence Estuary

(LSLE), under “chronic” and “acute” pollution scenarios. Mesocosms experiments were used as the methodological approach and maritime diesel as the source of pollution. The application of different methodologies for phytoplankton analyses enabled us to study different structural and functional attributes such as phytoplankton biomass, abundance, pigment and taxonomic composition, cell size, functional groups and the photosynthetic efficiency. Three main hypotheses were tested: (1. a) total biomass and cell density of phytoplankton assemblages will decline after HCs inputs; (1. b) sensitivity to HCs exposure will vary among phytoplankton taxonomic groups and (2) HCs inputs will diminish the photosynthetic efficiency of phytoplankton.

## 1.2 MATERIALS AND METHODS

### 1.2.1 Set-up

A mesocosms‘experiment was carried out during summer 2016 (June 21 - July 6) at the marine station (Pointe-au-Père, Canada) of the Institut des sciences de la mer de Rimouski (ISMER). The mesocosms system consists of two thermostated containers, each holding six 2.6 m<sup>3</sup> cylindrical mesocosms (Aquabiotech®) with a cone-shaped bottom. Each enclosure is sealed with a Plexiglas cover letting pass through between 80% and 90% of UV light and 90% of PAR. Each mesocosm has an independent control system for temperature (AQBT-Temperature sensor, accuracy ± 0.2°C) and probes connected to an automated record of pH (Hach® PD1P1 (± 0.02), dissolved oxygen and in vivo fluorescence (chlorophyll *a*) whose results are not presented in this study. Temperature in each mesocosms was measured every 15 minutes, and the control system triggered either a resistance heater (Process Technology TTA1.8215) located near the middle of the mesocosm or a pump activated glycol refrigeration system to maintain the set temperature.

Natural sea surface water (from 2 m depth) was sampled at the Les Escoumins harbor (48°19'06.9"N 69°24'44.8"W, Lower St. Lawrence Estuary), using an intake pump and transferred to a tanker truck. Water arrived at the Pointe-au-Père marine station three hours after sampling. To fill the mesocosms, the collected seawater was first filtered through a 300 µm Nitex mesh net to remove large zooplankton and avoid bias in the comparison of results among mesocosms. To ensure homogeneity in water characteristics among mesocosms at the start of the experiment, the seawater was mixed in an intermediary tank of 150 L and then distributed simultaneously to 9 mesocosms by gravity using 9 identical pipes originating from the intermediary tank. The regulating temperature system was activated once filling was completed. Seawater was mixed during the experiment using agitators (model Minn Kota RT55EM) with a fixed speed in each mesocosms, allowing to standardize the water temperature and vertical distribution of particles. Filling of the mesocosms was done on June 20, 2016 and water samples were taken from the following day (time 0), to check for homogeneity among mesocosms. No nutrients were added since local concentrations were high enough to allow for phytoplankton growth.

Two different diesel pollution scenarios were considered. According to the moment of the introduction of the contaminant and its concentration two pollution treatments were applied, named respectively chronic and acute, each one with three replicates. Three mesocosms where no diesel was added were included as the control treatment. For the chronic treatment, 10 mL of maritime diesel (density 0.845 g mL<sup>-1</sup> at 20°C) were added both on the 3<sup>rd</sup> (Jun 24) and 6<sup>th</sup> (Jun 27) experiment days, while for the acute treatment maritime diesel was added only in the 6<sup>th</sup> experiment day in a single injection of 20 mL. Diesel additions were done in the morning, just after the daily sampling. Diesel concentrations in the mesocosm were determined according to Brussaard et al. (2016). In the present study, an oil layer of 5 µm was simulated, which is equivalent to a concentration of 6.8 mg L<sup>-1</sup> of the pollutant in the mesocosm water taking into account a volume of diesel addition of 20 mL (Dal Santo Vidal, in prep.)

Daily sampling of the mesocosms was performed at 8:00 h am, using 20 L carboys and then water was transferred to specific bottles for further laboratory analysis (physical, chemical and biological) at ISMER.

### **1.2.2 Inorganic nutrients**

For inorganic nutrient analyses, 3 daily subsamples of 10 mL were prefiltered through a 25 mm polyethersulfone membrane filter (nominal porosity of 0.2 µm) placed on 60 mL acid washed syringes. The samples were stored in 12 mL acid washed polypropylene tubes previously rinsed twice with prefiltered samples and immediately frozen at -80°C until analysis. Nutrient concentrations were determined by automated procedures based on the colorimetric method adapted from Grasshoff et al. (1999), with a SEAL Auto Analyzer 3. Before analysis, samples were thawed in a bath of warm water, kept in the dark and analyzed within 1 h.

### **1.2.3 Chlorophyll *a***

Phytoplankton biomass was estimated fluorometrically using chlorophyll *a* (Chl *a*) as a proxy. Triplicate water samples (300 mL) were collected daily from each mesocosm to determine total concentrations. Samples were filtered through 25 mm glass fiber filters (Whatman GF/F; 0.7 µm nominal pore size). After filtration, filters were placed in tubes with 90% acetone during 24 h for the extraction of the pigment in a dark and cold (4-5°C) chamber. Fluorescence was measured using a Turner Design Fluorometer (TD 10-AU 005 CE) previously calibrated with pure Chl *a* (SIGMA no cat. C-6144). Chl *a* concentrations were calculated from the fluorescence of the extract according to Parsons et al. (1984).

### 1.2.4 Pigments analysis

Samples for pigment analysis (days 0, 4, 7, 12, 15) were chosen taking into account the Chl *a* fluorometry measurements evolution during the entire experiment, in order to identify the different stages of phytoplankton succession (prebloom, bloom and postbloom periods, respectively). Phytoplankton pigments were analyzed by high performance liquid chromatography (HPLC). Water samples of 0.7 to 1.5 L were gently filtered onto 25 mm diameter Whatman GF/F glass fiber filters. Filters with the filtrate were wrapped in aluminium foil, immediately frozen in liquid nitrogen and then stored at -80°C until analysis. Pigments were extracted in 95% methanol (MeOH), then sonicated for a few seconds and centrifuged in an IEC Clinical Centrifuge at 7100 rpm for 5 minutes. Pigment extracts were then filtered onto 0.2 µm polytetrafluoroethylene Gellman Acrodisc filters into amber glass vials and stored under argon gas at 4°C in darkness until measurement by reverse-phase HPLC within 24 h of extraction. The standard internal apo-carotene (trans-Bapo-8'-carotenal, Sigma-Aldrich) was added to each sample to correct for possible extraction and injection bias. The pigment extract was analyzed following Zapata et al. (2000) using eluent solution A (MeOH:acetonitrile:aqueous pyridine, 50:25:25, v:v) and solution B (MeOH:acetonitrile:acetone, 20:60:20, v:v) at a flow rate of 1 mL min<sup>-1</sup>. Pigments were separated on a reversed phase C8 Waters Symmetry column (150 × 4.6 mm, 3.5 µm) and detected using a Thermo Separation FL 3000 fluorescence detector in series with a photodiode array detector (Thermo Separation UV-6000). Pigment quantification was carried out at 450 nm. Pigment results are presented as volumetric concentrations (µg L<sup>-1</sup>) and their significance (Roy et al. 2011) is detailed in Table 1.

**Table 1:** Pigments identified in the present study and their taxonomic group and/or significance

Pigment	Taxonomic Group and/or significance
Chlorophyllide <i>a</i>	Chl <i>a</i> alteration product: senescent algae, damaged diatoms, zooplankton faecal pellets. Extraction artifact for algae with highly active chlorophyllase enzyme

MgDVP	Major pigment in prasinophyceae, trace amounts in most other algal groups
Chl <i>c2</i>	Minor pigment in most types of algae within the red algal lineage (Rhodophyceae)
Chl <i>c1</i>	Minor pigment in most types of algae within the red algal lineage (Rhodophyceae)
Pheophorbide <i>a</i>	Chl <i>a</i> alteration product: senescent algae, zooplankton faecal pellets and sediments
Fucoxanthin	Major pigment in most algal classes of the red algal lineage, especially diatoms
Neoxanthin	Photoprotective pigment in prasinophyceae and chlorophyceae
Prasinoxanthin	Major pigment in prasinophyceae
Violaxanthin	Photoprotective pigment in prasinophyceae and chlorophyceae
Micromonal	Major pigment in prasinophytes
Diadinoxanthin	Photoprotective pigment in diatoms and dinoflagellates
Antheraxanthin	Minor pigment in chlorophytes, prasinophytes, trebouxiophytes, mesostigmatophytes, some crysophytes and eustigmatophytes
Diadinoxanthin	Diadinoxanthin alteration product
Alloxanthin	Major pigment in crytophytes
Diatoxanthin	Photoprotective pigment, minor in euglenophytes, diatoms, bolidophytes, haptophytes, dictyochophytes, pelagophytes and some dinoflagellates
Zeaxanthin	Major pigment in cyanobacteria and prochlorophytes, minor in green algae as chlorophytes and prasinophytes
Lutein	Photoprotective pigment, dominant in chlorophytes and prasinophytes
Vaucherianthaxanthin ester	Major pigment in eustigmatophytes
Gyroxanthin	Major pigment in Gyroxanthin-containing dinoflagellates (i. e. the toxic algae <i>Gyrodinium breve</i> ) but also found in pelagophytes and haptophytes

---

Chl <i>b</i>	Major pigment in green algae, some prochlorophytes
Chl <i>a</i>	All photosynthetic algae
Pheophytine <i>a</i>	Chl <i>a</i> alteration product found in zooplankton faecal pellets, senescent algae and sediments
$\beta,\beta$ -Carotene	Major pigment in chlorophytes, prasinophytes, mesostigmatophytes, rhodophytes and one group of dinoflagellates. Minor in all other algal groups.
B-Fucox (*)	Major pigment in pelagophytes and dictyochophytes. Also present in some haptophytes; trace amounts in dinoflagellates

---

Note: (\*) trace levels, B-Fucox: 19'-butanoyloxyfucoxanthin, MgDVP : Mg-2,4-divinyl pheophorphyrin a5 monomethyl ester

Results of fluorometric and HPLC determination of Chl *a* were significantly correlated ( $p < 0.01$ ,  $r=0.92$ ,  $n=55$ ) following a Type II Simple Linear Regression ( $\text{Chl } a_{\text{Fluo}} = 1.14 \text{ Chl } a_{\text{HPLC}} + 0.21$ ;  $r^2 = 0.95$ ), showing that both techniques gave consistent results (Figure 1). Three aberrant points were ignored.

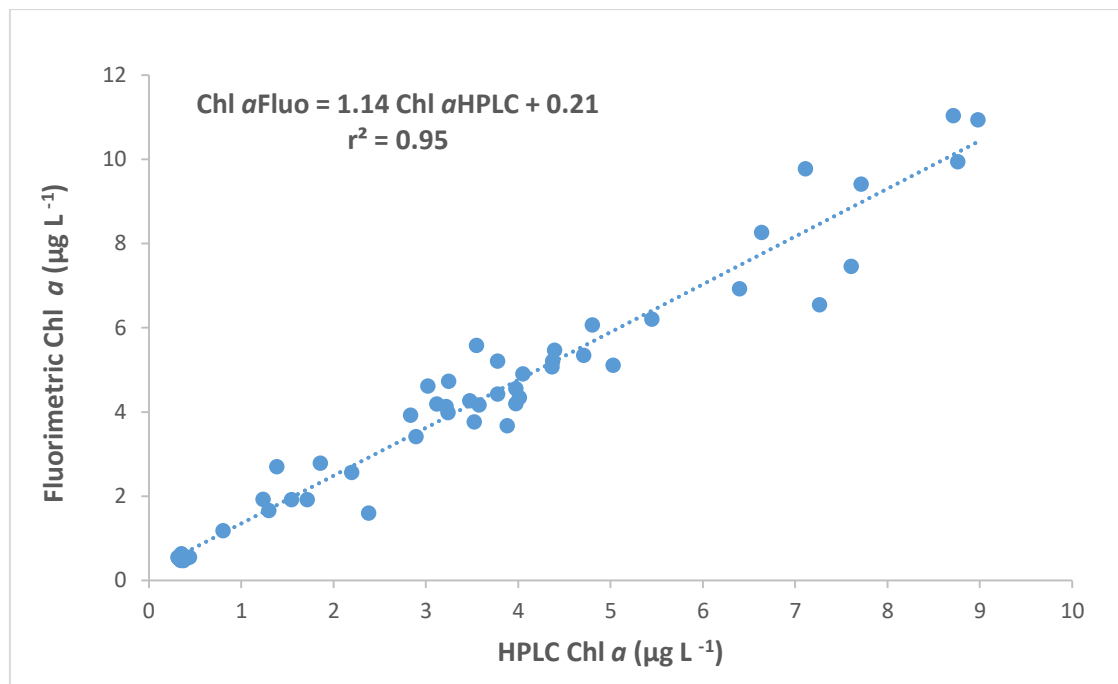


Figure 1: Simple Linear Regression between Chl *a* obtained by fluorometry and HPLC methods

### 1.2.5 Flow cytometry (FCM) analysis

For the determination of pico- and nanophytoplankton density, daily two-replicate subsamples (4 mL) were fixed with glutaraldehyde Grade I (Sigma), 0.1% final concentration, in the dark at 4°C for 15 min, flash-frozen in liquid nitrogen and then frozen at -80°C until analysis.

Abundances of autotrophs <20 µm, i.e. phycoerythrin-containing cyanobacteria, phycocyanin-containing cyanobacteria and autotrophic eukaryotes, were measured by flow cytometry. Samples for <20 µm autotroph abundances were analyzed using a CytoFLEX flow cytometer (Beckman Coulter) fitted with a blue (488 nm) and a red laser (638 nm). Using the blue laser, forward scatter, side scatter, orange fluorescence from phycoerythrin (582/42 nm BP), and red fluorescence from chlorophyll (690/50 nm BP) were measured. The red laser was used to measure the red fluorescence of phycocyanin (660/20 nm BP). Polystyrene microspheres of 2 µm diameter (Fluoresbrite YG, Polysciences) were added to each sample as an internal standard. Pico- (<2 µm) and nanoautotrophs (2-20 µm) were discriminated based on a forward scatter calibration using algal cultures (see below). The cytograms obtained were analyzed using Expo32 v1.2b software (Beckman Coulter).

In order to estimate the biovolume of the different nanoautotroph groups, a relationship was established between the mean forward scatter of glutaraldehyde-fixed algal cultures and the average equivalent spherical diameter (ESD, µm) of cultures of these algae measured with an inverted microscope (Axio Observer Z1, Carl Zeiss). The following linear regression was established using 15 algal cultures from 8 different algal species (*Coccomyxa* sp., *Dunaliella tertiolecta*, *Isocrysis galbana*, *Pavlova lutheri*, *Scenedesmus obliquus*, *Selenastrum* sp., *Tetraselmis suecica* and an unidentified flagellate) and covering the ESD range 3.3-11.2 µm:  $ESD = 0.49 \times FSC + 2.73$ ;  $r^2 = 0.955$ . FSC is the mean forward scatter of the cells normalized by the mean forward scatter of 2 µm Fluoresbrite beads. This linear regression was provided by Ph.D Claude Belzile.

Cell carbon content was estimated from volume calculated from the estimated spherical diameter (ESD) of the particle, according to Menden-Deuer & Lessard (2000).

For autotrophs with an ESD  $< 7 \mu\text{m}$ , volume-to-carbon conversion factor for taxonomically diverse protist plankton excluding diatoms ( $\text{pgC cell}^{-1} = 0.216 \times \text{volume}^{0.939}$ ) was considered. For autotrophs with an ESD  $\geq 7 \mu\text{m}$ , volume-to-carbon conversion factor for diatoms ( $\text{pgC cell}^{-1} = 0.288 \times \text{volume}^{0.811}$ ) was considered. For picocyanobacteria and picoeukaryotes, cell abundance to carbon biomass conversion factors ( $\text{pgC cell}^{-1}$ ) of two different species was considered: *Synechococcus* spp. (Buitenhuis et al. 2012) for picocyanobacteria and *Micromonas pusilla* (Durand et al. 2002) for picoeukaryotes. The time net biomass accumulation in each mesocosm for the whole experiment was approximated by the trapezoidal rule integration.

### **1.2.6 Light microscopy (LM) analysis**

Non-replicate 60 mL samples for LM and image analysis (section hereafter) were taken the same days as for HPLC pigments analysis, except for day 0, when no samples were taken due to sampling problems. These sub-samples (60 mL) were kept in amber glass bottles, preserved in acidic Lugol's solution (Parsons et al. 1984) and stored in the dark at 4°C until analysis. Eukaryotic cells  $> 2 \mu\text{m}$  were identified to the lowest possible taxonomic level and enumerated using an inverted microscope (ZEISS Germany, Axiovert 100) according to Lund et al. (1958). For each sample, at least 300 cells were counted. The main taxonomic references used for phytoplankton identification were Tomas (1997) and Bérard-Theriault et al. (1999).

### **1.2.7 Image analysis (FlowCAM)**

A total of 36 samples (taken and preserved as described above) were analyzed with a B/W FlowCam™ II benchtop instrument (Fluid Imaging Technologies), using the software

package Visual Spread Sheet (ViSP) version 1.5.16. All measurements in the present study were done using the automatic imaging mode. A 10 $\times$  objective was used in the FlowCAM and the dimension of the flow cell, determined by the objective, was 2  $\times$  0.1 mm (10 $\times$ ) flow cell, supplied from Fluid Imaging Technologies, Inc.

The automatic mode seems most useful for whole plankton community assessments and, depending on the lens used, is limited by the rather low sample volume processed (Jakobsen & Carstensen 2011). The samples were manually stirred and the dilution 9:10 was prepared with 900  $\mu$ l of the sample and 100  $\mu$ l of a tampon solution (TE-10X, Mat TE1000-1L) which was previously filtered (0.2  $\mu$ m) and then introduced in the FlowCam cell. The images were sorted as living versus non-living particles by visual inspection and particles in the 20 to 500  $\mu$ m range were analyzed. Biovolumes calculated from the ESD of the particle was converted to carbon content (MendenDeuer & Lessard 2000). The C: volume relationship from Menden-Deuer & Lessard (2000) for diatoms ( $\text{pgC cell}^{-1} = 0.288 \times \text{volume}^{0.811}$ ) was applied, since that microscopy identification and HPLC results revealed the diatom dominance for autotrophs  $> 20 \mu\text{m}$ .

### **1.2.8 Fluorescence induction analysis**

The fluorescence induction technique, known as Fast Repetition Rate Fluorometry (FRRF, Kolber et al. 1998) was used to investigate algal physiology conditions of photosystem II (PS II) using a FRR fluorometer (FRRf; Chelsea Instruments, UK). The photosynthetic parameters were measured from water samples (3 mL) collected daily after exposure to dark conditions during 30 min, to allow relaxation of fluorescence quenching. After this time, samples were illuminated with increasing irradiance of actinic light for measuring fluorescence emission according to Suggett et al. (2006). The photochemical efficiency or quantum yield, defined as the ratio of variable ( $F_v$ ) to maximal fluorescence ( $F_m$ ),  $F_v/F_m$ , was considered in this study as an index of the photosynthetic performance of phytoplankton. In this ratio,  $F_v$  is calculated as  $F_v = F_m - F_0$ , with  $F_0$  being the initial fluorescence (when all

photosystem II reaction centers are active or “open”) and  $F_m$  is the maximal fluorescence (when all reaction centers of photosystem II are “closed”). This parameter was used to examine the effects of HC pollution on the photosynthetic apparatus of phytoplankton.

### **1.2.9 Statistical analysis**

Data of nutrient and pigment concentrations, abundances, biomass estimates, and the photochemical efficiency parameter ( $F_v/F_m$ ) were independently compared with a Repeated Measures Analysis of Variance (RM-ANOVA) with two fixed factors (time in days (0 to 15) and treatment (Control versus Chronic and Control versus Acute, respectively) in a mixed model using the statistical package XL STAT version 10. Normality and homoscedascity of the model were checked by residual analysis and Kolmogorov-Smirnov test. If normality and/or homoscedasticity assumptions were not met, data were normalized with a log/ln transformation. Bonferroni and Tukey post-hoc tests were used to assess the significance of the differences between treatments within days. Probability levels  $< 0.05$  and  $< 0.01$  were considered as significant thresholds for the differences observed. Results from the first day (water filling; D0) were not considered in the statistical analyses as this was considered to be the initial stabilization period.

## **1.3 RESULTS**

### **1.3.1 Inorganic nutrients**

At the start of the experiment, mesocosms water was rich in nutrients, with concentrations of around  $6.82 (\pm 0.03)$ ,  $8.96 (\pm 0.05)$ , and  $1.14 (\pm 0.003)$   $\mu\text{mol L}^{-1}$  for nitrate + nitrite, silicate and phosphate, respectively (Figure 2). On the third day of the experiment, they decreased slightly in all mesocosms. Concentrations of nitrite + nitrate and silicate showed a

similar trend, but the largest drop for dissolved nitrogen occurred on day 6 while for silicate it happened some days later (i.e. days 7-9). Then, both nutrients remained exhausted in all mesocosms without significant differences between treatments.

Phosphate concentrations decreased from day 4 to day 6 and then remained relatively stable until day 11, declining in the last experimental days with significant differences between control and contaminated treatments. Phosphate concentrations were significantly higher in both, acute and chronic contaminated treatments, than in the control in the last experimental days. RM ANOVA results demonstrated an interactive effect of time and treatment ( $p < 0.01$ , see the Annex 1) on phosphate concentrations for both types of diesel addition.

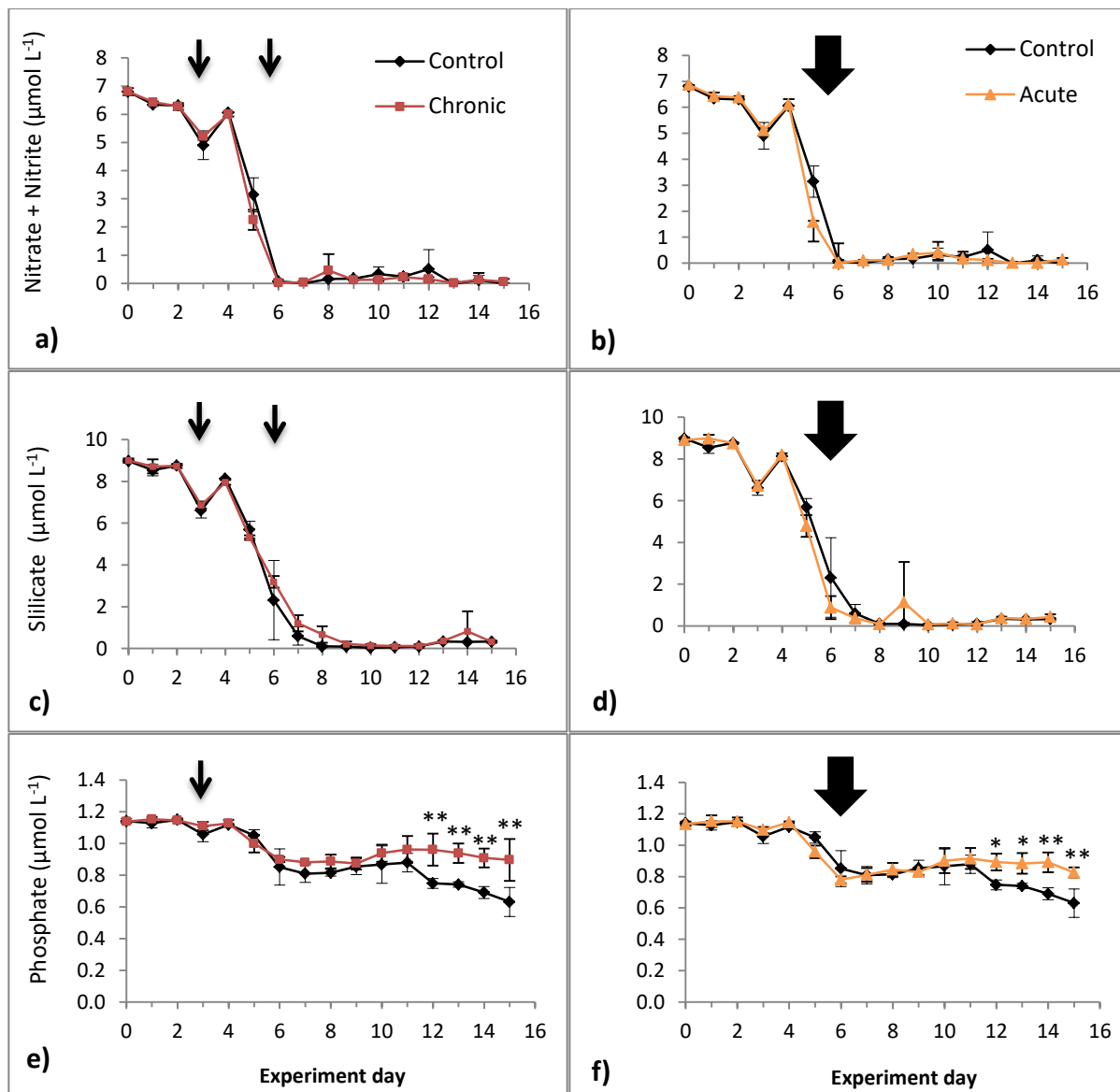


Figure 2: Temporal patterns for mean ( $\pm\text{SD}$ ) nutrient concentrations: a-b) Nitrate + Nitrite, c-d) Silicate, e-f) Phosphate. \*:  $p < 0.05$  \*\* =  $p < 0.01$ . Vertical bars indicate the standard errors. Arrows represent days when diesel injections were performed. The control treatment is shown in each figure for comparison purposes only

### 1.3.2 Chlorophyll *a* concentration evolution

Chl *a* evolution during the whole experiment (measured by the fluorometric method) is shown in Figure 3. When information on Chl *a* is combined with nutrient data, three periods can be distinguished: (i) pre-bloom, with relatively low Chl *a* levels and high nutrient concentrations (i.e. from day 0 to day 3); (ii) bloom, with relatively high Chl *a* levels and a marked nutrient decrease (i.e. from day 4 to day 7); and (iii) the post-bloom, with relatively low Chl *a* levels and low or exhausted nutrient concentrations (i.e. from day 8 to day 15). The bloom reached its maximum on the day 7 in all treatments - with Chl *a* levels between  $6.92 \pm 0.15$  and  $11.96 \pm 2.96 \mu\text{g L}^{-1}$ . Chl *a* in the chronic treatment was significantly lower than in the control after the day 11. In addition, RM ANOVA results evidenced an interactive effect between time and treatment ( $p < 0.0001$ , see the Annex 2) on Chl *a* concentration for the chronic treatment. In the acute treatment, Chl *a* concentration seemed to have the same trend as in the chronic one, but significant differences with the control were only found during the last experimental day. We detected significant effects eight days after diesel addition in the chronic treatment (considering the first input on day 3) and nine days for the acute one.

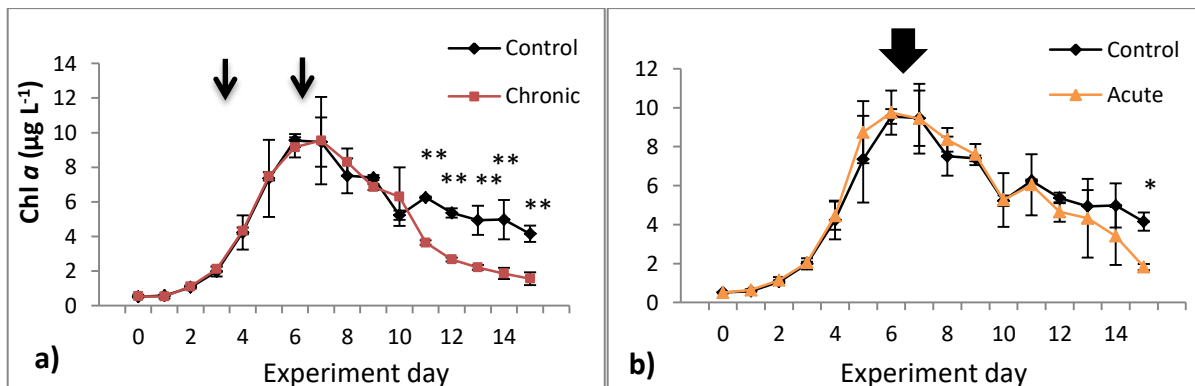


Figure 3: Temporal patterns for mean ( $\pm\text{SD}$ ) Chl *a* concentration measured by fluorimeter for the (a) chronic and (b) acute treatments \* =  $p < 0.05$  \*\* =  $p < 0.01$ . Vertical bars indicate the standard errors. Arrows represent days when diesel injections were performed. The control treatment is shown in each figure for comparison

### 1.3.3 Nano- and pico-phytoplankton densities and carbon estimations (FCM)

Temporal changes in density of phytoplankton cells <20 µm are depicted in Figure 4. Six groups were detected: eukaryotes (nano- and pico-eukaryotes) and cyanobacteria containing Phycoerythrin (nano-PE-cyanobacteria, pico-PE-cyanobacteria) or Phycocyanin (nano-PC-cyanobacteria and pico-PC-cyanobacteria). Nano-eukaryotes were the most important group comprising between 43% and 93% of nanophytoplankton density in the control treatment during the entire experiment, with maximum densities around  $1.6 \times 10^4$  cells mL<sup>-1</sup>. The contributions of pico-eukaryotes to total phytoplankton <20 µm varied during the experiment (4-47%), with maximal densities one order of magnitude lower than the other eukaryotes ( $\sim 9.16 \times 10^3$  cells mL<sup>-1</sup>).

Total phytoplankton <20 µm and both nano- and pico-eukaryotes densities (Figure 4) followed a similar trend to that of Chl *a* (Figure 3), and were significantly reduced by diesel inputs in the last period of the experiment (after day 11), notably in the chronic treatment. In addition, still for this latter treatment, RM ANOVA results showed an interactive effect of time and treatment in total phytoplankton <20 µm and in nano- and pico-eukaryotes densities ( $p < 0.01$ , see the Annex 3, 4, 5 respectively). Conversely, for the acute treatment an interactive effect of time and treatment was only observed on pico-eukaryotes densities ( $p < 0.01$ , see the Annex 5).

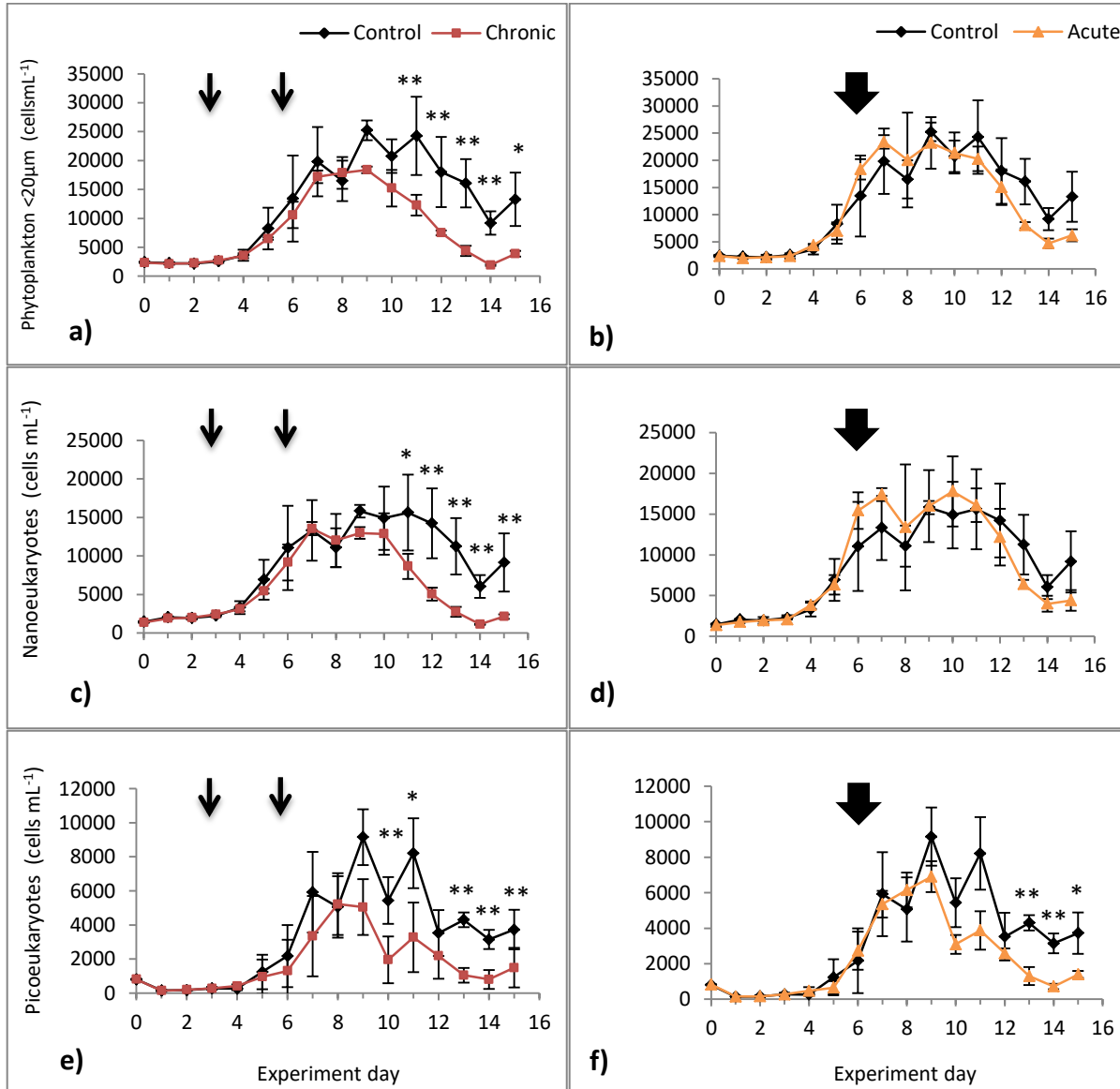
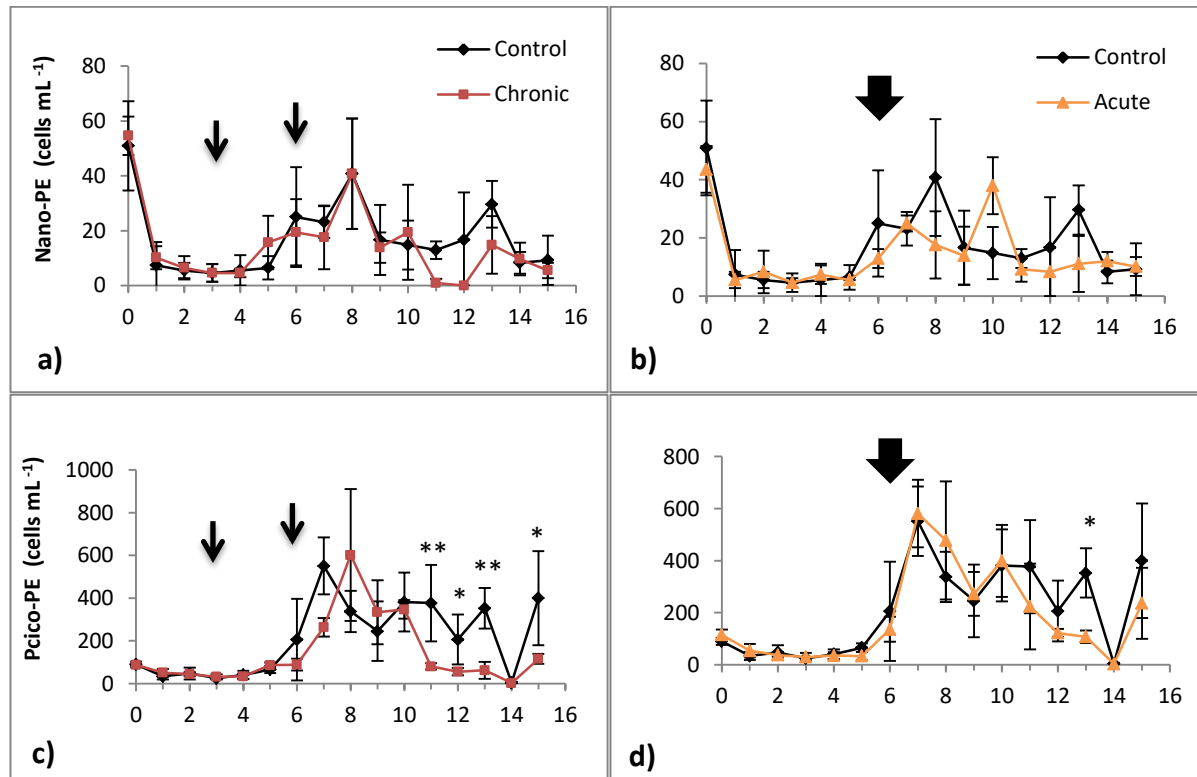


Figure 4: Temporal patterns for mean ( $\pm \text{SD}$ ) phytoplankton densities measured by Flow Cytometry: a-b) Total phytoplankton ( $<20\text{ }\mu\text{m}$ ), c-d) Nano-eukaryotes, e-f) Pico-eukaryotes. \* =  $p < 0.05$  \*\* =  $p < 0.01$ . Vertical bars indicate the standard errors. Arrows represent diesel inputs. The control treatment is shown in each figure for comparison purposes only

Cyanobacteria were not abundant (in many cases, they were even not detectable), representing less than 10% of total phytoplankton community  $<20\text{ }\mu\text{m}$  during the entire experiment and in all treatments (Figure 5). However, density of some groups was either significantly reduced or stimulated by the effect of diesel additions, especially in the post

bloom period. In this regard, RM ANOVA results showed an interactive effect of time and treatment in nano-PC-cyanobacteria densities for both contaminated treatments ( $p < 0.01$ ,  $p < 0.05$  for chronic and acute respectively, see the Annex 6). Similar results were found for pico-PE-cyanobacteria densities for the chronic treatment ( $p < 0.01$ , see the Annex 7). It is important to highlight that nano-PC-cyanobacteria was the only group of nanophytoplankton being significantly stimulated by diesel addition.



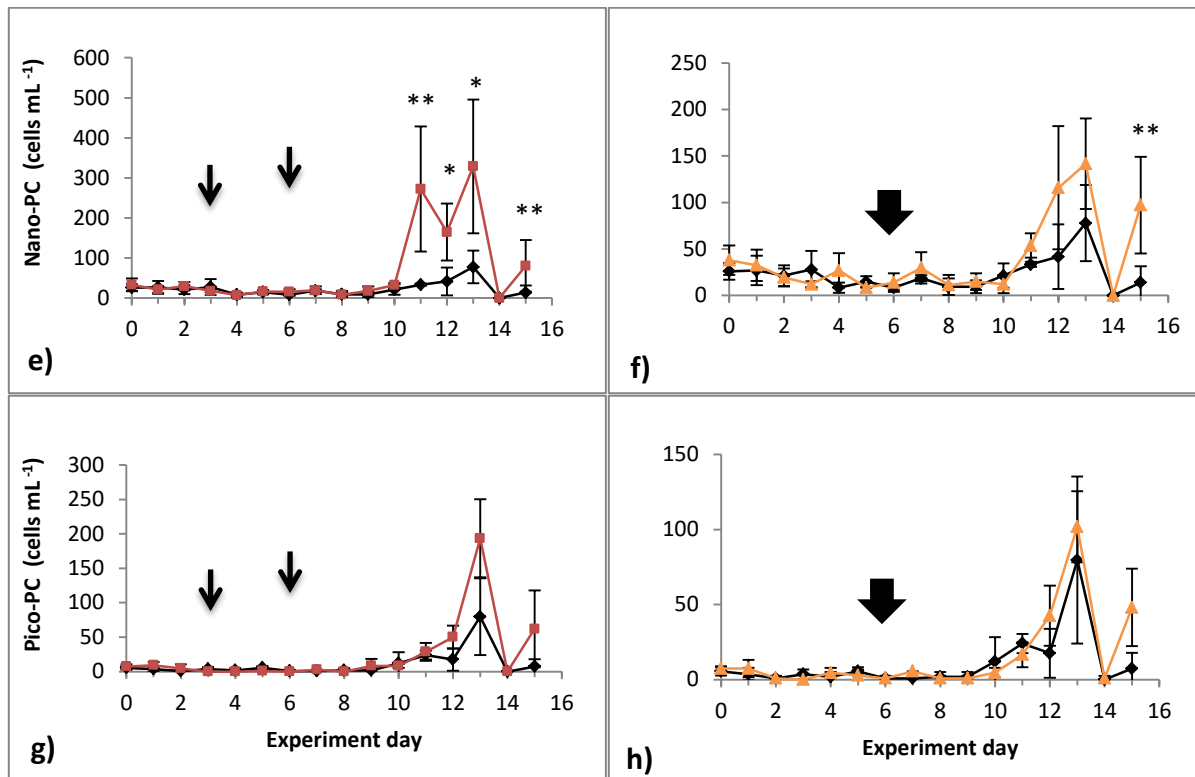


Figure 5: Temporal patterns for average ( $\pm \text{SD}$ ) cyanobacteria densities measured by Flow Cytometry: a-b) Nano-PE, c-d) Pico-PE, e-f) Nano-PC, g-h) Pico-PC \* =  $p < 0.05$  \*\* =  $p < 0.01$ . Vertical bars indicate standard errors. Arrows represent diesel inputs.

Estimations of carbon biomass obtained from cell volume of pico- and nanophytoplankton are depicted in Figure 6. Total phytoplankton carbon biomass in control treatments ranged between  $21 \mu\text{g C L}^{-1}$  ( $\pm 5$ ) at the beginning of the experiment and  $355 \mu\text{g C L}^{-1}$  ( $\pm 37$ ) on day 11, decreasing in the post bloom. Nanoeukaryotes were the prevalent group, comprising from 88 to 99% of phytoplankton carbon biomass in the control ( $20-347 \mu\text{g C L}^{-1}$ ), showing a pattern similar to that of total phytoplankton  $<20 \mu\text{m}$ .

Significant differences in phytoplankton carbon biomass between the control and contaminated treatments were evidenced in the last period (especially for the chronic treatment), which suggests a significant loss of phytoplankton carbon related to diesel addition.

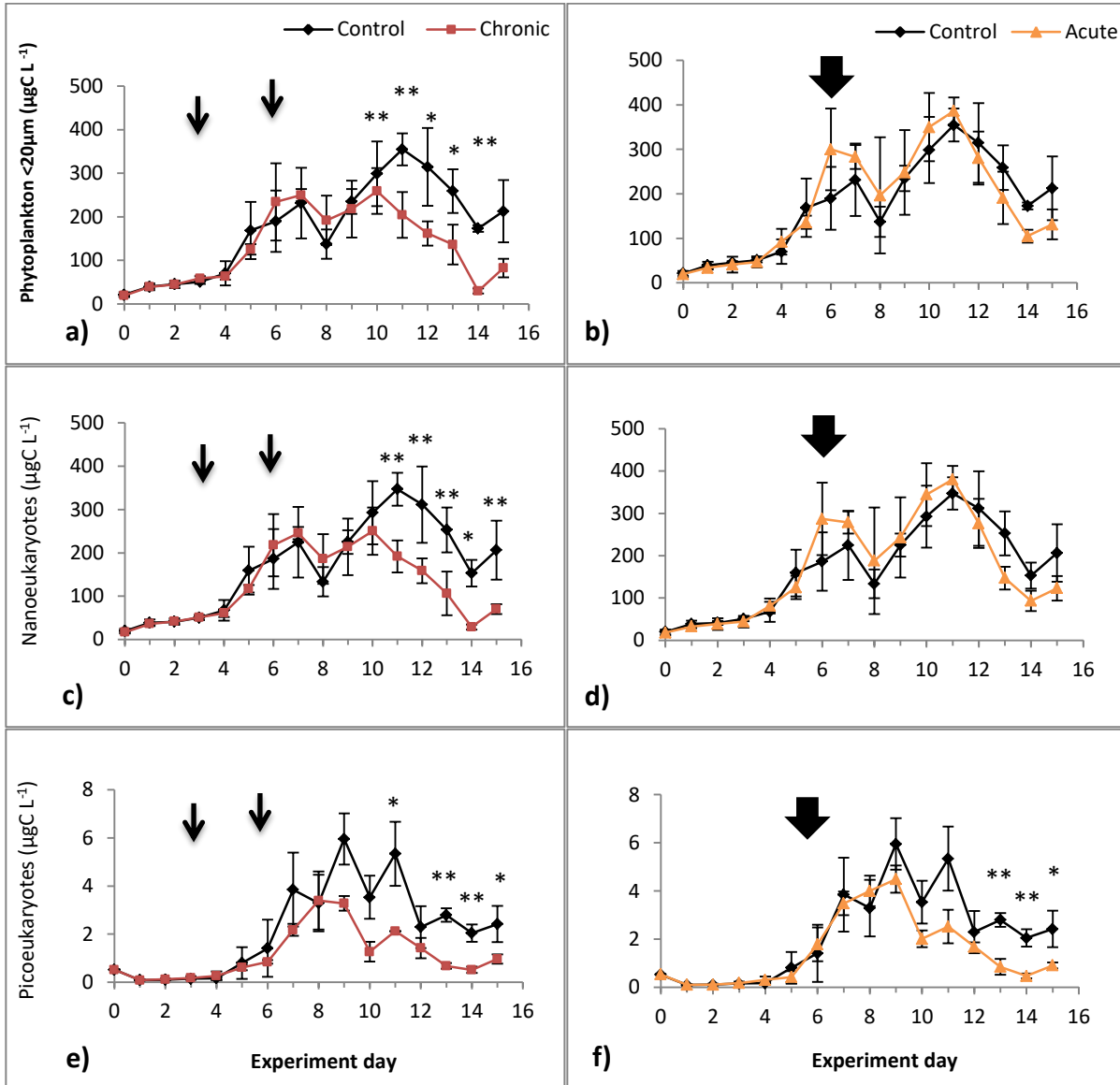


Figure 6: Temporal patterns for mean ( $\pm\text{SD}$ ) phytoplankton carbon biomass estimated from volume (ESD), a-b) Total phytoplankton  $<20\text{ }\mu\text{m}$ , c-d) Nano-eukaryotes, e-f) Pico-eukaryotes \* =  $p < 0.05$  \*\* =  $p < 0.01$ . Vertical bars indicate the standard errors. Arrows represent diesel inputs.

Interactions between time and treatment were evident in total phytoplankton  $<20\text{ }\mu\text{m}$ , nano-eukaryotes and pico-eukaryotes biomass for the chronic treatment ( $p < < 0.01$ , see the Annex 8-10), and only in picoeukaryotes biomass for the acute one ( $p < < 0.01$ , see the Annex

10). In general, biomass was significantly reduced by diesel inputs after day 10. Pico-eukaryotes seemed to be affected earlier but this difference was not significant.

Net carbon accumulation for nano- and pico-eukaryotes estimated from day 10 on, during the post-bloom, is depicted in Figure 7. Carbon loss in nanoeukaryotes was 47% and 14% for the chronic and acute treatments, respectively. ANOVA results for net carbon accumulation showed significant differences between treatments ( $p \leq 0.01$ , see the Annex 11) with the chronic treatment being significantly lower than the control and the acute ones ( $p = 0.01$  and  $p < 0.05$  respectively, see the Annex 12). The acute treatment was not significantly different than the control ( $p = 0.467$ , see the Annex 12). Carbon loss in pico-eukaryotes was higher than in nano-eukaryotes, namely 61% and 56% for chronic and acute treatment, respectively. Net carbon accumulation was significantly different between treatments ( $p < 0.01$ , see the Annex 11), with chronic and acute treatments being significantly lower than the control ( $p < 0.01$ , see the Annex 12). In this case, there were no significant differences between both contaminated treatments.

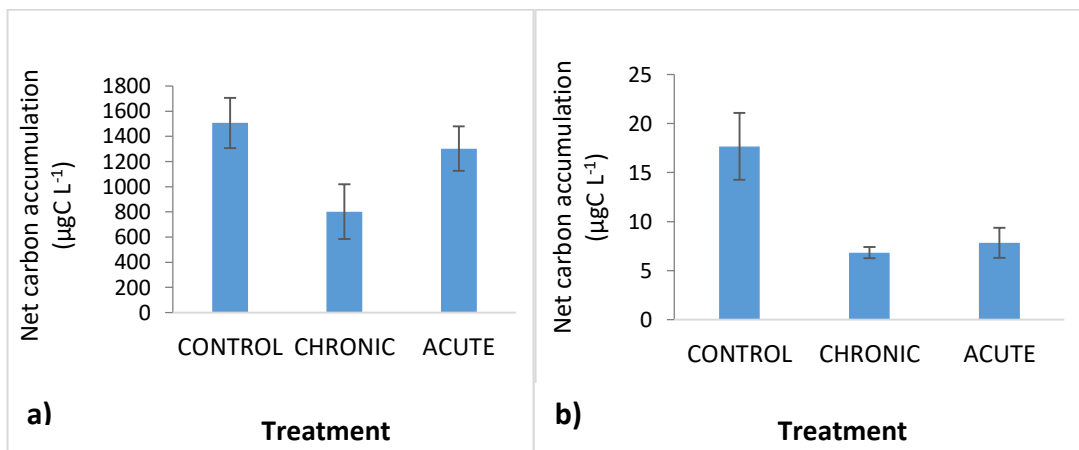


Figure 7: Net carbon accumulation for nano- (a) and pico-eukaryotes (b) estimated from day 10 on for all treatments. Vertical bars indicate standard errors

### 1.3.4 Microphytoplankton densities and carbon estimations (FlowCAM)

Temporal changes in density and biomass (carbon) of microphytoplankton (cells >20  $\mu\text{m}$ ), obtained by imaging analysis (FlowCAM), are depicted in Figure 8. Both variables increased during the experiment in the control treatment but were significantly reduced from day 12 on in the contaminated treatments. Results of RM ANOVA showed an interaction effect between time and treatment in Microphytoplankton density ( $p << 0.01$ , see the Annex 13) and biomass ( $p << 0.01$ , see the Annex 14) for both contaminated treatments.

Phytoplankton carbon estimations for microphytoplankton ranged from 196 ( $\pm 29$ )  $\mu\text{g CL}^{-1}$  to 390 ( $\pm 89$ )  $\mu\text{g CL}^{-1}$  in the control treatment for the period analyzed. Microphytoplankton carbon biomass significantly increased on day 7 in the chronic treatment.

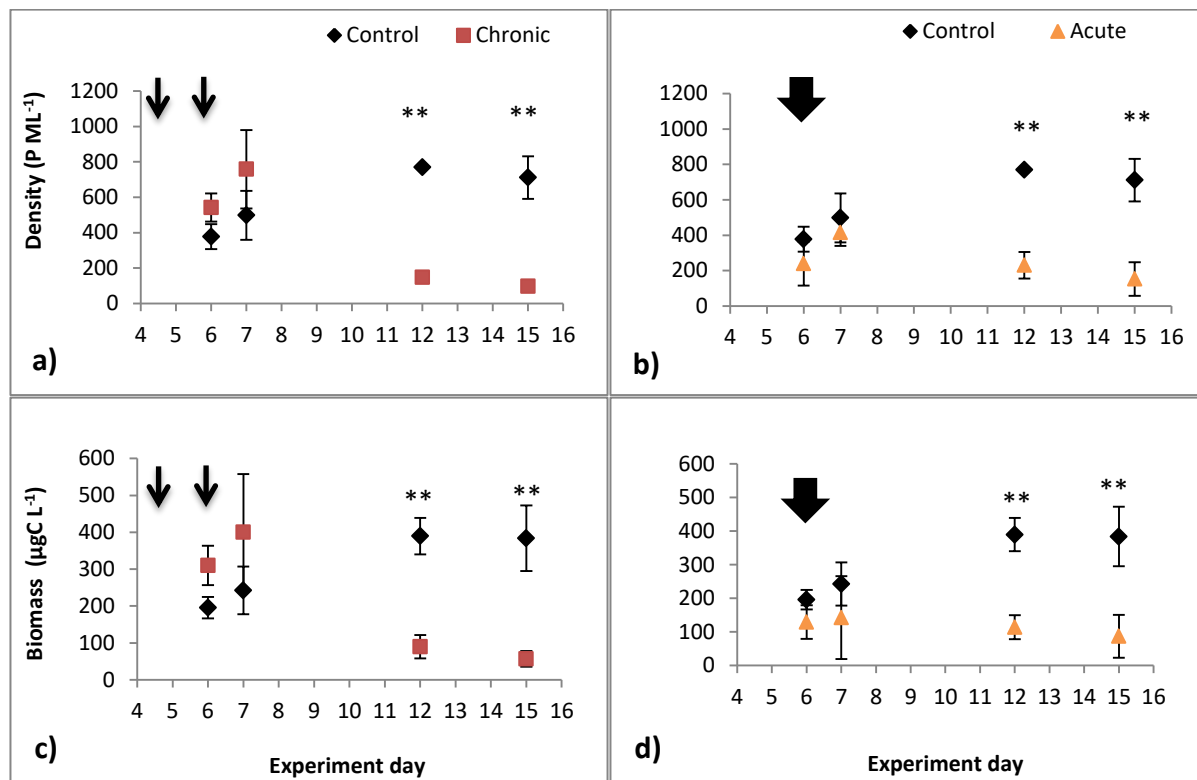


Figure 8: Temporal patterns for mean ( $\pm\text{SD}$ ) microphytoplankton densities (a-b) and carbon biomass (c-d) estimated from the biovolume. \* =  $p < 0.05$  \*\* =  $p < 0.01$ . Vertical bars indicate the standard errors. PML: Particles per mL. Arrows represent diesel inputs

Net carbon accumulation for Microphytoplankton was estimated from day 6 on (Figure 9). Carbon loss was 40% and 58% for chronic and acute treatment respectively, but it is important to note that it is not directly comparable with nano- and picoeukaryotes results because of low number of samples and different intervals of time. ANOVA results for net carbon accumulation showed significant differences between treatments ( $p << 0.01$ , see the Annex 15), with the chronic and acute treatments being significantly lower than the control ( $p < 0.01$ , see the Annex 16). There were no significant differences between both contaminated treatments.

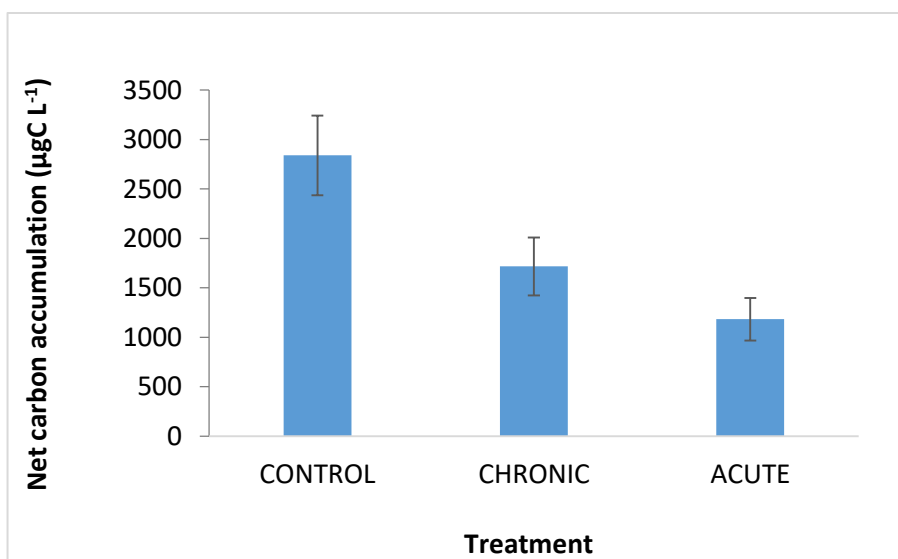


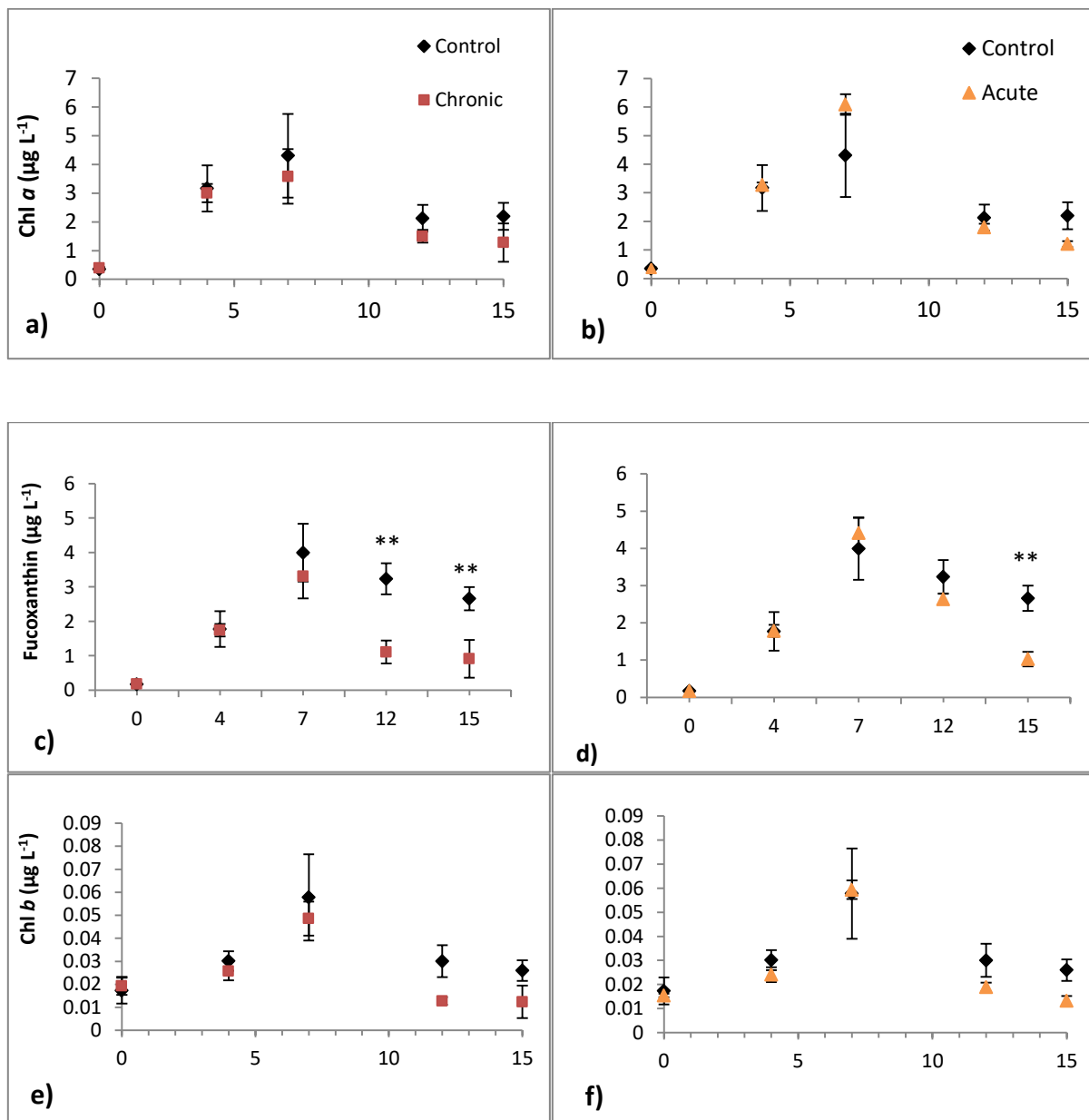
Figure 9: Net carbon accumulation for microphytoplankton estimated from day 6 on for all treatments. Vertical bars indicate the standard errors

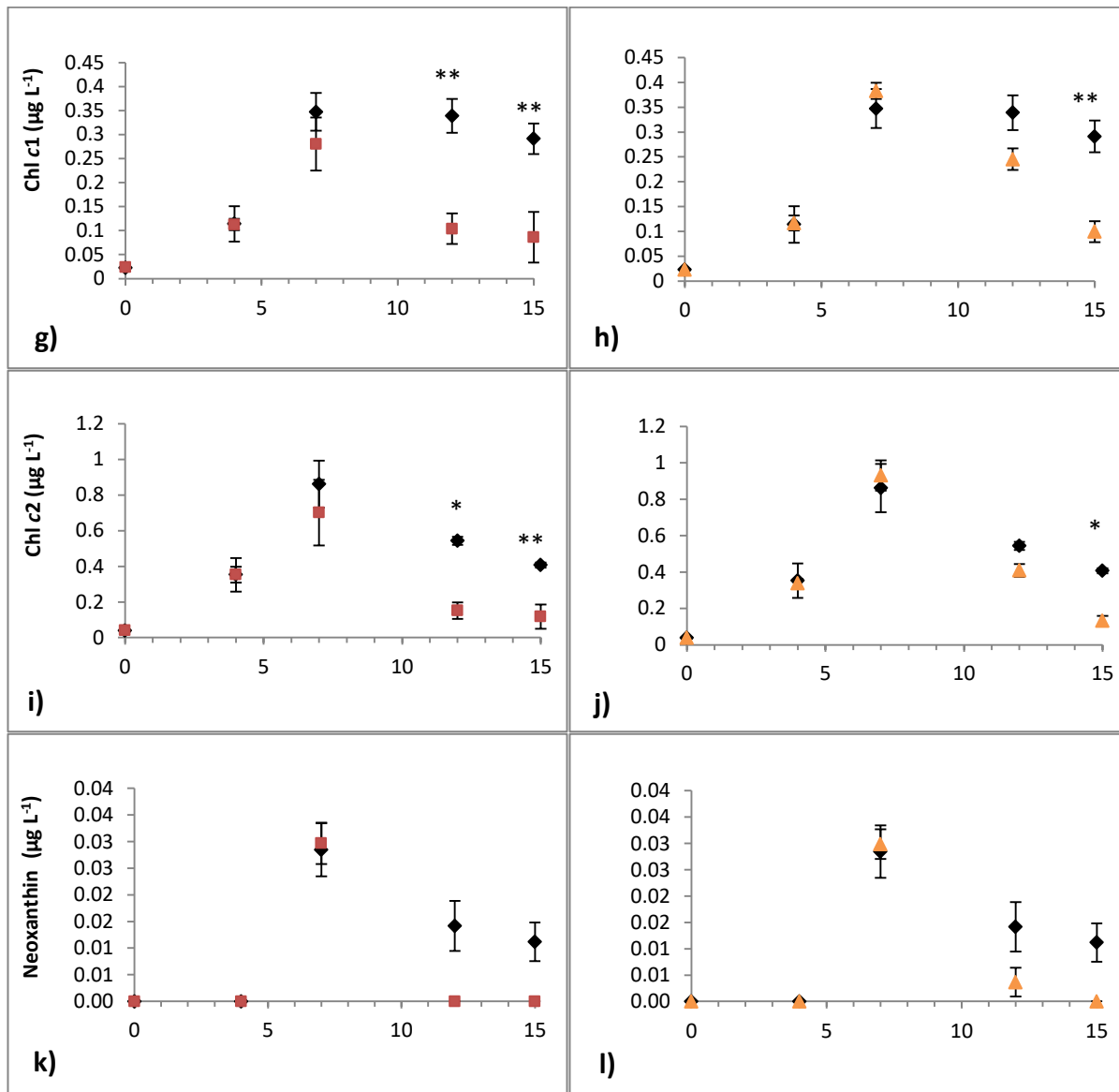
### 1.3.5 Pigments analyses (HPLC)

A total of 25 pigments were identified in the present study, whose concentrations varied during the experiment and between treatments. Fucoxanthin was the most abundant accessory pigment with a maximum concentration of  $3.9 \pm 0.84 \mu\text{g L}^{-1}$  in the control treatment.

Concerning the most important pigments, two trends can be identified: accessory pigments having a trend similar to that of Chl *a* (Chl *b*, Chl *c1*, chl *c2*, MGDVP fucoxanthin, neoxanthin and violaxanthin), with an increase in their concentrations from day 1 to day 7 and a decrease from that day until the end of the experiment (Figure 10), and pigments showing a different trend than Chl *a* (i.e. zeaxanthin, prasinoxanthin and alloxanthin; Figure 11). Alloxanthin was detected on the first day of the experiment (at relative low concentrations: 0.007 µg L<sup>-1</sup>) and then decreased in all treatments. Contrastingly, eeaxanthin had two peaks, the first one day 4, before the maximum of Chl *a* concentration and the other one (and the highest) on the last day of the experiment. Prasinoxanthin reached its maximum concentration on day 12 for all treatments, except for the chronic one.

Moreover, differences between the control and contaminated treatments were identified in the last period, revealing that some phytoplankton groups are sensitive to diesel inputs. Pigments with the same trend as Chl *a* experienced a bigger fall in their concentrations (significant for fucoxanthin, Chl *c1* and *c2* and violaxanthin) in contaminated treatments than in the control. Chl *b* and Alloxanthin seemed to follow the same trend, but their concentrations were probably too low to show significant differences. Prasinoxanthin concentrations were significantly reduced in the last period in the contaminated treatments. On the other hand, zeaxanthin concentrations were stimulated by diesel inputs. Results of RM ANOVA showed an interactive effect of time and treatment in the concentrations of several pigments, namely fucoxanthin, Chl *c1*, Chl *c2*, neoxanthin, prasinoxanthin and zeaxanthin for both, chronic and acute treatments. For violaxanthin, the interaction was significant only in the chronic treatment (see the Annex 17-26).





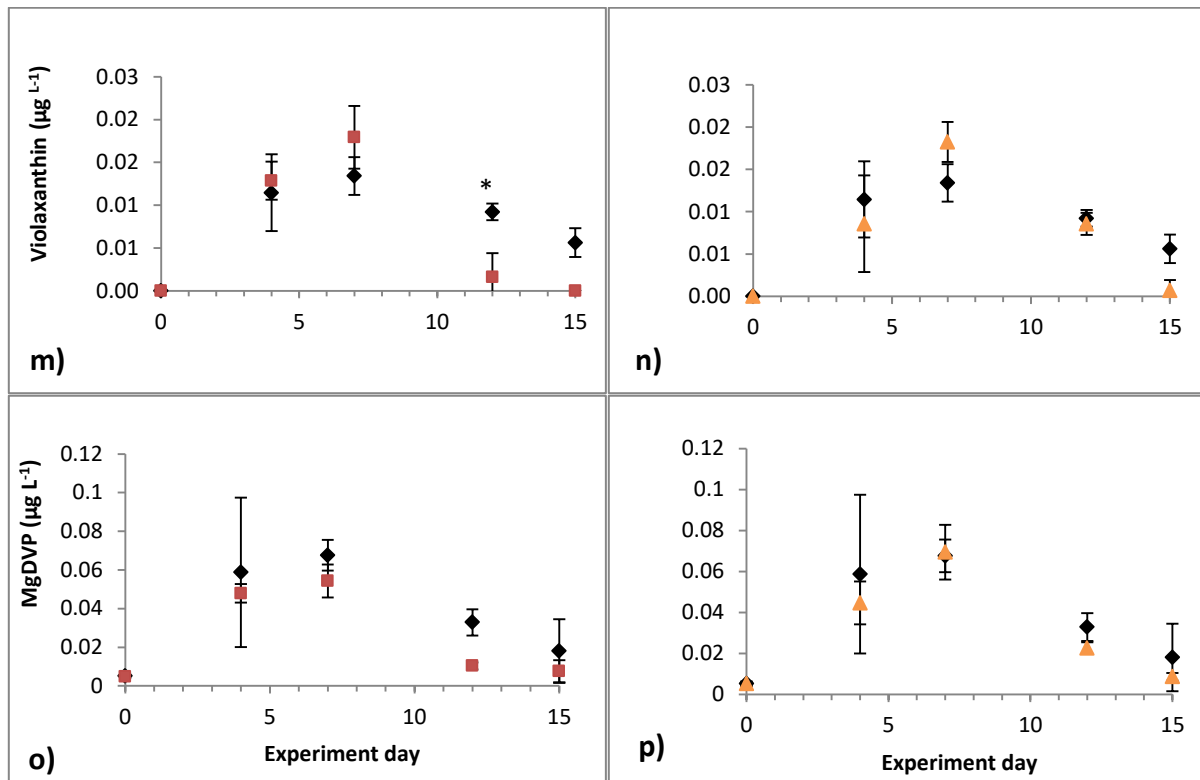


Figure 10: Temporal patterns for average ( $\pm\text{SD}$ ) Chl *a* (a-b) and accessory pigment concentrations ( $\mu\text{g L}^{-1}$ ) with similar trends than Chl *a*: c-d) fucoxanthin, e-f) Chl *b*, g-h) Chl *c1*, i-j) Chl *c2*, k-l) neoxanthin, m-n) violaxanthin, o-p) MgDVP \* =  $p < 0.05$  \*\* =  $p < 0.01$ . Vertical bars indicate the standard errors

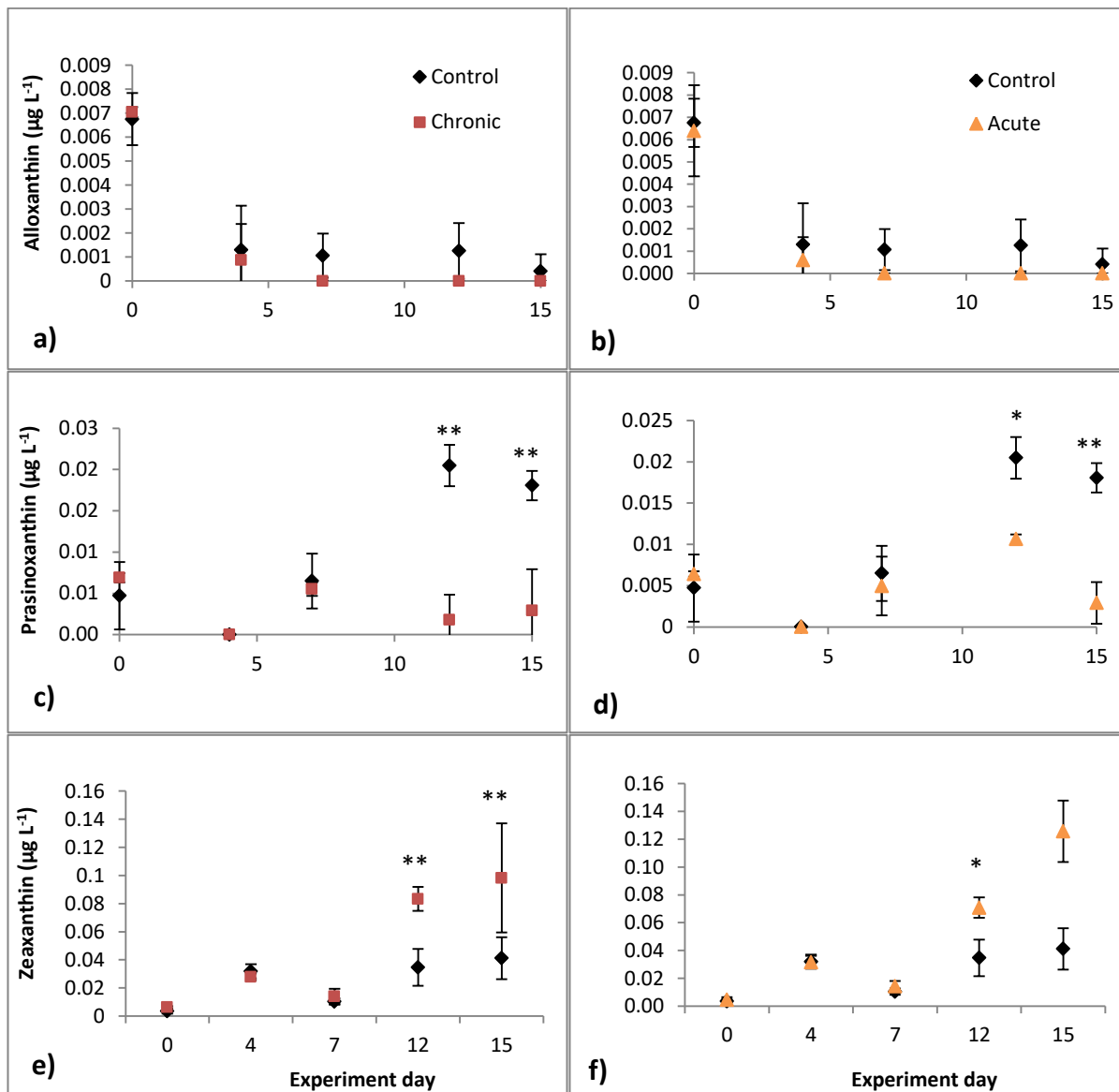


Figure 11: Temporal patterns for average ( $\pm\text{SD}$ ) accessory pigment concentrations ( $\mu\text{g L}^{-1}$ ) with a different trends than those of Chl  $a$ : a-b) alloxanthin, c-d) prasinoxanthin, e-f) zeaxanthin \* =  $p < 0.05$  \*\* =  $p < 0.01$ . Vertical bars indicate the standard errors.

### 1.3.6 Light microscopy (LM)

Microscopic identification confirmed the dominance of diatoms in terms of density and biomass during the study, with *Skeletonema costatum* as the most important species, but also the presence of some dinoflagellates (*Alexandrium tamarensis*, *Protoperidinium* sp., *Gymnodinium* sp., *Gyrodinium* sp.), Euglenophyceae (*Eutreptia* sp.), Prasinophyceae (*Tetraselmis* sp.), Cryptophyceae, Prymnesiophyceae and nanoflagellates of different sizes (with a diameter lower than 5 µm or between 5 µm and 10 µm) and small numbers of mixotrophic organisms (*Chrysochromulina* sp., Choanoflagellates, etc.).

The densities of total phytoplankton were generally  $\sim 10^3$  cells mL<sup>-1</sup> during the period and treatments analyzed (Figure 12). In the control treatment, maximum cell density was  $4.5 \times 10^3$  cells mL<sup>-1</sup> on day 12. The diatom bloom had started some days earlier. Nanoflagellates densities increased from this moment up to the end of the experiment.

Cell densities declined because of diesel inputs in both contaminated treatments. This effect was detected earlier in the chronic than in the acute one (from day 7), probably related to the first diesel input on day 3 in the chronic treatment. However, at the end of the experiment, cell densities were lower in the acute treatment than in the chronic one.

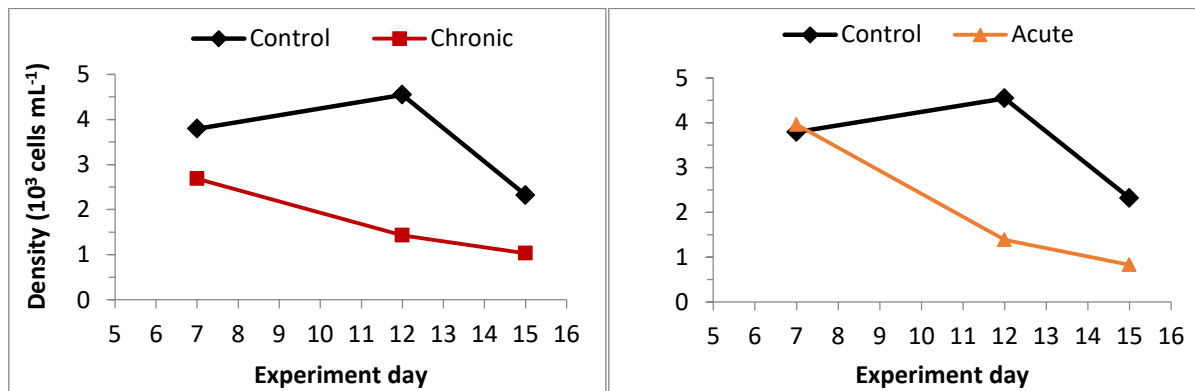


Figure 12: Total densities of phytoplankton determined by microscopic analyses during the experiment

The contribution of different algal groups to total phytoplankton is shown in Figure 13. It is important to highlight the shift in the phytoplankton assemblage's structure, with diatoms densities decreasing and nanoflagellates densities increasing at the end of the experiment in all treatments. However, this trend was more evident in the contaminated treatments and it was detected earlier than in the control, especially in the chronic treatment.

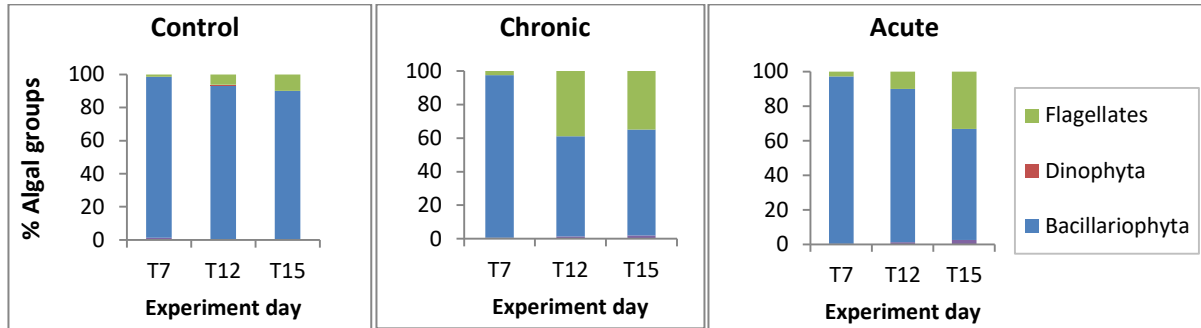


Figure 13: Percentage of the main phytoplankton groups in the control and contaminated treatments

The density contribution of different Bacillariophyta species is depicted in Figure 14 revealing the dominance of centric diatoms. *S. costatum*, *Chaetoceros* spp. (*C. decipiens*, *C. C. gelidus*, *C. debilis*), *Attheya septentrionalis* and different species included in the groups Centric spp. < 10 µm and Centric spp. 10 µm – 20 µm as *Thalassiora* spp., *Leptocylindrus* sp., and *Melosira* like species, were the most important taxa in terms of their contribution. There were some differences in diatoms composition between contaminated treatments and the control from day 12, especially concerning the dominant species. In general, *S. costatum* seemed to be replaced by *A. septentrionalis*, Centric spp. < 10 µm, Centric spp. 10-20 µm and Pennates (*Licmophora* spp, *Nitzschia* spp., *Pseudo-nitzschia* spp., *Cylindroteca closterium*, *Navicula* spp. *Fragilariopsis cylindrus* like).

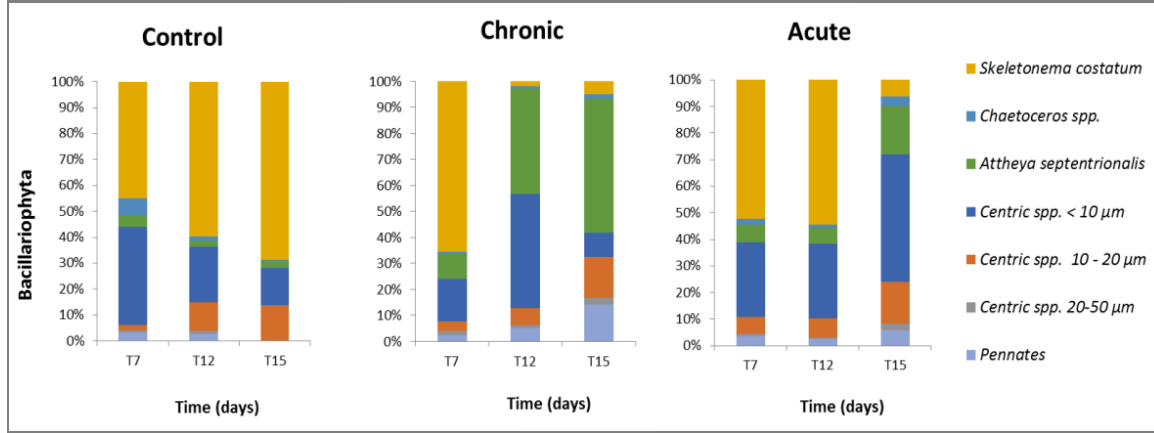


Figure 14: Percentage of different species for Bacillariophyta in control and contaminated treatments

*S. costatum* was the dominant species reaching maximum densities of  $10^3$  cells  $\text{mL}^{-1}$ , accounting for more than 50% of total phytoplankton in the control during the period analyzed. However, its densities largely declined (between one and two orders of magnitude) after day 7 in the treatments contaminated with diesel. This species was generally observed forming long chains of up to eleven cells (usually five cells). The number of cells per chain was also notably reduced on day 12 in the contaminated treatments (especially in chronic one) and in all treatments on the last days of the experiment. The formation of aggregations of *S. costatum* cells was also observed during the last period (days 12 to 15) for all treatments, but these aggregates were more frequent and detected earlier in the contaminated treatments, especially in chronic one (Figure 15).

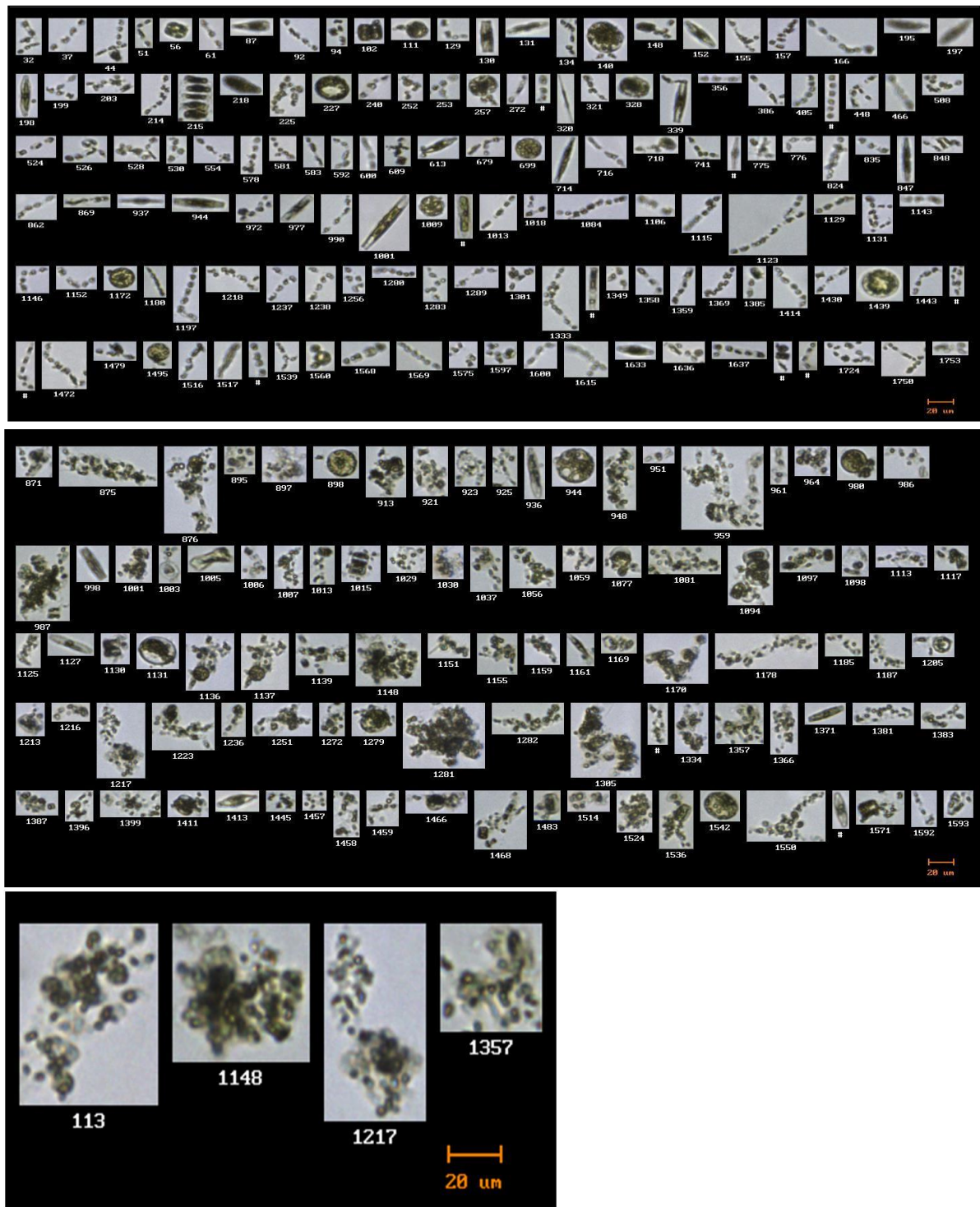


Figure 15: FlowCAM images showing *S. costatum* cells mostly forming chains in the control (upper) and aggregated in the chronic treatment (middle) on day 12. Detail of aggregations (lower)

It is important to highlight that most of the species identified by microscopy had a cell diameter <20 µm, with only some dinoflagellates, and pennate and centric diatoms having a larger size. This suggests that an important fraction of the cells analyzed by microscopy corresponded to the nanophytoplankton size class observed by flow cytometry, especially those corresponding to the nanoeukaryotes group. This is true for the density, but regarding biomass, it seems to be equivalent when comparing nano (Figure 6, a-b) with microphytoplankton (Figures 7, c-d). In addition, a visual inspection of FlowCAM images revealed that most of the particles in the 20 to 500 µm range were chains of the diatoms *S. costatum*, *Chaetoceros* spp. and *Thalassiosira* spp. However, it is important to note that Flow Cytometry and FlowCAM methods count particles and take in account their spherical diameter (ESD) not being able to quantify cells within a chain, in contrast to microscopy counts. For this reason, we suggest that nanoeukaryotes identified by Flow cytometry probably includes most of the species detected by microscopy, mainly all the chains of *S. costatum*, *Chaetoceros* spp. and other chain forming diatoms, individually having a diameter (ESD) <20 µm. For example, *S. costatum* would be present forming chains of around five cells if we consider its average cell diameter of 5 µm, while longer chains belong to the micro-phytoplankton fraction identified by FlowCAM image analysis.

### **1.3.7 Flow cytometry (FCM) versus - HPLC results**

A comparison between flow cytometry and HPLC results is shown below. Significant, positive correlations were found between Chl *a* concentration and the density of total phytoplankton <20 µm ( $p < 0.001$ ,  $r=0.68$ ,  $n=19$ ) as well as between Chl *b* concentration and pico-eukaryotes' density ( $p \leq 0.001$ ,  $r=0.76$ ,  $n=19$ ). In both cases, the best fit between the dependent and the independent variables followed a linear relationship ( $r^2$  of 0.47 and 0.57 for Chl *a* and Chl *b* concentrations vs density, respectively) (Figure 16).

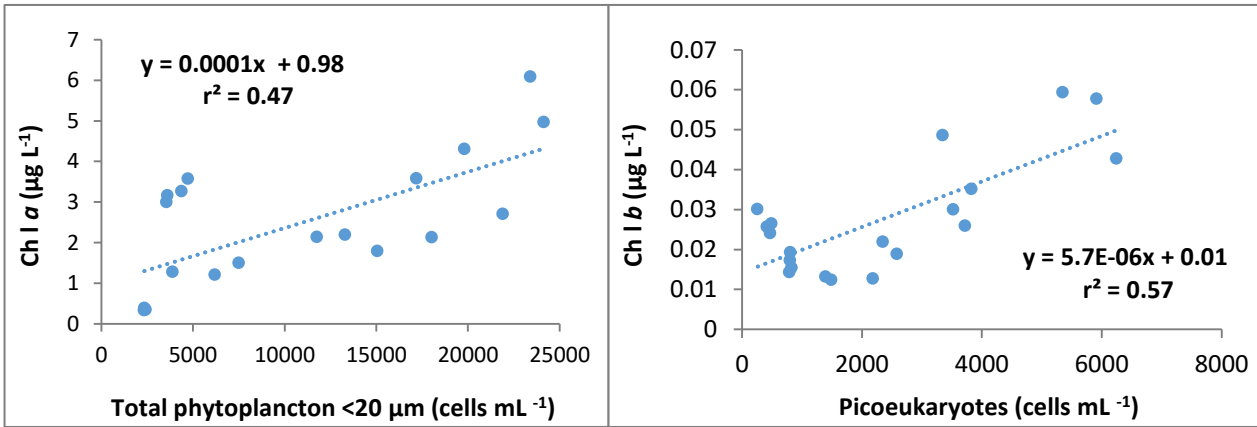


Figure 16: Simple linear regression between total phytoplankton <20 µm density (cells mL⁻¹) and Chl *a* concentration obtained by HPLC (left) and between Picoeukaryotes density (cells mL⁻¹) and Chl *b* concentration (right).

Fucoxanthin concentration was significantly and positively correlated to the density of nano-eukaryotes ( $r=0.94$ ,  $p <<< 0.0001$ ,  $n=19$ ), showing a significant fit for the simple linear regression model ( $y = 0.0002x + 0.41$ ;  $r^2 = 0.88$ ) (Figure 17).

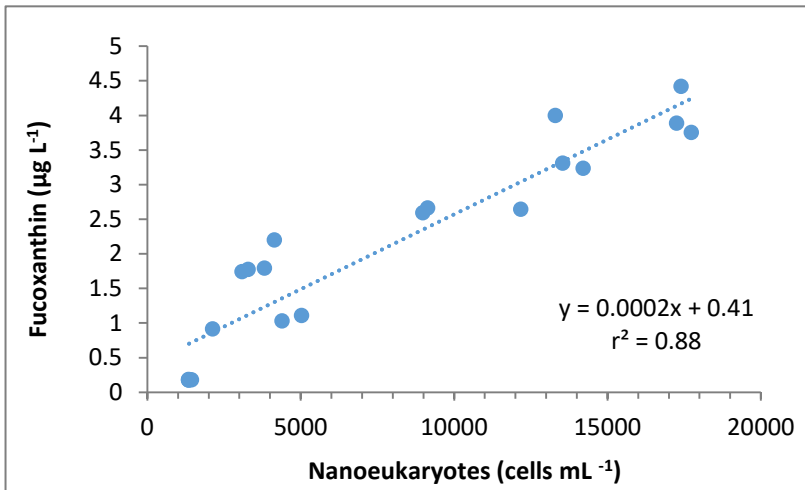


Figure 17: Simple linear regression between nanoeukaryotes density (cells mL⁻¹) and fucoxanthin concentration (µg L⁻¹)

Zeaxanthin concentration was significantly correlated with density of pico- and nanocyanobacteria containing PC ( $r=0.72$ ,  $p << 0.0001$  and  $r=0.58$ ,  $p <<< 0.0001$  respectively). Unexpectedly, zeaxanthin concentration was negatively correlated with

cyanobacteria containing PE ( $r=-0.53$ ,  $p << 0.0001$ ) and not correlated with pico-PE-cyanobacteria. On the other hand, zeaxanthin and Chl *b* ( $R=-0.46$ ,  $p = 0.04$ ) were not significantly correlated. In turn, alloxanthin concentration varied according to the density of nanocyanobacteria containing PE ( $R=0.93$ ,  $p < 0.0001$ ).

### 1.3.8 Physiological status of phytoplankton - Fluorescence Induction

Values of the photochemical quantum yield of PSII, expressed as the  $F_v/F_m$  ratio, were relatively stable in the control, varying between  $0.32 \pm 0.03$  on day 13 and  $0.39 \pm 0.04$  on day 7 during the bloom. This photosynthetic parameter did not show a clear response to diesel addition during the pre-bloom and bloom periods, even if punctual differences with respect to the control were observed in certain days in the contaminated treatments (days 2 and 5 for chronic and acute treatments, respectively). However, after day 10  $F_v/F_m$  values decreased (sometimes significantly) in the contaminated treatments (Figure 18). Results of RM ANOVA showed an interactive effect of time and treatment on photosynthetic efficiency of PSII assessed by the  $F_v/F_m$  parameter ( $p < 0.01$ , see the Annex 27) for both, the chronic and acute contaminated treatments.

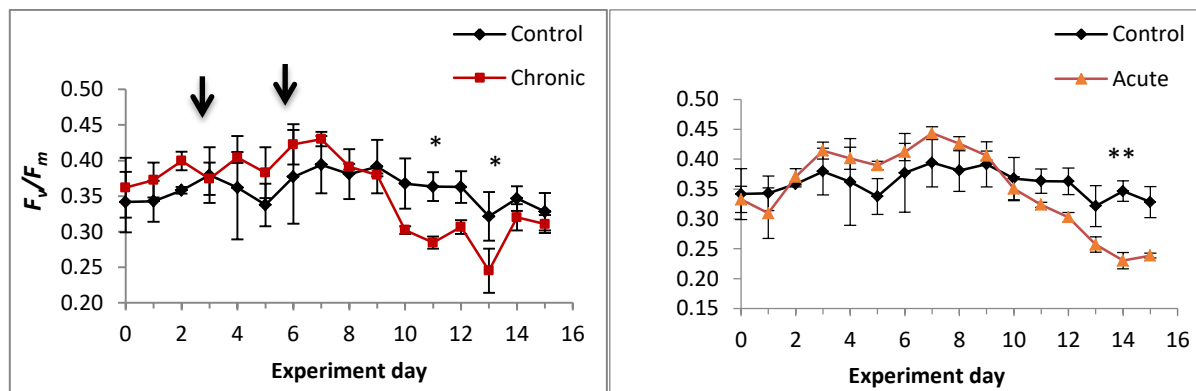


Figure 18: Temporal changes (mean  $\pm$ SD) in photochemical quantum yield of PSII ( $F_v/F_m = (F_m - F_0)/F_m$ ) as measured by FRRF during the experiment. \* =  $p < 0.05$  \*\* =  $p < 0.01$ . Vertical bars indicate the standard errors. Arrows represent diesel inputs. The control treatment is also shown in each figure.

## 1.4 DISCUSSION

The present study provides new insights on the functional and structural responses of natural phytoplankton assemblages in a low oil pollution scenario. Maritime diesel, the form of oil used in the present study, had significant effects on the cold temperate/subpolar, phytoplankton assemblages of the LSLE. So far, the impacts of diesel have been understudied, comparatively to the effects of other kinds of oil, even if it is actually one of the most extensively used petroleum hydrocarbons and a key pollutant on water surface through leaks and accidental spills (Ramadass et al. 2017). Since both globally and in the studied area, there is a growing trend towards an increase in marine transport and diesel is the principal carburant used by ships, the results of the present study contribute to the understanding of the potential risk of diesel spills for pelagic food webs in this environment.

Diesel concentrations such as those used in the present study can be encountered in the immediate vicinity of oil spills and in chronically polluted coastal waters from the Marina of Rimouski (Dal Santo Vidal, in prep) and in others places (Prouse et al. 1976, Nayar et al. 2005, Brussaard et al. 2016). They are lower in comparison with those reported from highly impacted coastal ecosystems in other parts of the world such as Boston (Ahmed et al. 1974) and Halifax Harbour (Michalick & Gordon 1971), coastal waters of Malaysia (Abdullah 1995), Saudi Arabia and Qatar (El-Samara et al. 1986). Considering diesel slicks covering a surface of 1 km<sup>2</sup> before dissipating from the surface, the thickness of the layer simulated in the present study would represent a volume between 6000 and 13000 L of diesel spilled. This volume is between 8 to 16 times lower than some diesel spills that occurred recently in Canadian waters. Therefore, diesel concentrations used in this experiment reasonably reflect chronic exposures of phytoplankton to diesel in LSLE waters.

### 1.4.1 Chlorophyll *a* and nutrients' concentrations

Three different periods of the plankton ecological succession were distinguished in the control mesocosms: i) the pre-bloom (days 0-3), with relatively low Chl *a* and high nutrient

concentrations; (ii) the bloom (days 4-7), with relatively high Chl *a* and a sharp decrease in nutrient concentrations; and (iii) the post-bloom (days 8-15), with relatively low Chl *a* and low or exhausted nutrient concentrations. Previous studies showed that nutrients are generally not limiting in this environment (Levasseur et al. 1984) but during our experiment, nitrate + nitrite were depleted faster than silicate and phosphate, meaning that nitrogen was probably the limiting nutrient. Nitrate + nitrite and silicate were exhausted after days 6 and 9 of the experiment, respectively, being rapidly consumed by phytoplankton during the exponential growth phase, mainly by diatoms. Daily Chl *a* concentrations from this study ( $0.52 \pm 0.02$  to  $9.46 \pm 1.42 \mu\text{g L}^{-1}$ ) were within the ranges of *in situ* values published for the LSLE (Roy et al. 1996) for the May - September period, as well as in a mesocosm experiment (Lionard et al. 2012) performed in August. In both cases, maximum values corresponded to a diatom bloom events, consistent with our results.

Diesel addition resulted in a decline in Chl *a* concentration (significant for the chronic treatment) in both pollution scenarios in the last, post-bloom period. A similar trend has been reported for phytoplankton exposed to hydrocarbon *in situ* (Sheng et al. 2011) in the month following the Montara oil spill in the Northwest Shelf of Australia and in microcosms experiments using low or sub-lethal concentrations of different kinds of oil (Sargian et al. 2007, Gilde & Pinckney 2012). Decrease in Chl *a* concentration has also been reported in a mesocosms experiment with St. Lawrence Estuary waters at the end of the winter, but in this case the authors used dispersed and adsorbed crude oil in concentrations expected after a massive oil spill (Siron et al. 1996). The results of the present study revealed that refined oil (i.e. diesel) could also be highly toxic for phytoplankton assemblages, causing Chl *a* concentrations to decline, even at low pollution levels.

Decline in Chl *a* concentration may be due to inhibition of growth, cell mortality or a combination of both. Hing et al. (2011) suggested that diesel affected phytoplankton by preventing growth rather than inducing mortality. However, other studies contradicted this finding, detecting a higher cell mortality (El-Dib et al. 2001) or decreases in cell density after the addition of hydrocarbons (Adekunle et al. 2010, Echeveste et al. 2010b, Tas et al. 2011). In

the present study, density of all phytoplankton groups (pico-, nano- and microphytoplankton) decreased in contaminated treatments and mortality by grazing was not detected (Olmedo Masat, in prep.). Furthermore, an additional dilution experiment (Olmedo Masat, in prep.) carried out simultaneously with ours showed that pico- and nanophytoplankton growth rates were affected by diesel addition. It is therefore likely that both cell death and growth diminution in some functional groups, contributed to a significant decrease in Chl *a* concentration in contaminated treatments during the last period.

#### **1.4.2 Pico-, nano- and microphytoplankton density and phytoplankton carbon estimations**

Total phytoplankton <20 µm was mainly composed by nano- and pico-eukaryotes, which followed a similar trend to that of Chl *a* in the control. Although much less abundant or absent in many samples, and nano- and picocyanobacteria followed this same trend. Microphytoplankton was composed by some few dinoflagellates, pennate and long chains of the centric diatom (*S. costatum*, *Chaetoceros* spp. and *Thalassiosira* spp.) whose densities increased in the control in the last days of the experiment. However, mesocosms' assemblages were characterized by the numerical dominance of small sized species, corresponding mainly to the nanophytoplankton fraction, which agrees with the natural community described in previous studies in this area (Levasseur et al. 1984, Roy et al. 1996).

Brussaard et al. (2016) reported total phytoplankton abundance of the North Sea decreasing by 50% after a crude oil spill simulated in mesocosms. Phytoplankton (with Chrysophyceae, Prasinophyceae and Prymnesiophyceae as the dominant algal groups) disappeared almost completely within the next few days, mainly as a result of decrease in various groups of eukaryotic phytoplankton, such as reported in the present study. Diesel addition resulted in a decline in density of nanoeukaryotes, picoeukaryotes and microphytoplankton cells in both scenarios of diesel pollution in the last days of our experiment. Some cyanobacteria groups also responded significantly to diesel addition, being

either affected (Pico-PE-cyanobacteria) or stimulated (Nano-PC-cyanobacteria) in the contaminated treatments during the last days which is coincident with previous studies using other kinds of oil or different methodological approaches (Palmer 1969, Gaur and Kumar 1985, Nayar et al. 2005, Gilde & Pinckney 2012, Brussaard et al. 2016).

Decline in phytoplankton density in almost all functional groups also meant a substantial loss of phytoplankton biomass (estimated as carbon biomass) in contaminated treatments, comparatively to the control. Carbon loss in nano and picoeukaryotes as well as in micro phytoplankton was 47%, 61% and 40% respectively for chronic and 14%, 56% and 58% respectively for the acute treatment. ANOVA results for net carbon accumulation estimated from day 10 on demonstrated that carbon biomass of picoeukaryotes was significantly reduced in both pollution scenarios while carbon biomass of nanoeukaryotes was only significantly affected by the chronic exposure. Even if we cannot directly compare microphytoplankton net carbon accumulation with that of the other functional groups because of the lower number of samples and time of analyses, carbon biomass in microphytoplankton was also significantly reduced in both pollution scenarios. Since microzooplankton showed very low densities and no significant control of the biomass by grazing was confirmed during the same experiment (Olmedo Masat, in prep.), this important loss in carbon biomass in all phytoplankton size categories can be interpreted as a direct negative impact of diesel addition in the water column.

González et al. (2009) analyzed WSF effects (naphthalene and its alkylated derivates basically) on the carbon biomass of oceanic and coastal marine phytoplankton assemblages in microcosm experiments. In their work, biomass of nanoflagellates, the most important group in the nanophytoplankton, showed an initial decrease between the first and the 3<sup>rd</sup> day, consistent with our results but contrasting with our results, it recovered at the end of their experiment (5<sup>th</sup> day). On the other hand, oceanic picophytoplankton biomass was drastically reduced in the three analysed compartments (picoeukaryotes, *Prochlorococcus* and *Synechococcus*). It was especially severe for the cyanobacteria, which were the most abundant group. This is similar to our observations, except in that pico-eukaryotes were the most abundant functional group in the mesocosms. Diatoms, which were the most important

microphytoplankton component during their experiment, were negatively affected by HCs, consistent with our results. However small diatoms (<20 mm) were apparently stimulated by HCs, contrasting with our observations. These authors explained differences in diatoms responses by indirect trophic interactions resulting in the release of predation on smaller species or different sensitivities of species to PAHs. This differs largely with our results, since grazing did not seem to be a control factor of phytoplankton grown in our experiment. Therefore, the present study shows mostly direct effects of HCs on phytoplankton.

Phytoplankton carbon loss in all functional groups found in this study suggests a significant impact in terms of carbon fluxes mediated by phytoplankton. We showed that relatively low refined hydrocarbons (i.e. diesel) may significantly affect the fate of the carbon incorporated via photosynthesis, consequently reducing the capacity of the oceanic biological pump (Agustí et al. 1998, Kirchman 1999). Moreover, different size groups of grazers in the micro- and mesozooplankton, such as small heterotrophic nanoflagellates and ciliates (Reckermann 1997, Raven 1998, Raven et al. 2005), medium protozoa (5 to 10  $\mu\text{m}$ ) (Samuelsson & Andersson 2003), dinoflagellates, micro-sized (20-200  $\mu\text{m}$ ) and copepods (Perissinotto 1992) could be directly impacted by this differential loss in phytoplankton carbon biomass. On average, microzooplankton and mesozooplankton consume 67% and 23%, respectively, of daily primary production in surface oceans (Calbet 2001) and therefore a total 90% of the daily primary production can be consumed by herbivores in the ocean. Consequently, both phytoplankton composition changes and carbon loss can severely affect carbon transfer within the marine food web, as well as export via the biological pump.

Our results show that nutrient uptake and assimilation processes were uncoupled, since nitrate + nitrite deficiency after the 5<sup>th</sup> experimental day did not prevent phytoplankton biomass (Chl *a* - carbon) increase under uncontaminated conditions. It has been shown that some phytoplankton groups, especially diatoms, have evolved to adapt to periods of nutrient limitation by a fast uptake down to depletion in the first days of blooms development (—luxury uptake) (Vincent 1981, White et al. 1986), with internal assimilation afterwards when the ambient pool became depleted. Ability of N-deficient cells to take up and store

nitrogen far in excess of current growth requirements have been proven for several diatom species (Lalli & Parsons 1997, Vincent 1981). Luxury uptake could be responsible for 8-16 times the minimum quota needed by phytoplankton, theoretically sustaining 3-4 cells doublings after exhaustion of one limiting nutrient (Reynolds 2006).

In the contaminated treatments, effects of diesel on carbon biomass were observed at least 4 days after nitrate + nitrite drop. In this case, luxury assimilation could have been the reason for no significant biomass responses after nitrogen depletion. However, putting together these results with our photochemical observations, the results suggest that under damage conditions of the photosynthetic apparatus (from day 10 on), nitrogen was less efficiently used in the metabolic processes of biomass synthesis, resulting in the observed biomass decay under both pollution scenarios.

#### **1.4.3 Pigments (HPLC) - Light microscopy (LM)**

Some pigments here identified (e.g., fucoxanthin, alloxanthin, zeaxanthin, chlorophyll *b* and 19'-butanoyloxy-fucoxanthin) are considered diagnostic pigments for specific phytoplankton groups (notably diatoms, cryptophytes, cyanobacteria, chlorophytes and pelagophytes, respectively) (Roy et al. 2011). Moreover, diatoxanthin and diadinoxanthin are photo protective pigments generally found in diatoms and dinoflagellates, whereas prasinoxanthin, lutein, violaxanthin, and neoxanthin are found in prasinophyceae and chlorophyceae. Fucoxanthin was the most abundant marker pigment confirming the diatom dominance. However, it can also be attributed to the presence of other phytoplankton groups such as haptophyceae, crysophyceae and dinoflagellates (Bidigare 1989, Bidigare et al. 1990, Jeffrey & Wright 1994, Roy et al. 2011). Some marker pigments such as Chl *b*, Chl *c1* chl *c2*, MGDVP, fucoxanthin, neoxanthin and violaxanthin followed a similar trend than Chl *a*, while others such as alloxanthin or zeaxanthin and prasinoxanthin had higher concentrations at the beginning or in the last days of the experiment, respectively. Taking into account these differences in markers pigments trends, phytoplankton succession could be described by the presence of cryptophyceae at the beginning, followed by an important abundance of diatoms in

the bloom period but also the presence of prymnesiophyceae, dinoflagellates and green algae and finally, in the post-bloom, prasinophyceae and cyanobacteria as the most abundant groups.

Most of the taxonomic pigments detected in the present study have been previously reported for this area (Roy et al. 1996, Lionard et al. 2012). However, peridinin and HFU (19'-hexanoyloxy-fucoxanthin), were not detected in this study, which are marker pigments for dinoflagellates and haptophytes, respectively (Roy et al. 2011). Most of dinoflagellates genera identified in the present study, namely *Gymnodinium*, *Gyrodinium* and *Peridinium* have been recognized to have fucoxanthin derivatives in place of peridinin (Jeffrey et al. 1975, Bjørnland & Tangen 1979, Tangen & Bjørnland 1981, Johnsen & Sakshaug 1993, Millie et al. 1995). This could explain why no peridinin was detected. It is also important to note that dinoflagellates were rare in the mesocosms, being only detected in microscopic qualitative analyses and certain FlowCAM images. HFU has been sporadically detected at very low concentrations between May to September (Roy et al. 1996) which means a longer time of analyses and more probabilities to detect the pigment in comparison with us.

Roy et al. (1996) described the phytoplankton temporal succession in the LSLE, where diatoms and flagellates dominated, with a major centric diatom bloom event in July, which agrees with our results. Moreover, the general pattern reported for this area (Sinclair 1978, Levasseur et al. 1984, Roy et al. 1996) and for the northern temperate coastal waters (Smayda 1980) shows Chrysophyceae and Cryptophyceae dominating in May, pennate diatoms and unidentified flagellates in June, centric diatoms in July and, at much lower abundances Prymnesiophyceae, Chrysophyceae, Clorophyceae and Cryptophyceae in September. Many of these taxonomic groups have also been detected in the present study and phytoplankton succession in our treatment control reasonably mimics the succession in the field.

Diesel inputs affected significantly most of the marker pigments concentrations in the contaminated treatments in comparison with the control. Fucoxanthin, Chl *c1*, Chl *c2*, violaxanthin and prasinoxanthin concentration were significantly reduced in the last days. Therefore, we suggest that mainly diatoms, but also dinoflagellates, prymnesiophyceae and

prasinophytes were sensitive to diesel in both pollution scenarios. Green algae and cryptophyceae seemed to be also affected, but concentrations of their specific marker pigments, Chl *b* and alloxanthin, were too low to obtain significant results. In addition, the significant correlation of Chl *b* and picoeukaryotes suggest the prevalence of green algae for this FCM identified group. Since picoeukaryotes densities and carbon biomass were significantly reduced by diesel addition and green algae were a main component for this FCM group, we could also suggest some sensitivity of green algae to diesel in the present study.

On the contrary, zeaxanthin was the only marker pigment being stimulated by diesel addition in the last days in both pollution scenarios. Significant correlation of zeaxanthin and PC-cyanobacteria (pico- and nano-) revealed its provenance from these two FCM groups. Therefore, we could confirm cyanobacteria containing PC as the only group favored by diesel addition. However, since zeaxanthin is also a minor pigment in green algae (Roy et al. 2011), we tested its relationship with Chl *b*, but they were not significantly correlated, confirming that zeaxanthin probably did not come from green algal groups, which are characterized by the presence of Chl *b*. The PE containing nanocyanobacteria group was highly correlated with alloxanthin (pigment of cryptophytes). Therefore, we suggest that this FCM group could also have been PE containing cryptophytes, since this group can also contain PE (Kirk 1994). Then, we propose to rename this FCM group as nano-PE-cryptophytes.

Microscopic identification confirmed both density and biomass dominance of diatoms during the present study with centric diatoms such as *S. costatum*, *Chaetoceros* spp. (*C. decipiens*, *C. gelidus*, *C. debilis*), *A. septentrionalis*, *Thalassiora* spp., *Leptocilindrus* sp. as the most important taxa in terms of their contribution to total phytoplankton in the control. Their densities were sensibly reduced in the last days by effect of diesel additions in both pollution scenarios, notably in the chronic one. Diatom sensitivity has been previously reported in microcosm experiments using oil WSF (Sargian et al. 2007) and in an *in situ* mesocosm experiment in a tropical estuary (Nayar et al. 2005) using diesel fuel. Siron et al. (1996) showed a high susceptibility of diatoms of the St. Lawrence Estuary to dissolved hydrocarbons from crude oil in which naphthalene and its alkylated analogues were the major toxic

compounds. Sargian et al. (2007) explained that porous silica structure is a good absorbent of hydrocarbons, and that frustules of diatoms absorb and retain these compounds, facilitating subsequent toxicity. This expresses as a reduction in the expression of genes for photosynthetic pigments, as well as for some silica-associated proteins necessary for cell division (Bopp & Lettieri 2007). This could also be the reason for the significant decline in fucoxanthin and the principal photosynthetic pigments detected in the contaminated treatments in this study. Nevertheless, results on the effects of oil on diatoms are sometimes contradictory. Diatoms have also been recognized as more resistant than other phytoplankton in microcosm's studies on estuarine phytoplankton using crude oil (Gilde & Pinckney 2012) and on natural costal assemblages using WSF (González et al. 2009). This has been ascribed to their lower surface-to-volume ratio (Echeveste et al. 2010a). The absence of a consistent response of diatoms to HCs in different studies may indicate not only species-specific responses to different types of oil and concentrations assessed but also differences in the experimental approaches adopted which make it difficult to draw general conclusions about diatoms as a single group.

In this study, the chain forming diatom *S. costatum* showed a high sensitivity to diesel in terms of biomass and density, which is consistent with previous results from both, cold-temperate waters of St. Lawrence (Siron et al. 1996) and the Norwegian polar coastal waters, in mesocosms (Dahl et al. 1983), as well as in microcosm experiments (Østgaard et al. 1984), considering several types of oil. However, this phytoplankton species has also been found to be oil tolerant in a more temperate area, the Narragansett Bay (Vargo et al. 1982) and in laboratory cultures (Dunstan et al. 1975). The oil sensitivity of this ubiquitous diatom seems to be greatly influenced by the origin of the population and/or by seasonal (climatic) factors such as seawater temperature, light cycle and nutrients (Siron et al. 1996). In addition, results could vary depending on the type of oil and the experimental approach used. Since *S. costatum* has been recognized as a major component of the natural community in waters from the St. Lawrence Estuary (Sinclair 1978, Levasseur et al. 1984, Siron et al. 1996), the present results suggest that this species could be used as a bioindicator species of water quality in monitoring programs assessing the oil pollution in this area.

The formation of aggregations of *S. costatum* cells as well as the reduction in cell numbers per chain, such as observed in the present study, have been previously associated with nutrient-limiting conditions (Takabayashi et al. 2006) and interpreted as characteristics of the termination of blooms. Since aggregates were more frequent and detected earlier in our contaminated treatments than in the control, we suggest the existence of a synergistic effect of nutrient limitation and diesel. This is consistent with Karidys (1981), who reported that nutrient deficiencies as being lethal in combination with crude oil for this species. In addition, Granum et al. (2002) suggested the release of extracellular products in *S. costatum* (“unhealthy”) cells exposed to various physical or biological stress factors. These extracellular products could also contribute to aggregation.

Concerning other taxonomic groups, sensitivity of prasinophytes and green algae to diesel such as found in the present study has been previously shown for crude oil (Gilde & Pinckney 2012) or WAF (Sargian et al. 2007) in microcosm experiments. These results, agree with ours for prasinophytes but not for green algae, since some euglenophytes and chlorophytes would be resistant to other kinds of oil. We did not find a clear response for cryptophytes, despite that they have been recognized as sensitive to crude oil in microcosms (Gilde & Pinckney 2012) and in an experimental open sea spill (Brussaard et al. 2016).

Cyanobacteria resistance to diesel such as found in the present study has been previously reported for crude oil in microcosms (Gilde & Pinckney 2012). The capacity of cyanobacteria to tolerate moderate levels of organic pollution and thrive in waters receiving effluents containing petroleum hydrocarbons have been suggested (Palmer 1969, Gaur and Kumar 1985). Cyanobacteria abundance also increased in mesocosms experiments using other kinds of oil (Nayar et al. 2005, Brussaard et al. 2016) but in these studies microscopic examination revealed the dominance of the picocyanobacteria *Synechococcus* sp. The response of cyanobacteria to oil pollution seems to be dependent on the size (pico- or nanocyanobacteria), species composition and methodological approach. The significant decline in pico-PE-cyanobacteria densities after diesel inputs such as found in this study has been previously reported for PAHs on natural and cultured phytoplankton populations

(Echeveste et al. 2010b). González et al. (2009) have also shown a decline in picophytoplankton biomass in WSF exposure microcosm studies, which was driven by severe reductions and the eventual disappearance of pico-cyanobacteria *Prochlorococcus* and *Synechococcus*. Nevertheless, the low cyanobacteria densities found in the present study, which has been previously reported in this area (Annane et al. 2015), make it difficult to draw better conclusions.

Our microscopic analyses showed that densities of small nanoflagellates ( $<5\text{ }\mu\text{m}$ ) increased in contaminated treatments comparatively to the control while diatoms declined. Previous studies have reported the dominance of nanoflagellates in newly formed assemblages following an oil stress event (Lee et al. 1977, Dahl et al. 1983, Harrison et al. 1986). Siron et al. (1996) described a similar trend and ascribed the decrease of Chl *a* cellular content to the low photosynthetic capacity of the nanoflagellates in comparison with diatoms. This could also explain the decline in Chl *a* observed in our results in the last days.

Despite the short duration of our mesocosm experiment, we were able to detect some trends related to phytoplankton composition, in which diatom-based assemblages of the beginning of the experiment and especially of the bloom were replaced by small nanoflagellates and nanocyanobacteria in the diesel contaminated treatments. This could have important consequences not only in terms of the plankton community structure but also in terms of transfer of energy through the food web and carbon export (biological pump). A shift in the phytoplankton size structure from large nano- and microphytoplankton to small-sized species may induce significant shifts in the pelagic food web dynamics. In this sense, it represents a change from an herbivorous food web (with dominance of large phytoplankton and copepods and rapid sedimentation of particulate matter) to a microbial food web dominated by small phytoplankton and zooplankton such as ciliates and flagellates. These changes may result in faster carbon cycling in the ocean surface with the consequent decrease in the biological pump (Pomeroy 1974, Azam et al. 1983, Laws et al. 2000), and lead the ocean to release CO<sub>2</sub> to the atmosphere and act as a source (Legendre & Rassoulzadegan 1996).

Together, these results support the first two hypotheses (a-b) of the present study, which proposed that total biomass and density of phytoplankton assemblages decline because of diesel pollution and that sensitivity to diesel exposure varies among taxonomic groups. Only some cyanobacteria groups and small nanoflagellates were stimulated (increasing their densities) leading to a change in phytoplankton assemblages' structure. However, concerning the diverse responses of the phytoplankton taxonomic groups found in this study, which agree or not with those previously reported in the literature, we suggest they would be related to different types of oil and concentrations assessed, the initial phytoplankton assemblages enclosed, and the different experimental approaches adopted. We have to highlight, though, that almost no results were reported using diesel, so that the effects we measured on phytoplankton are one of the major, original contributions of the present work.

#### **1.4.4 Physiological status of phytoplankton - fluorescence induction**

The photosynthetic efficiency of PSII, expressed as the  $F_v/F_m$  ratio, was affected by diesel addition during the last six and five experimental days (chronic and acute treatments, respectively). Such a negative effect on photosynthetic efficiency has been previously reported (Gilde el at. 2012, Perhar & Arhonditsis 2014). It has been related to the accumulation of the relatively hydrophobic PAHs in the hydrophobic thylakoid membranes of the cells (Marwood et al. 1999, Sargian et al. 2005), where PSII is located, interfering with electron transport and photosynthesis light reactions (Duxbury et al. 1997, Koshikawa et al. 2007, Aksmann & Tukaj 2008). Interference with membrane function and integrity due to HCs hydrophobicity may lead to organelles in general, and chloroplasts in particular (Sikkema et al. 1995), becoming disorganized and losing functionality (Wang & Zheng 2008). Since a substantial loss in phytoplankton carbon biomass was found in the present study after oil addition, we could also suggest interference in photosynthesis dark reactions blocking the  $\text{CO}_2$  fixation. To our knowledge, no information exists concerning oil effects in this particular photosynthesis phase.

Concerning the second hypothesis of the present study, which evaluated the effect of diesel addition on the physiology of phytoplankton assemblages, our results confirmed a decrease in photosynthetic efficiency of PSII.

#### **1.4.5 Time of exposure - Ecological succession**

We are not able to compare the effects of diesel between contaminated treatments, because the chronic one consisted of two additions of 10 mL while the acute one consisted of a single addition of 20 mL. Moreover, the duration of phytoplankton cells exposure to diesel varied in among treatments, being larger in the chronic treatment (twelve days) than in the acute one (nine days). Mironov & Lanskaya (1968) reported death or retardation of cell division on marine planktonic algae exposed to black oil and kerosene. Such effects varied not only with the species tested but also with the oil concentrations and the duration of exposure. In another mesocosm experiments (Hjort 2007) phytoplankton assemblages also responded differently depending on the time and the level of pyrene exposure. Survival rates of three marine Arctic diatoms species decreased with increasing exposure times to three types of oils contamination (Hsiao 1978). This response has been ascribed to the duration of the experiment, which would have meant greater changes in the oil composition, concentration and toxicity (Prouse et al. 1976). In our experiment, Dal Santo Vidal (in prep.) found naphthalene, ace naphthene, fluorene, phenanthrene, anthracene, fluoranthene, pyrene and benzo (b) fluoranthene as the most toxic PAHs, which were probably the main responsibles for the diesel toxicity in mesocosm water (Ramadass et al. 2017). The larger exposure time of phytoplankton cells to these toxicants could serve to explain the significant effects observed in general in this treatment, not only for Chl *a* but also for most variables measured.

Taking into account the time of diesel inputs for each treatment, phytoplankton assemblages were disturbed in different periods of the ecological succession; during the pre-bloom and bloom periods for the chronic treatment and during the bloom period for the acute one. Phytoplankton composition and abundance were different at those two periods, in terms

of the dominant taxonomic and functional groups, which showed different sensitivities to diesel pollution. As discussed above, our results show that phytoplankton assemblages in the pre-bloom period could have been more sensitive to diesel addition given their lower abundances.

#### **1.4.6 Synergy effects - Trophic interactions**

The decline of nitrate + nitrite on day 5, earlier than other nutrients, could have been an extra stress for phytoplankton cells in treatments contaminated. Previous studies have suggested that the expressions of phytoplankton stress response to toxicants could be nutrient dependent (Karydis 1981, Hjorth et al. 2007, Perhar & Arhonditsis 2014). Ozhan & Bargu (2014) showed more sensitivity of the Gulf of Mexico phytoplankton communities to crude oil under nutrient-limited conditions, which agree with our results.

Phosphate trend observed in the control in the present study showed relatively stable concentrations during five days after day 6, which could have meant no uptake by phytoplankton during this period. This could be explained by the fact that nitrates + nitrites were exhausted after day 6 and algal cells need both nutrients (N and P) for their growth (Healey 1979, Goldman 1981, Hecky and Kilham 1988). The decline in phosphate concentrations after day 11 can be explained by a new phytoplankton uptake period which suggests the input of a new source of nitrogen available in the water. Since nitrates + nitrites were exhausted at that time, we suggest that the microbial community could have regenerated nitrogen as ammonium from the organic matter accumulated at the end of the bloom (Legendre & Rassoulzadegan 1995). We did not perform ammonium measurements. However, these results could be supported by the observed increase in heterotrophic bacteria, notably of particulate-attached HNA bacteria, from day 10 to the end of the experiment (Gadoin, 2018). In addition, values of community metabolism in the same experiment were positive between days 1 to 7 ( $0.1 - 0.6 \text{ mL O}_2 \text{ L}^{-1} \text{ d}^{-1}$ ) and turned negative after this time ( $-0.1 - -0.2 \text{ mL O}_2 \text{ L}^{-1} \text{ d}^{-1}$ ) (Putzeys et al. in prep.), suggesting a metabolic change in the plankton community in

mesocosm water, becoming more heterotrophic than autotrophic, additionally supporting our hypothesis.

Significantly higher phosphate concentrations in contaminated treatments after day 11 could be directly related to phytoplankton cell death (especially diatoms) due to diesel inputs. Then, the phosphate stored in diatom vacuoles could probably have been set free to the environment after breakdown of cells stressed by diesel. Storage of water and water-soluble compounds such as inorganic phosphate,  $\text{Ca}^{2+}$ ,  $\text{NH}_4^+$  or  $\text{NO}_3^-$  in vacuoles has been demonstrated for most algae (Raven 1997). However, in this period P was higher in the contaminated than in the uncontaminated treatments, but there were no changes comparing with previous values in days 7-11. Then, another possibility could be the lack of P uptake, due to bad state of the cells and the lack of capacity to take the regenerated N. This is also supported by the fact that  $\text{NO}_3^-$  did not change. Leak of P due to vacuole disruption could also have been liberated  $\text{NO}_3^-$ .

Phytoplankton cell death could also have been caused by viral infection. Viruses, which are remarkably abundant in marine plankton, have been recognized to play an essential role in the cycle of nutrients in the marine environment as well as in the population dynamics of phyto- and bacterioplankton (Fuhrman 1999, Brussaard 2004, Suttle 2005). Even if most marine viruses infect bacteria, prokaryotes and eukaryotes phytoplankton have shown evidence of viral infection in nature (Fuhrman 1999). Viruses could act as important agents of mortality for phytoplankton, causing release of nutrients bound in cellular biomass and relieving competitive pressure by dominant species (Larsen et al. 2001, Martínez-Martínez et al. 2006). In addition, Larsen et al. (2007) suggested that large dsDNA viruses infecting algae constitute a major part of high fluorescence virus (HFV) and nanoeukaryotes are mainly assumed to host HFV. In the present study, this kind of virus was detected in higher densities in contaminated treatments compared to control in the last period after time 10 (Starr, pers. comm.). Therefore, we suggest that viral infection of phytoplankton affected by diesel pollution (especially nanoeukaryotes, which was the most abundant phytoplankton group) could represent a mortality source to explain phytoplankton biomass loss.

## 1.5 CONCLUSIONS

In conclusion, even if the effect of oil and its constituents on phytoplankton natural assemblages remains still largely unknown, our results show for the first time that a refined oil such as diesel in concentrations that simulate a low pollution scenario, would have substantial consequences (structural and functional) on the phytoplankton assemblages and the pelagic food webs in the area of study. The existence of a synergistic effect with nutrient limitation as well as viral lysis could amplify the diesel effects on phytoplankton assemblages during certain periods. With the increase of maritime transportation, the frequency of small spills is likely to increase rather than decrease, leading the plankton community to frequent short-term and chronic exposure of available and toxic oil compounds with potential long-term adverse effects. The results of the present study could contribute in helping decision-making processes concerned with oil spills in subarctic environments like the LSLE. *S. costatum* could be used as a bioindicator species of water quality in monitoring programs, given its high sensitivity to diesel and its important role as a major component of the natural phytoplankton assemblages in this area.

Our mesocosms were not open to the atmosphere and temperature was constant. At a first glance, the results of the present study would seem to be applicable only to worst pollution case scenarios, in which there is neither HCs evaporation nor temperature effect (dissolution). However, diesel fuel does not readily evaporate unlike lighter fuels such as gasoline (Clark 1989). This renders it being persistent in the environment meaning that our mesocosm experience, even its limitations, could partially reflect what is occurring in the natural environment.

## **CONCLUSION GÉNÉRALE**

Le phytoplancton joue un rôle clé dans les écosystèmes marins; elles sont les principaux acteurs de la régulation marine du carbone atmosphérique. Pour cette raison des changements dans leurabondance, leur composition et leur biomasse peuvent entraîner des impacts significatifs pour l'ensemble de ces écosystèmes (Ozhan et al. 2014). Compte tenu que la structure et le fonctionnement des réseaux trophiques pélagiques marins dépendent essentiellement de l'énergie et de la matière fournie par la photosynthèse du phytoplancton, étudier l'impact de l'un des facteurs majeurs de contamination marine, les hydrocarbures (HCs), sur les associations phytoplanctoniques s'avère essentiel. Dans ce contexte, les connaissances existantes sont peu claires et parfois contradictoires. La plupart des études ont été conduites en conditions de laboratoire, qui ne sont pas assez représentatives de l'environnement naturel. Certaines études *in situ* ont suivi les réponses des organismes phytoplanctoniques dans des environnements naturels qui ont été affectées par des déversements accidentels de pétrole (Linden et al. 1979, Ramachandran et al. 2004, Salas et al. 2006, Varela et al. 2006, Díez et al. 2009), mais les effets à court terme n'ont pas pu être étudiés à cause des délais entre les déversements accidentels et les échantillonnages. De plus, certaines formes de pétrole, dont le diesel, ont été moins étudiées que d'autres, même s'il s'agit, comme dans le cas du diesel, d'un contaminant clé sur la surface de l'eau à cause des fuites ou des petits déversements accidentels, ainsi que l'un des plus extensivement utilisés (Ramadass et al. 2017).

Les résultats de cette recherche contribuent à l'amélioration des connaissances sur les effets potentiels du diesel sur les écosystèmes estuariens, en particulier celui du Saint-

Laurent, un environnement qui pourrait être fragilisé par l'augmentation du transport global de produits pétroliers (Institut Maritime du Québec 2014). Cette étude a permis de faire une première analyse des effets du diesel sur les associations phytoplanctoniques dans un scénario de faible pollution, ce qui est difficile à évaluer directement dans l'environnement, où certains comportements pourraient être masqués par des processus plus importants. Les études futures *in situ*, ainsi que la modélisation de scénarios de pollution, pourront se baser sur ces résultats qui combleront certaines informations manquantes.

L'objectif général de ce projet a été d'étudier les réponses structurelles et fonctionnelles de la communauté planctonique face à une perturbation anthropique telle que la contamination par des hydrocarbures. Le but a été d'étudier, par une approche expérimentale en mésocosme, les effets d'une exposition « aiguë » et d'une exposition « chronique » au diesel maritime comme source de contamination. La méthodologie utilisée a permis d'établir des liens entre les différents niveaux trophiques tels que le phytoplancton (présente étude), le bactérioplancton (Gadoïn 2017) et le microzooplancton (Olmedo Masat en prep.) ainsi que la chimie des hydrocarbures (Dal Santo Vidal en prep.) dans un scénario de faible pollution par des hydrocarbures. Un aspect central de mon projet de recherche réside en l'utilisation des différentes méthodologies d'étude de phytoplancton (fluorométrie, HPLC, cytométrie en flux, FowCAM, microscopie, FRRF) pour évaluer les réponses du phytoplancton soumis au stress par hydrocarbures, en considérant les possibles effets directs ou indirects avec les autres composants de la communauté planctonique.

Le premier objectif spécifique de ce projet de recherche était de déterminer comment les ajouts d'HCs affectaient les attributs structurels (biomasse, densité, composition) des associations phytoplanctoniques. La plupart des effets ont été détectés dans les derniers jours de l'expérience, correspondant à la période de postfloraison de la succession phytoplanctonique. Les concentrations de Chl *a* ont été réduites dans les deux traitements contaminés. Les principales composantes de tous les groupes fonctionnels de fitoplancton (picoeucaryotes, nanoeucaryotes et microphytoplancton) ont été sensiblement affectés par les ajouts du diesel, en déclinant leurs densités et biomasses de carbone totales. Ces pertes

de biomasse, étant supérieures à 50% dans la plupart des cas, peuvent être interprétés comme un effet direct négatif de la pollution par diesel étant donné que le microzooplancton a été très peu abondant et le contrôle de la biomasse par le broutage n'a pas été significatif (Olmedo Masat, en prep.). La succession écologique dans le traitement control, qui a été représentative de celle présente dans l'environnement naturel, peut être décrite par la présence des crytophytées au début de l'expérience, suivi par une importante abondance des diatomées et quelques prymnesiophytes, dinoflagellés et d'algues vertes pendant la période de floraison et finalement des prasinophytes et des cyanobactéries dans la période de postfloraison.

D'ailleurs, nous avons pu constater qu'au niveau de la composition des assemblages, quelques groupes de cyanobactéries telles que les Pico-PE ont été négativement affectées par le diesel et d'autres, telles que les Nano-PC, ont été stimulées. Plus en détail, les analyses pigmentaires ont permis d'établir la succession écologique dans l'eau des mésocosmes ainsi que les principaux groupes taxonomiques affectés ou stimulés par le diesel.

Les concentrations des pigments marqueurs fucoxanthine, Chl *c1*, Chl *c2*, violaxanthine et prasinoxanthine ont été significativement réduites dans les deux traitements contaminés, ce qui suggère une diminution des abondances des groupes taxonomiques qu'ils représentent. Pour cette raison, on a pu constater que les diatomées principalement, mais aussi certains dinoflagellés, prymnesiophycees et prasinophytes, ont été les groupes les plus affectés par le diesel. D'autres groupes tels que les algues vertes et les cryptophytes semblent être sensibles au diesel, mais cette réponse n'a pas été claire en raison des faibles concentrations de leurs pigments marqueurs. La zéaxanthine a été le seul pigment stimulé par le diesel, indiquant une augmentation des cyanobactéries, spécifiquement les nano-PC.

L'identification microscopique a confirmé la dominance des diatomées (spécialement centriques) pendant l'expérience ainsi que la stimulation des pico- et nanoflagellés au détriment des diatomées dans les traitements contaminés. En raison de sa forte sensibilité au diesel, la diatomée *S. costatum* a été proposée comme espèce potentielle indicatrice de la

qualité de l'eau pour des programmes de suivis de monitorage de la pollution par HCs dans cette aire d'étude.

Ces résultats nous permettent d'accepter les deux premières hypothèses de départ qui stipulaient que la biomasse et la densité totale des associations phytoplanctoniques diminueraient après les ajouts d'HCs et que les divers groupes taxonomiques répondraient de façon différentielle à l'exposition aux hydrocarbures. Dans cette étude, les associations dominées par des diatomées au début de l'expérience étaient remplacées progressivement par des pico et nanoflagellées et des nanocyanobactéries dans les traitements contaminés.

La Figure 19 montre un modèle conceptuel qui résume les résultats principaux de cette étude concernant la composition, la biomasse ainsi que les conclusions générales vis-à-vis les flux de carbone régulés par le phytoplancton dans deux scénarios différents: le contrôle, non contaminé et celui contaminé par HCs.

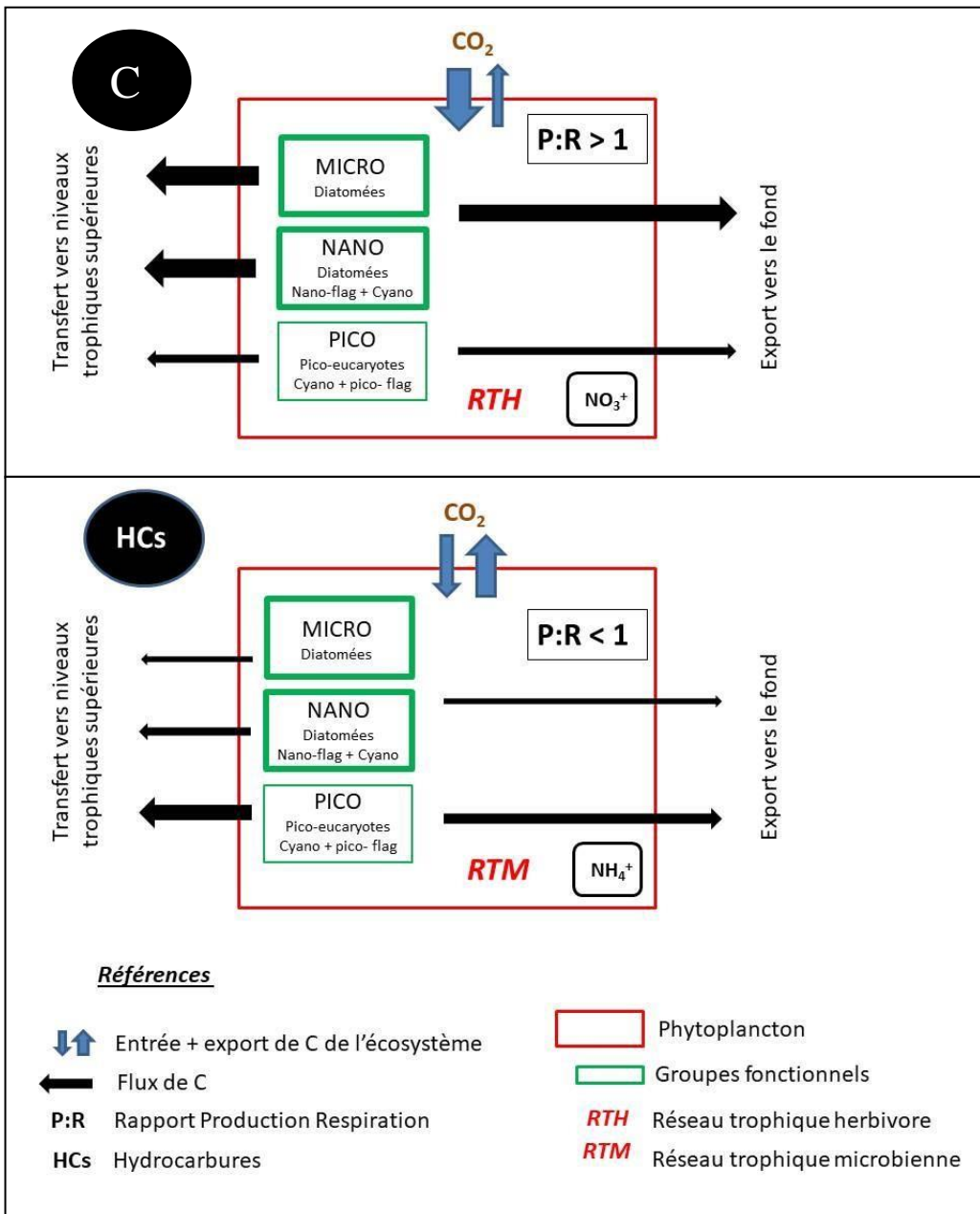


**Figure 19:** Résultats principaux de cette étude concernant la composition, la biomasse et les flux de carbone (C) dans deux scénarios différents: non contaminé (supérieure) et contaminé par HC<sub>s</sub> (inférieure). Cyano: cyanobactéries, Nano-flag : nanoflagellées, Pico-flag : picoflagellées. Micro: microphytoplancton, Nano: nanophytoplancton, Pico: picophytoplancton, RTH and RTM (Legendre & Rassoulzadegan 1996, Azam et al. 1983, Laws et al. 2000).

Un changement dans la structure des tailles du phytoplancton comme celui observé dans cette étude, avec une transition dès une dominance d'espèces de grande taille dans la gamme du nano- et du microphytoplancton vers une dominance d'espèces de petite taille (les nanocyanobactéries et les pico-nano flagelles), peut entraîner un changement dans le type de réseau trophique pélagique. Ainsi, d'un réseau trophique herbivore dominé par de grands copépodes (prédateurs du nano- et microphytoplancton) avec une sédimentation plus rapide de la matière organique, le système peut évoluer vers un système dominé par un réseau trophique microbien dominé par du microzooplancton de plus petite taille (ciliées, flagellées) avec un recyclage relativement plus rapide du carbone, une sédimentation plus lente de la matière organique et, par conséquent, une diminution dans l'intensité de la pompe biologique (Pomeroy 1974, Azam et al. 1983, Laws et al. 2000), ce qui contribuera à l'augmentation du dégazage de CO<sub>2</sub> vers l'atmosphère.

De plus, une perte de biomasse (en termes de carbone) dans tous les groupes fonctionnels par effet direct du diesel comme celle mesurée dans cette étude représente un énorme impact en matière du flux de carbone régulé par le phytoplancton dans le réseau trophique marin. L'incorporation de carbone via la photosynthèse serait réduite ainsi que la quantité et la qualité de carbone disponible pour les niveaux trophiques supérieurs. Cela entraînerait une diminution du transfert de carbone à travers le broutage.

Le deuxième objectif spécifique de ce projet de recherche était d'évaluer l'effet des ajouts d'HCs sur la physiologie des associations phytoplanctoniques. À l'aide de la technique de FRRF, l'efficacité photosynthétique, représentée par le rapport F<sub>v</sub>/F<sub>m</sub>, a été mesurée. Ce rapport a montré une diminution lors de l'addition de diesel dans les derniers jours de l'expérience. D'autres auteurs expliquent que l'accumulation des HAPs, relativement hydrophobes dans les membranes tilacoidelles des cellules (Marwood et al. 1999, Sargian et al. 2005), où le photosystème II est situé, peut entraîner une interférence du transport électronique vers le photosystème I et de la chaîne de réactions de la photosynthèse qui dépendent de la lumière (Duxbury et al. 1997, Koshikawa et al. 2007, Akemann & Tukaj 2008). En raison de la substantielle perte de biomasse de carbone

phytoplanctonique, nous suggérons aussi une possible interférence des réactions photosynthétiques qui ne sont pas dépendantes de la lumière, car c'est dans cette étape que la fixation de CO<sub>2</sub> se produit. Cependant, à notre connaissance il n'existe pas d'information concernant les effets des HCs dans la phase obscure de la photosynthèse.

Ces résultats nous permettent d'accepter la deuxième hypothèse de départ (2) qui stipulait que les ajouts d'HCs diminueraient l'efficacité photosynthétique du phytoplancton.

## **PERSPECTIVES**

Malgré les efforts mis dans la réalisation de ces expériences et les résultats que nous avons obtenus, il y a toujours place à l'amélioration, et c'est dans ce sens que les paragraphes suivants discutent des aspects à tenir en compte pour des expériences futures.

### **L'étude du microphytoplancton**

Cette étude permet d'avoir un aperçu général des effets du diesel sur la densité, la biomasse et la composition des associations phytoplanctoniques en considérant les groupes fonctionnels. Cependant, concernant le microphytoplancton il serait très utile d'ajouter des analyses de cytométrie en flux (i.e., CitoSub) afin de mieux les comparer avec les résultats de la cytométrie en flux utilisée, qui permet juste l'analyse des plus petits groupes.

Concernant la microscopie, il aurait été idéal de faire une analyse complète des échantillons depuis le début jusqu'à la fin de l'expérience. Malheureusement, nous avons eu un problème d'échantillonnage qui nous a empêché d'analyser les premiers jours d'expérience. Cependant, grâce à l'utilisation des diverses techniques d'étude nous avons pu surmonter ce problème et obtenir des résultats clairs sur tous les stades de la succession écologique analysée.

### **Nouvelles perspectives d'analyses**

D'autres perspectives d'analyses pourraient aussi être considérées pour des recherches futures, comme par exemple des études sur la génétique à niveau de l'expression

différentielle des gènes dans des divers scénarios de pollution, ou bien sur la composition lipidique des membranes des cellules.

### **Paramètres photosynthétiques et production primaire**

Comme les tendances du paramètre  $F_v/F_m$  n'ont pas été complètement claires pendant les périodes pré floraison et floraison, il serait intéressant de prolonger le temps d'analyse et d'ajouter d'autres paramètres photosynthétiques afin d'avoir un aperçu global des réponses fonctionnelles du phytoplancton à la pollution par le diesel.

La photosynthèse est intimement liée à la production primaire, laquelle a été définie comme la quantité de matière produite par le phytoplancton durant un intervalle de temps donné. La diminution de la production primaire totale à cause des certains hydrocarbures (e.g. Miller et al. 1978, Karydis 1981, González et al. 2009) a déjà été reporté dans le passé.

Pour cette raison, il serait pertinent d'inclure cette variable d'analyse afin de mieux comprendre les effets globaux de la pollution par les HCs dans une communauté planctonique. Dans ce contexte, la mesure de la respiration en combinaison avec la production (P : R) pourrait nous permettre de suivre le métabolisme de la communauté et d'en tirer des conclusions plus complètes sur le rôle de la communauté étudiée.

### **Plan expérimentale**

Afin d'étudier la photochimie des HCs, les mésocosmes utilisés ont été fermés, empêchant tout échanges gazeux avec l'atmosphère. Ainsi, l'évaporation d'HCs, qui constitue l'un des processus d'altération des HCs les plus significatifs à court terme (heures à jours) a été éliminée de l'expérience. L'évaporation consiste en la perte physique des composants de faibles masses moléculaires d'un pétrole vers l'atmosphère par volatilisation (Lee et al. 2015). Cependant, certaines études indiquent que le diesel ne s'évapore pas aisément contrairement aux carburants plus légers comme l'essence (Clark 1989). Cela le rend plus persistant dans l'environnement ce qui indique que notre expérience, même avec cette limitation, pourrait partiellement reproduire ce qui se passe dans la nature. Pour des

futures expériences, il serait important de considérer de travailler avec les mésocosmes ouverts à l‘extérieur, pour mieux simuler les processus d‘altération d‘HCs qui se produisent dans l‘environnement naturel.

En revanche, l‘ouverture des mésocosmes peut contribuer à ajouter d‘autres facteurs de variabilité environnementale tels que les pluies (qui peuvent contribuer à la dilution de l‘eau ou à l‘ajout des nutriments) ou le vent (qui pourrait accélérer les processus de dégradation d‘HCs via le mélange ainsi qu‘ajouter de la matière en suspension pouvant modifier les conditions de lumière et l‘analyse de flux de carbone). Les facteurs environnementaux tels que la température, la lumière, les sédiments en suspension et l‘action des marées (énergie) sont des paramètres clés dans les processus de modification de la concentration du pétrole dans l‘environnement (Lee et al. 2015). Dans cette expérience, la température a été maintenue constante et le mélange a été simulé. Le choix du dessin expérimental pour travailler avec des mésocosmes est intimement lié aux objectifs d‘étude et aux hypothèses de départ. En fonction de cela, le système devrait s‘adapter pour simuler partiellement les conditions environnementales en même temps qu‘étudier en détail certains aspects (variables) de la communauté planctonique.

Malgré la myriade d‘effets possibles, certaines observations du phytoplancton lors de déversements de pétrole réels ne montrent généralement aucun effet significatif (Banks 2003, Varela et al. 2006). Les communautés phytoplanctoniques sont sujettes à de fortes variations naturelles, ce qui peut empêcher que les changements observés ne puissent pas être distingués des fluctuations naturelles (Diez et al., 2009). Dans certains cas, le phytoplancton peut s‘adapter à la présence de pétrole brut (López-Rodas et al. 2009), mais cela est peu probable lorsque ces déversements se produisent dans des zones où les concentrations naturelles des HCs sont faibles. Le facteur d‘atténuation le plus probable est la dégradation des HCs par des bactéries hétérotrophes (Leahy et Colwell 1990). Ces réactions, combinées à la dilution naturelle, à la dispersion et à l‘altération du pétrole, réduiront probablement les effets du pétrole bien en deçà de ceux observés dans la présente étude.

## **Nutriments - azote**

Quant aux nutriments, les concentrations d'ammonium n'ont pas pu être mesurées dans cette expérience, ce qui pourrait ajouter de l'information afin de mieux comprendre le cycle de l'azote et de son lien avec la communauté planctonique. Cela pourrait également permettre d'évaluer les effets potentiels de synergie entre le manque de nutriments et l'exposition au diesel sur le phytoplancton. Pour cette raison, il est fortement recommandé de mesurer tous les composants de l'azote, en y incluant l'ammonium, dans des futures études.

## **Comparaison des traitements chronique et aigu**

Le plan expérimental utilisé dans cette expérience ne permet pas de comparer les deux scénarios de contamination, car un des traitements était composé de deux ajouts de 10 mL de diesel (chronique) tandis que l'autre (aigu) n'était composé que d'un seul ajout de 20 mL. Pour cette raison, le temps d'exposition au diesel de cellules phytoplanctoniques a été plus long dans le traitement chronique (douze jours) en comparaison avec le traitement aigu (neuf jours). La plus grande durée de l'exposition aux HCs toxiques pourrait servir à expliquer les résultats significatifs et les tendances plus explicites observées en général pour le traitement chronique pour la plupart des variables mesurées. Cependant, pour évaluer spécifiquement l'effet de la durée un autre plan expérimental devrait être mis en place, composé par différents traitements avec des ajouts du diesel de volumes constants à différents temps chacun. Un tel plan expérimental pourra aussi permettre d'évaluer quelle est la période de la succession écologique la plus sensible à la contamination par des HCs.

Les résultats de cette étude montrent des changements dans la composition, la densité et la biomasse de carbone totales des associations phytoplanctoniques au long de la succession écologique, qui pourraient servir à expliquer pourquoi les effets les plus toxiques ont été détectés dans le traitement chronique (où le premier ajout de diesel a été réalisé dans la période de préfloraison). Les associations phytoplanctoniques de la période préfloraison

peuvent avoir été plus sensibles à l'addition du diesel en raison d'une sensibilité différentielle, ainsi qu'au la faible densité des cellules.

Finalement, concernant le traitement aigu et étant donné que les résultats de la plupart des variables sont similaires à ceux du traitement chronique, il aurait peut-être fallu prolonger de quelque jours l'expérience pour vérifier la présence d'effets significatifs, ainsi que pour confirmer si les réponses différaient ou s'accentuaient relativement à l'autre traitement. En même temps, il faudrait essayer les effets de volumes de diesel plus élevés relativement à celui utilisé, mais en considérant toujours un scénario global de faible pollution d'HCs.

## RÉFÉRENCES BIBLIOGRAPHIQUES

- Abdullah, M. P. (1995). Oil related pollution status of coastal waters of Peninsular Malaysia. In: *Proceedings of the ASEAN - Canada Technical Conference on Marine Science*, EVS Environment Consultants and NSTB, Singapore, 215-224.
- Adekunle, I. M., Ajijo, M. R., Adcofun, C. O., & Omoniyi, I. T. (2010). Response of four phytoplankton species found in some sectors of Nigerian coastal waters to crude oil in controlled ecosystem. *International Journal of Environmental Research*, 4, 65–74.
- Agustí, S., Satta, M. P., Mura, M. P., & Benavent, E. (1998). Dissolved esterase activity as tracer of phytoplankton lysis: Evidence of high phytoplankton lysis rates in the NW Mediterranean. *Limnology and Oceanography*, 43, 1836–1849.
- Ahmed, S. M., Beasley, M. D., Efronson, A. D., & Hites, R. A. (1974). Sampling errors in the quantification of petroleum in Boston Harbor water. *Analytical Chemistry*, 46, 1858-1860.
- Aksmann, A., & Tukaj, Z. (2008). Intact anthracene inhibits photosynthesis in algal cells: a fluorescence induction study on *Chlamydomonas reinhardtii* cw92 strain. *Chemosphere*, 74(1), 26-32.
- Annane, S., St-Amand, L., Starr, M., Pelletier, E., & Ferreyra, G. A. (2015). Contribution of transparent exopolymeric particles (TEP) to estuarine particulate organic carbon pool. *Marine Ecology Progress Series*, 529, 17–34.
- Azam, F., Fenchel, T., Field, J. G., Gray, J. S., Meyer-Reil, L. A., & Thingstad, F. (1983). The ecological role of water-column microbes in the sea. *Marine Ecology Progress Series*, 10, 257–263.
- Bælum, J., Borglin, S., Chakraborty, R., Fortney, J. L., Lamendella, R., Mason, O. U., ... & Malfatti, S. A. (2012). Deep-sea bacteria enriched by oil and dispersant from the Deepwater Horizon spill. *Environmental Microbiology*, 14(9), 2405-2416.
- Banks, S. (2003). SeaWiFS satellite monitoring of oil spill impact on primary production in the Galapagos Marine Reserve. *Marine Pollution Bulletin*, 47(7-8), 325-330.
- Bérard-Theriault, L., Poulin, M., & Bossé, L. (1999). Guide d'identification du phytoplancton marin de l'estuaire et du golfe du Saint-Laurent incluant également certains protozoaires. *Canadian Manuscript report of Fisheries and Aquatic Sciences*, 128, 387 pp.
- Bidigare, R. R. (1989). Photosynthetic pigment composition of the brown tide alga: unique chlorophyll and carotenoid derivatives. In *Novel phytoplankton blooms*, Springer, Berlin, Heidelberg, 57-75.

- Bidigare, R. R., Kennicutt II, M. C., Ondrusek, M. E., Keller, M. D., & Guillard, R. R. L. (1990). Novel chlorophyll-related compounds in marine phytoplankton: distributions and geochemical implications. *Energy and Fuels*, 4, 653-657.
- Bjørnland, T., & Tangen, K. (1979). Pigmentation and morphology of a marine Gyrodinium (Dinophyceae) with a major carotenoid different from peridinin and fucoxanthin. *Journal of Phycology*, 15(4), 457-463.
- Boehm, P. D., & Page, D. S. (2007). Exposure Elements in Oil Spill Risk and Natural Resource Damage Assessments : A Review. *Human and Ecological Risk Assessment: An International Journal*, 13(2), 418–448.
- Bopp, S. K., & Lettieri, T. (2007). Gene regulation in the marine diatom *Thalassiosira pseudonana* upon exposure to polycyclic aromatic hydrocarbons (PAHs). *Gene*, 396, 293–302.
- Brussaard, C. P. (2004). Viral control of phytoplankton populations - a review. *Journal of Eukaryotic Microbiology*, 51(2), 125-138.
- Brussaard, C. P. D., Peperzak, L., Beggah, S., Wick, L. Y., Wuerz, B., Weber, J., ... Van Der Meer, J. R. (2016). Immediate ecotoxicological effects of short-lived oil spills on marine biota. *Nature Communications*, 7, 1–11.
- Buitenhuis, E. T., Li, W. K. W., Vaulot, D., Lomas, M. W., Landry, M. R., Partensky, F., ... McManus, G. B. (2012). Picophytoplankton biomass distribution in the global ocean. *Earth System Science Data*, 4(1), 37–46.
- Calbet, A., Landry, M. R., & Nunnery, S. (2001). Bacteria-flagellate interactions in the microbial food web of the oligotrophic subtropical North Pacific. *Aquatic Microbial Ecology*, 23(3), 283-292.
- Cadaillon A., Ferreyra G, Schloss I, Starr M & Vidussi F. (in prep.) Functional and structural responses of natural phytoplankton assemblages to anthropic perturbations: the case of a low concentration oil spill scenario.
- Camilli, R., Reddy, C. M., Yoerger, D. R., Van Mooy, B. A., Jakuba, M. V., Kinsey, J. C., ... & Maloney, J. V. (2010). Tracking hydrocarbon plume transport and biodegradation at Deepwater Horizon. *Science*, 330(6001), 201-204.
- Canadian Press, 2017. Bella Bella, B.C. Oil Spill Likely Caused By Sleeping Crew On Tugboat: Report [in line] <https://www.independent.ie/business/irish/caterpillar-fined-fordiesel-spill-into-irish-sea-36199096.html> (consulted 20 February 2018)
- Clark, R.B., 1989. Marine Pollution, (2<sup>ed</sup>). Clarendon Press, Oxford.

- Chan, K., & Chiu, S. Y. (1985). The Effects of Diesel Oil and Oil Dispersants on Growth, Photosynthesis, and Respiration of *Chlorella salina*. *Archives of Environmental Contamination and Toxicology*, 33(14), 325–331.
- Dahl, E., Laake, M., Tjessem, K., Eberlein, K., & Bøhle, B. (1983). Effects of Ekofisk crude oil on an enclosed planktonic ecosystem. *Marine Ecology Progress Series*, 14, 81–91.
- Díez, I., Secilla, A., Santolaria, A., & Gorostiaga, J. M. (2009). Ecological monitoring of intertidal phytoplankton communities of the Basque Coast ( N . Spain ) following the Prestige oil spill. *Environmental Monitoring and Assessment*, 159, 555–575.
- Dal Santo Vidal, M (in prep.) *Mesure de la présence et de la dynamique environnementale des hydrocarbures aromatiques polycycliques (HAPs) à l'aide des matrices d'excitation-émission de fluorescence*. Master's thesis. University of Quebec in Rimouski. Quebec.
- Dunstan, W. M., Atkinson, L. P., & Natoli, J. (1975). Stimulation and inhibition of phytoplankton growth by low molecular weight hydrocarbons. *Marine Biology*, 31(4), 305–310.
- Dupuis, A., & Ucán-Marín, F. (2015). *A literature review on the aquatic toxicology of petroleum oil: An overview of oil properties and effects to aquatic biota*. Canadian Science Advisory Secretariat, 51 pp.
- Durand, M. D., Green, R. E., Sosik, H. M., Olson, R. J., & Manton, B. (2002). Diel Variations in Optical Properties of. *Journal of Phycology*, 1142, 1132–1142.
- Duxbury, C. L., Dixon, D. G., & Greenberg, B. M. (1997). Effects of simulated solar radiation on the bioaccumulation of polycyclic aromatic hydrocarbons by the duckweed *Lemna gibba*. *Environmental Toxicology and Chemistry*, 16(8), 1739–1748.
- Echeveste, P., Agustí, S., & Dachs, J. (2010a). Cell size dependent toxicity thresholds of polycyclic aromatic hydrocarbons to natural and cultured phytoplankton populations. *Environmental Pollution*, 158(1), 299–307.
- Echeveste, P., Dachs, J., Berrojalbiz, N., & Agustí, S. (2010b). Decrease in the abundance and viability of oceanic phytoplankton due to trace levels of complex mixtures of organic pollutants. *Chemosphere*, 81(2), 161–168.
- El-Dib, M. A., Abou Waly, H. F., & El Naby, A. H. (2001). Fuel oil effect on the population growth, species diversity and chlorophyll (a) content of freshwater microalgae. *International Journal of Environmental Health Research*, 11(2), 189–197.

- El-Sheekh, M. M., El-Naggar, A. H., Osman, M. E. H., & Haieder, A. (2000). Comparative studies on the green algae *Chlorella homosphaera* and *Chlorella vulgaris* with respect to oil pollution in the River Nile. *Water Air and Soil Pollution*, 124, 187-204.
- Fan, C., & Reinfelder, J. R. (2003). Phenanthrene Accumulation Kinetics in Marine Diatoms. *Environmental Science and Technology*, 37, 3405–3412.
- Faksness, L. G., Brandvik, P. J., & Sydnes, L. K. (2008). Composition of the water accommodated fractions as a function of exposure times and temperatures. *Marine Pollution Bulletin*, 56(10), 1746-1754.
- Finkel, Z. V., Beardall, J., Flynn, K. J., Quigg, A., Rees, T. A. V., & Raven, J. A. (2010). Phytoplankton in a changing world: Cell size and elemental stoichiometry. *Journal of Plankton Research*, 32(1), 119–137.
- Fuhrman, J. A. (1999). Marine viruses and their biogeochemical and ecological effects. *Nature*, 399(6736), 541–548.
- Gadoin, E (2018). « Effets de contaminations chronique et aiguë au diesel maritime sur la structure et le métabolisme de la communauté bactérienne de l'estuaire du saint Laurent ». Master's thesis. University of Quebec in Rimouski. Quebec.
- Gao, Z. H., Yang, J. Q., & Wang, P. G. (2007). Theory, method, and case study of ecological lost assessment on themarine oil spill .Beijing: *Ocean Press*, 291–358.
- Gaur, J.P. & Kumar, H.D. (1985). The influence of oil refinery effluents on the structure of algal communities. *Archiv fur Hydrobiologie*. 103, 305–23.
- Gilde, K., & Pinckney, J. L. (2012). Sublethal Effects of Crude Oil on the Community Structure of Estuarine Phytoplankton. *Estuaries and Coasts*, 35(3), 853–861.
- González, J. J., Viñas, L., Franco, M. A., Fumega, J., Soriano, J. A., Grueiro, G., ... Albaiges, J. (2006). Spatial and temporal distribution of dissolved/dispersed aromatic hydrocarbons in seawater in the area affected by the Prestige oil spill. *Marine Pollution Bulletin*, 53(5–7), 250–259.
- González, J., Figueiras, F. G., Aranguren-Gassis, M., Crespo, B. G., Fernández, E., Morán, X. A. G., & Nieto-Cid, M. (2009). Effect of a simulated oil spill on natural assemblages of marine phytoplankton enclosed in microcosms. *Estuarine, Coastal and Shelf Science*, 83(3), 265–276.
- González, J., Fernández, E., Figueiras, F. G., & Varela, M. (2013). Subtle effects of the water soluble fraction of oil spills on natural phytoplankton assemblages enclosed in mesocosms. *Estuarine, Coastal and Shelf Science*, 124, 13–23.

- Granum, E., Kirkvold, S., & Myklestad, S. M. (2002). Cellular and extracellular production of carbohydrates and amino acids by the marine diatom *Skeletonema costatum*: diel variations and effects of N depletion, 242(Werner 1977), 83–94.
- Grasshoff, K., Ehrhardt, M., & Kremling, K. (1999). *Methods of seawater analysis*, 3ed. Wiley-VCH, New York, NY. 577 pp.
- Harrison, P. J., Cochlan, W. P., Acreman, J. C., Parsons, T. R., Thompson, P. A., Dovey, H. M., & Xiaolin, C. (1986). The effect of crude oil and Corexit 9527 on marine phytoplankton in an experimental enclosure. *Marine Environmental Research*, 18, 93109.
- Healey, F. P., (1979). Short-term responses of nutrient deficient algae to nutrient addition. *Journal of Phycology*, 15(3), 289-299.
- Hing, L. S., Ford, T., Finch, P., Crane, M., & Morritt, D. (2011). Laboratory stimulation of oil-spill effects on marine phytoplankton. *Aquatic Toxicology*, 103(1–2), 32–37.
- Hjorth, M., Vester, J., Henriksen, P., Forbes, V., & Dahllöf, I. (2007). Functional and structural responses of marine plankton food web to pyrene contamination. *Marine Ecology Progress Series*, 338, 21–31.
- Hsiao, S. I. (1978). Effects of crude oils on the growth of arctic marine phytoplankton. *Environmental Pollution* (1970), 17(2), 93-107.
- Incardona, J. P., Gardner, L. D., Linbo, T. L., Brown, T. L., Esbaugh, A. J., Mager, E. M., ... & Tagal, M. (2014). Deepwater Horizon crude oil impacts the developing hearts of large predatory pelagic fish. *Proceedings of the National Academy of Sciences*, 111(15), E1510-E1518.
- Institut Maritime du Québec (2014). Bilan des connaissances. Transport maritime des hydrocarbures. Innovation Maritime. QC, Canada, 110 pp.
- Jakobsen, H., & Carstensen, J. (2011). FlowCAM: Sizing cells and understanding the impact of size distributions on biovolume of planktonic community structure. *Aquatic Microbial Ecology*, 65(1), 75–87.
- Jeffrey, S. W., Sielicki, M., & Haxo, F. T. (1975). Chloroplast pigment patterns in dinoflagellates. *Journal of Phycology*, 11, 374-384.
- Jeffrey, S. W., & Wright, S. W. (1994). Photosynthetic pigments in the Haptophyta. In: *The Haptophyte algae*. Green, J. C., & Leadbeater, BSc (eds). *Systematics Association Special, Clarendon Press*, Oxford, 51, 111-132.

- Jeffrey, S. W., & Wright, S. W. (2006). Photosynthetic pigments in marine microalgae: insights from cultures and the sea. In: *Algal cultures, analogues of blooms and applications*. Subba Rao, D. V. (eds). *Science Publishers*, Enfield, NH, 1, 33–90.
- Jiang, Z., Huang, Y., Xu, X., Liao, Y., Shou, L., Liu, J., ... & Zeng, J. (2010). Advance in the toxic effects of petroleum water accommodated fraction on marine plankton. *Acta Ecologica Sinica*, 30(1), 8-15.
- Johnsen, G., & Sakshaug, E. (1993). Bio-optical characteristics and photoadaptive responses in the toxic and bloom-forming dinoflagellates *Gyrodinium aureolum*, *Gymnodinium galatheanurn*, and two strains of *Prorocentrum minimum*. *Journal of Phycology*, 29(5), 627-642.
- Jung, S. W., Kwon, O. Y., Joo, C. K., Kang, J. H., Kim, M., Shim, W. J., & Kim, Y. O. (2012). Stronger impact of dispersant plus crude oil on natural plankton assemblages in short-term marine mesocosms. *Journal of Hazardous Materials*, 217, 338–349.
- Karydis, M. (1981). The toxicity of crude oil for the marine alga *Skeletonema costatum* (Greville) Cleve in relation to nutrient limitation. *Hydrobiologia*, 85(2), 137–143.
- Kelly, L. D., McGuinness, L. R., Hughes, J. E., & Wainright, S. C. (1999). Effects of phenanthrene on primary production of phytoplankton in two New Jersey estuaries. *Bulletin of Environmental Contamination and Toxicology*, 63, 646–653.
- Kemp, W. M., Petersen, J. E., & Gardner, R. H. (2001). Scale-dependence and the problem of extrapolation: implications for experimental and natural coastal ecosystems. In: *Scaling relations in experimental ecology*. Gardner, R. H., Kemp, W. M., Kennedy, V. S., & Petersen, J. E. (eds), *Columbia University Press*, New York, NY, 3–57.
- Kirchman, D. L. (1999). Phytoplankton death in the sea. *Nature*, 398, 293–294.
- Kirk, J. T. O. (1994). Light and photosynthesis in aquatic ecosystems (2ed). *Cambridge University Press*, 509 pp.
- Kolber, Z. S., Prášil, O., & Falkowski, P. G. (1998). Measurements of variable chlorophyll fluorescence using fast repetition rate techniques: defining methodology and experimental protocols. *Biochimica et Biophysica Acta (BBA)-Bioenergetics*, 1367(13), 88-106.
- Koshikawa, H., Xu, K. Q., Liu, Z. L., Kohata, K., Kawachi, M., Maki, H., ... & Watanabe, M. (2007). Effect of the water-soluble fraction of diesel oil on bacterial and primary production and the trophic transfer to mesozooplankton through a microbial food web in Yangtze estuary, China. *Estuarine, Coastal and Shelf Science*, 71(1-2), 68-80.

- Kusk, K. O. L. E. (1978). Effects of Crude Oil and Aromatic Hydrocarbons on the Photosynthesis of the Diatom *Nitzschia palea*. *Physiologia Plantarum*, 43, 1–6.
- Lalli, C. M. & Parsons, T. R. (1997). Biological Oceanography: an introduction (2ed). Butterworth-Heinemann, Oxford, 314 pp.
- Larsen, A., Castberg, T., Sandaa, R. A., Brussaard, C. P. D., Egge, J., Heldal, M., ... Bratbak, G. (2001). Population dynamics and diversity of phytoplankton, bacteria and viruses in a seawater enclosure. *Marine Ecology Progress Series*, 221, 47–57.
- Larsen, J. B., Larsen, A., Thyrhaug, R., Bratbak, G., & Sandaa, R. A. (2007). Marine viral populations detected during a nutrient induced phytoplankton bloom at elevated pCO<sub>2</sub> levels. *Biogeosciences Discussion*, 4, 3961–3985.
- Laws, E. A., Falkowski, P. G., Smith, W. O., Ducklow, H., & McCarthy, J. J. (2000). Temperature effects on export production in the open ocean. *Global Biogeochemical Cycles*, 14(4), 1231-1246.
- Leahy, J. G., & Colwell, R. R. (1990). Microbial degradation of hydrocarbons in the environment. *Microbiological reviews*, 54(3), 305-315.
- Lee, R. F., Takahashi, M., Beers, J. R., Thomas, W. H., Seibert, D. L. R., Koeller, P., & Green, D. R., (1977). Controlled ecosystems: their use in the study of the effects of pet-roleum hydrocarbons on plankton. In: *Physiological responses of marine biota to pollutants*. Vernberg, F. J., Calabrese, A., Thurberg, F. P., & Vernberg, W. B. (eds). Academic Press, London, 323-342.
- Lee, K., Boufadel, M., Chen, B., Foght, J., Hodson, P., Swanson, S., & Venosa, A. (2015). The behaviour and environmental impacts of crude oil released into aqueous environments. *The Royal Society of Canada*, Ottawa. 460 pp.
- Le Devoir, 2016. Hydro-Québec sévèrement critiquée pour un déversement de diesel [in line] <https://www.independent.ie/business/irish/caterpillar-fined-for-diesel-spill-into-irishsea-36199096.html> (consulted 20 February 2018)
- Legendre, L., & Rassoulzadegan, F. (1995). Plankton and nutrient dynamics in coastal waters. *Ophelia*, 41, 153–172.
- Levasseur, M., Therriault, J.-C., & Legendre, L. (1984). Hierarchical control of phytoplankton succession by physical factors. *Marine Ecology Progress Series*, 19, 211–222.
- Linden, O., Elmgren, R., & Boehm, P. (1979). The Tsesis oil spill: Its impact on the coastal ecosystem of the Baltic Sea. *Ambio*, 8(6), 244–253.

- Lionard, M., Roy, S., Tremblay-Létourneau, M., & Ferreyra, G. A. (2012). Combined effects of increased UV-B and temperature on the pigment-determined marine phytoplankton community of the St. Lawrence Estuary. *Marine Ecology Progress Series*, 445, 219–234.
- López-Rodas, V., Carrera-Martínez, D., Salgado, E., Mateos-Sanz, A., Báez, J. C., & Costas, E. (2009). A fascinating example of microalgal adaptation to extreme crude oil contamination in a natural spill in Arroyo Minero, Rio Negro, Argentina. In: *Anales de la Real Academia Nacional de Farmacia*, 75(4), 883-899.
- Lund, J. W. G., Kipling, G., & Le Creen, E. D. (1958). The inverted microscope method of estimating algae numbers and the statistical basis of estimation by counting. *Hydrobiologia*, 11, 143–170.
- Martínez-Martínez, J., Norland, S., Thingstad, T. F., Schroeder, D. C., Bratbak, G., Wilson, W. H., & Larsen, A. (2006). Variability in microbial population dynamics between similarly perturbed mesocosms. *Journal of plankton research*, 28(8), 783-791.
- Marwood, C. A., Smith, R. E. H., Solomon, K. R., Charlton, M. N., & Greenberg, B. M. (1999). Intact and Photomodified Polycyclic Aromatic Hydrocarbons Inhibit Photosynthesis in Natural Assemblages of Lake Erie Phytoplankton Exposed to Solar Radiation. *Ecotoxicology and Environmental Safety*, 44, 322–327.
- Menden-Deuer, S., & Lessard, E. J. (2000). Carbon to volume relationships for dinoflagellates, diatoms, and other protist plankton. *Limnology and Oceanography*, 45(3), 569–579.
- Michalick, P. A., & Gordon Jr, D. C. (1971). Concentration and distribution of oil pollutants in Halifax Harbour, 10 June to 20 August, 1971. *Fisheries Research Board of Canada Technical Report*, 284, 26 pp.
- Miller, M. C., Alexander, V., & Barsdate, R. J. (1978). The Effects Of Oil Spills On Phytoplankton The Effects In An Arctic Lake And Ponds. *Arctic*, 31(3), 192–218.
- Millie, D. F., Kirkpatrick, G. J., & Vinyard, B. T. (1995). Relating photosynthetic pigments and in vivo optical density spectra to irradiance for the Florida red-tide dinoflagellate *Gymnodinium breve*. *Marine Ecology Progress Series*, 120, 65-75.
- Mironov, O. G., & Lanskaya, L. A. (1968). The capacity of survival in seawater polluted with oil products inherent in some marine planktonic and benthoplanktonic algae. *Botanicheskii Zhurnal.*, 53, 661-669.
- Nayar, S., Goh, B. P. L., & Chou, L. M. (2005). Environmental impacts of diesel fuel on bacteria and phytoplankton in a tropical estuary assessed using *in situ* mesocosms. *Ecotoxicology*, 14(3), 397–412.

- Neff, J. N. M., Ostazeski, S., Gardiner, W., & Stejskal, I. (2000). Effects of Weathering on the Toxicity of Three Offshore Australian Crude Oils and a Diesel Fuel To Marine Animals. *Environmental Toxicology and Chemistry*, 19(7), 1809–1821.
- Østgaard, K., Hegseth, E. N., & Jensen, A. (1984). Species-dependent sensitivity of marine planktonic algae to Ekofisk crude oil under different light conditions. *Botanica marina*, 27(7), 309-318.
- Olmedo Masat, M (in prep.) *Effets des hydrocarbures sur le broutage par le microzooplancton et sur le taux de croissance du phytoplancton de l'estuaire maritime du Saint-Laurent en conditions expérimentales (Québec-Canada)*. Master's thesis. University of Quebec in Rimouski. Quebec.
- Oviatt, C., Frithsen, J., Gearing, J., & Gearing, P. (1982). Low chronic additions of No.2 fuel oil: chemical behavior, biological impact and recovery in a simulated estuarine environment. *Marine Ecology Progress Series*, 9, 121–136.
- Ozhan, K. , & Bargu, S. (2014). Distinct responses of Gulf of Mexico phytoplankton communities to crude oil and the dispersant Corexit EC9500A under different nutrient regimes. *Ecotoxicology*, 23, 370–384.
- Ozhan, K., Parsons, M. L., & Bargu, S. (2014). How were phytoplankton affected by the deepwater horizon oil spill? *BioScience*, 64(9), 829–836.
- Palmer, C.M. (1969). A composite rating of algae tolerating organic pollution. *Journal of Phycology*. 5, 78–82
- Parab, S. R., Pandit, R. A., Kadam, A. N., & Indap, M. M. (2008). Effect of Bombay high crude oil and its water-soluble fraction on growth and metabolism of diatom *Thalassiosira* sp. *Indian Journal of Marine Sciences*, 37, 251–255.
- Parsons, T. R., Maita, Y. & Lalli, C. M. (1984). A Manual of Chemical and Biological Methods for Seawater Analysis. *Pergamon Press*, New York, 395, 475-490.
- Pérez, P., Fernández, E., & Beiras, R. (2010)a. Fuel toxicity on Isochrysis galbana and a coastal phytoplankton assemblage: Growth rate vs. variable fluorescence. *Ecotoxicology and Environmental Safety*, 73(3), 254–261.
- Pérez, P., Tecnológico, C., Cet, F., & Fernández, E. (2010)b. Use of Fast Repetition Rate Fluorometry on Detection and Assessment of PAH Toxicity on Microalgae. *Water Air Soil Pollution*, 209, 345–356.
- Perhar, G., & Arhonditsis, G. B. (2014). Aquatic ecosystem dynamics following petroleum hydrocarbon perturbations: A review of the current state of knowledge. *Journal of Great Lakes Research*, 40(S3), 56–72.

- Petersen, J. E., Kemp, W. M., Bartleson, R., Boynton, W. R., Chen, C., Cornwell, J. C., ... Suttles, S. E. (2003). Multiscale Experiments in Coastal Ecology : Improving Realism and Advancing Theory. *BioScience*, 53(12), 1181–1197.
- Pomeroy, L. R. (1974). The ocean's food web, a changing paradigm. *BioScience*, 24(9), 499–504.
- Prouse, N. J., Gordon Jr., D. C., & Keizer, P. D. (1976). Effects of Low Concentrations of Oil Accommodated in Sea Water on the Growth of Unialgal Marine Phytoplankton Cultures. *Journal of the Fisheries Research Board of Canada*, 33(4), 810–818.
- Ramachandran, S. D., Hodson, P. V., Khan, C. W., & Lee, K. (2004). Oil dispersant increases PAH uptake by fish exposed to crude oil. *Ecotoxicology and environmental safety*, 59(3), 300-308.
- Ramadass, K., Megharaj, M., Venkateswarlu, K., & Naidu, R. (2017). Toxicity of diesel water accommodated fraction toward microalgae, *Pseudokirchneriella subcapitata* and *Chlorella* sp. MM3. *Ecotoxicology and Environmental Safety*, 142, 538–543.
- Raven, J.A. (1987). The role of vacuoles. *New Phytologist* 106, 357–422.
- Raven, J.A. (1998). The twelfth Tansley Lecture. Small is beautiful: The picophytoplankton. *Functional Ecology*, 12(4), 503–513.
- Raven, J. a, Finkel, Z. V, & Irwin, A. J. (2005). Phytoplankton: bottom-up and top-down controls on ecology and evolution. *Vie et Milieu*, 55, 209–215.
- Reckermann, M., & Veldhuis, M. J. W. (1997). Trophic interactions between picophytoplankton and micro- And nanozooplankton in the western Arabian Sea during the NE monsoon 1993. *Aquatic Microbial Ecology*, 12(3), 263–273.
- Reynolds, C. S. (2006). The ecology of phytoplankton. *Cambridge University Press*. 524 pp.
- Richardson, T. L., Jackson, G. A. (2007). Small phytoplankton and carbon export from the surface ocean. *Science*, 315 (5813), 838–840.
- Roy, S., Chanut, J. P., Gosselin, M., & Sime-Ngando, T. (1996). Characterization of phytoplankton communities in the lower St. LawrenceEstuary using HPLC-detected pigments and cell microscopy. *Marine Ecology Progress Series*, 142(1–3), 55–73.
- Roy, S., Llewellyn, C. A., Egeland, E. S., & Johnsen, G. (Eds.). (2011). Phytoplankton pigments: characterization, chemotaxonomy and applications in oceanography. *Cambridge University Press*.

- Salas, N., Ortiz, L., Gilcoto, M., Varela, M., Bayona, J. M., Groom, S., ... & Albaiges, J. (2006). Fingerprinting petroleum hydrocarbons in plankton and surface sediments during the spring and early summer blooms in the Galician coast (NW Spain) after the Prestige oil spill. *Marine Environmental Research*, 62(5), 388–413.
- Samuelsson, K., & Andersson, A. (2003). Predation limitation in the pelagic microbial food web in an oligotrophic aquatic system. *Aquatic Microbial Ecology*, 30(3), 239–250.
- Sargian, P., Mas, S., Pelletier, É., & Demers, S. (2007). Multiple stressors on an Antarctic microplankton assemblage: Water soluble crude oil and enhanced UVBR level at Ushuaia (Argentina). *Polar Biology*, 30(7), 829–841.
- Sargian, P., Mostajir, B., Chatila, K., Ferreyra, G. A., Pelletier, É., & Demers, S. (2005). Non-synergistic effects of water-soluble crude oil and enhanced ultraviolet-B radiation on a natural plankton assemblage. *Marine Ecology Progress Series*, 294, 63–77.
- Shaw, D. G. (1992). The Exxon Valdez Oil-spill: Ecological and Social Consequences. *Environmental Conservation*, 19(3), 253–258.
- Sikkema, J., de Bont, J. A., & Poolman, B. (1995). Mechanisms of membrane toxicity of hydrocarbons. *Microbiological reviews*, 59(2), 201-222.
- Sinclair, M. (1978). Summer phytoplankton variability in the lower St. Lawrence estuary. *Journal of the Fisheries Board of Canada*, 35(9), 1171-1185.
- Siron, R., Giusti, G., Berland, B., Morales-Loo, R., & Pelletier, É. (1991). Water-soluble petroleum compounds: chemical aspects and effects on the growth of microalgae. *The Science of the Total Environment*, 104, 211–227.
- Siron, R., Pelletier, E., & Roy, S. (1996). Effects of dispersed and adsorbed crude oil on microalgal and bacterial communities of cold seawater. *Ecotoxicology*, 5, 229–251.
- Smayda, T. J. (1980). Phytoplankton species succession. In: *The physiological ecology of phytoplankton*. Morris 1 (eds). University of California Press. Berkeley, 493-570.
- Suggett, D. J., Moore, C. M., Oxborough, K., & Geider, R. J. (2006). Fast Repetition Rate (FRR) Chlorophyll a Fluorescence Induction Measurements. *Chelsea Technologies Group*, 49 pp.
- Suttle, C. A. (2005). Viruses in the sea. *Nature*, 437(7057), 356.
- Takabayashi, M., Lew, K., Johnson, A., Marchi, A. L., Dugdale, R., & Wilkerson, F. P. (2006). The effect of nutrient availability and temperature on chain length of the diatom, *Skeletonema costatum*. *Journal of Plankton Research*, 28(9), 831-840.

- Tangen, K., & Björnland, T. (1981). Observations on pigments and morphology of *Gyrodinium aureolum* Hulbert, a marine dinoflagellate containing 19'hexanoyloxyfucoxanthin as the main carotenoid. *Journal of Plankton Research*, 3, 389-401.
- Tas, S., Okus, E., Unlu, S., & Altiock, H. (2011). A study on phyto- plankton following ‘Volgoneft-248’ oil spill on the north-eastern coast of the Sea of Marmara. *Journal of the Marine Biological Association of the United Kingdom*, 91, 715–725.
- Thomas, W. H., Rossi, S. S., & Seibert, D. L. R. (1981). Effects of some representative petroleum refinery effluent compounds on photosynthesis and growth of natural marine phytoplankton assemblages: Part 1—cresols. *Marine Environmental Research*, 4(3), 203-215.
- Tomas, C. R. (1997). Identifying Marine Phytoplankton. Academic Press, San Diego, CA, 858 pp.
- Tukaj, Z. (1987). The effects of crude and fuel oils on the growth, chlorophyll *a*‘content and dry matter production of a green alga *Scenedesmus quadricauda* (Turp.) bréb. *Environmental Pollution*, 47(1), 9-24.
- Vandermeulen, J. & Singh, J. (1994). ARROW oil spill, 1970-90: Persistence of 20-yr weathered Bunker C fuel oil. *Canadian Journal of Fisheries and Aquatic Sciences*, 51, 845–855.
- Varela, M., Bode, A., Lorenzo, J., Álvarez-Ossorio, M. T., Miranda, A., Patrocinio, T., ...Groom, S. (2006). The effect of the Prestige oil spill on the plankton of the N-NW Spanish coast. *Marine Pollution Bulletin*, 53(5–7), 272–286.
- Vargo, G. A., Hutchins, M., & Almquist, G. (1982). The effect of low, chronic levels of No.2 fuel oil on natural phytoplankton assemblages in microcosms: 1. Species composition and seasonal succession. *Marine Environmental Research*, 6, 245-264.
- Villeneuve, S. (2001). Les répercussions environnementales de la navigation commerciale sur le Saint- Laurent. *Le naturaliste canadien*, 125(2), 49-67.
- Vincent, W. F. (1981). Rapid physiological assays for nutrient demand by the plankton. I. Nitrogen. *Journal of Plankton Research*, 3(4), 685–697.
- Volk, T., & Hoffert, M. I. (1985). Ocean carbon pumps: analysis of relative strengths and efficiencies in ocean-driven atmospheric CO<sub>2</sub> changes. In: *The Carbon Cycle and Atmospheric CO<sub>2</sub>: Natural Variations Archean to Present*. W. S. Sundquist, E. T. and Broecker (eds), American Geophysical Union, Washington, DC, 99–110.

- Wolfe, M. F., Olsen, H. E., Gasuad, K. A., Tjeerdema, R. S., & Sowby, M. (1999). Induction of heat shock protein (hsp) 60 in *Isochrysis galbana* exposed to sublethal preparations of dispersant and Prudhoe Bay crude oil. *Marine Environmental Research*, 47, 473–489.
- Yin, F., Hayworth, J. S., & Clement, T. P. A. (2015). Tale of two recent spills-comparison efficiencies in ocean-driven atmospheric CO<sub>2</sub> changes. In: *The Carbon Cycle and Atmospheric CO<sub>2</sub>: Natural Variations Archean to Present*. W. S. Sundquist, E. T. and Broecker (eds), *American Geophysical Union*, Washington, DC, 99–110.
- Wang, Z., & Fingas, M. (2006). Oil and petroleum product fingerprinting analysis by gas chromatographic techniques. *Chromatographic Science Series*, 93, 1027.
- Wang, L., Zheng, B., & Meng, W. (2008). Photo-induced toxicity of four polycyclic aromatic hydrocarbons, singly and in combination, to the marine diatom *Phaeodactylum tricornutum*. *Ecotoxicology and Environmental Safety*, 71(2), 465–472.
- White, E., Payne, G., Pickmere, S., & Woods, P. (1986). Nutrient demand and availability related to growth among natural assemblages of phytoplankton. *New Zealand Journal of Marine and Freshwater Research*, 20(2), 199–208.
- Yin, F., Hayworth, J. S., & Clement, T. P. A. (2015). Tale of two recent spills-comparison of 2014 Galveston Bay and 2010 Deepwater Horizon oil spill residues. *PLoS ONE*, 10(2).
- Zapata, M., Rodríguez, F., & Garrido, J. L. (2000). Separation of chlorophylls and carotenoids from marine phytoplankton: a new HPLC method using a reversed phase C8 column and pyridine containing mobile phases. *Marine Ecology Progress Series*, 195, 29–45.

## ANNEXES

**Annex 1.** RM ANOVA results obtained for phosphate concentrations. Upper table: Chronic treatment, lower table: Acute treatment.

Effects	df	Sq	F	Pr > F
TIME	15	64	34,393	<b>&lt; 0,0001</b>
TREAT	1	64	47,713	<b>&lt; 0,0001</b>
TIME*TREAT	15	64	3,982	<b>&lt; 0,0001</b>
Effects	df	Sq	F	Pr > F
TIME	15	64	52,733	<b>&lt; 0,0001</b>
TREAT	1	64	17,544	<b>&lt; 0,0001</b>
TIME*TREAT	15	64	4,330	<b>&lt; 0,0001</b>

**Annex 2.** RM ANOVA results obtained for chlorophyll *a* concentration (by the Fluor metric method). Upper table: Chronic treatment, lower table: Acute treatment

Effects	df	Sq	F	Pr > F
TIME	15	64	75,130	<b>&lt; 0,0001</b>
TREAT	1	64	20,491	<b>&lt; 0,0001</b>
TIME*TREAT	15	64	4,389	<b>&lt; 0,0001</b>
Effects	df	Sq	F	Pr > F
TIME	15	64	56,316	<b>&lt; 0,0001</b>
TREAT	1	64	0,556	0,458
TIME*TREAT	15	64	1,167	0,320

**Annex 3.** RM ANOVA results obtained for Total phytoplankton (<20 µm) densities. Upper table: Chronic, lower table: Acute.

Effects	df	Sq	F	Pr > F
TIME	13	56	22,123	<b>&lt; 0,0001</b>
TREAT	1	56	47,997	<b>&lt; 0,0001</b>
TIME*TREAT	13	56	3,129	<b>0,001</b>
<hr/>				
Effects	df	Sq	F	Pr > F
TIME	14	60	26,270	<b>&lt; 0,0001</b>
TREAT	1	60	2,584	0,113
TIME*TREAT	14	60	1,738	0,071

**Annex 4.** RM ANOVA results obtained for Nano-eukaryotes densities. Upper table: Chronic, lower table: Acute.

Effects	df	Sq	F	Pr > F
TIME	15	64	71,757	<b>&lt; 0,0001</b>
TREAT	1	64	85,698	<b>&lt; 0,0001</b>
TIME*TREAT	15	64	11,556	<b>&lt; 0,0001</b>
<hr/>				
Effects	df	Sq	F	Pr > F
TIME	15	64	21,506	<b>&lt; 0,0001</b>
TREAT	1	64	0,051	0,822
TIME*TREAT	15	64	1,325	0,214

**Annex 5.** RM ANOVA results obtained for Pico-eukaryotes densities. Upper table: Chronic, lower table: Acute.

Effects	df	Sq	F	Pr > F
TIME	15	64	88,267	<b>&lt; 0,0001</b>
TREAT	1	64	43,395	<b>&lt; 0,0001</b>
TIME*TREAT	15	64	4,320	<b>&lt; 0,0001</b>
Effects	df	Sq	F	Pr > F
TIME	15	64	93,224	<b>&lt; 0,0001</b>
TREAT	1	64	19,888	<b>&lt; 0,0001</b>
TIME*TREAT	15	64	4,476	<b>&lt; 0,0001</b>

**Annex 6.** RM ANOVA results obtained for Nano-PC-cyanobacteria densities. Upper table: Chronic, lower table: Acute.

Effects	df	Sq	F	Pr > F
TIME	15	64	18,835	<b>&lt; 0,0001</b>
TREAT	1	64	19,865	<b>&lt; 0,0001</b>
TIME*TREAT	15	64	2,374	<b>0,009</b>
Effects	df	Sq	F	Pr > F
TIME	15	64	12,160	<b>&lt; 0,0001</b>
TREAT	1	64	5,889	<b>0,018</b>
TIME*TREAT	15	64	1,912	<b>0,038</b>

**Annex 7.** RM ANOVA results obtained for Pico-PE-cyanobacteria densities. Upper table: Chronic, lower table: Acute.

Effects	df	Sq	F	Pr > F
TIME	15	64	40,439	<b>&lt;0,0001</b>
TREAT	1	64	16,202	<b>0,000</b>
TIME*TREAT	15	64	3,665	<b>0,000</b>
Effects	df	Sq	F	Pr > F
TIME	15	64	39,253	<b>&lt;0,0001</b>
TREAT	1	64	2,918	0,092
TIME*TREAT	15	64	1,114	0,363

**Annex 8.** RM ANOVA results obtained for Total Phytoplankton <20 µm carbon biomasses estimations. Upper table: Chronic, lower table: Acute.

Effects	df	Sq	F	Pr > F
TIME	14	60	19,736	<b>&lt;0,0001</b>
TREAT	1	60	20,755	<b>&lt;0,0001</b>
TIME*TREAT	14	60	3,757	<b>0,000</b>
Effects	df	Sq	F	Pr > F
TIME	15	64	24,972	<b>&lt;0,0001</b>
TREAT	1	64	0,070	0,792
TIME*TREAT	15	64	1,394	0,178

**Annex 9.** RM ANOVA results obtained for Nano-eukaryotes carbon biomasses estimations. Upper table: Chronic, lower table: Acute.

Effects	df	Sq	F	Pr > F
TIME	15	64	24,179	< 0,0001
TREAT	1	64	25,601	< 0,0001
TIME*TREAT	15	64	4,149	< 0,0001
Effects	df	Sq	F	Pr > F
TIME	15	64	26,229	< 0,0001
TREAT	1	64	0,005	0,941
TIME*TREAT	15	64	1,666	0,081

**Annex 10.** RM ANOVA results obtained for Pico-eukaryotes carbon biomasses estimations. Upper table: Chronic, lower table: Acute.

Effects	df	Sq	F	Pr > F
TIME	15	64	87,466	< 0,0001
TREAT	1	64	43,430	< 0,0001
TIME*TREAT	15	64	4,267	< 0,0001
Effects	df	Sq	F	Pr > F
TIME	15	64	92,419	< 0,0001
TREAT	1	64	19,981	< 0,0001
TIME*TREAT	15	64	4,433	< 0,0001

**Annex 11.** ANOVA results obtained for net carbon accumulation between the 10<sup>th</sup> and the 15<sup>th</sup> experiment days. Upper table: nano-eukaryotes, lower table: pico-eukaryotes.

Source	df	Sq	Squares Average		
			F	Pr > F	
Modèle	2	789405,089	394702,545	9,980	<b>0,012</b>
Erreur	6	237290,093	39548,349		
Total corrigé	8	1026695,183			

*Calculé contre le modèle Y=Moyenne(Y)*

Source	df	Sq	Squares Average		
			F	Pr > F	
Modèle	2	215,056	107,528	22,637	<b>0,002</b>
Erreur	6	28,500	4,750		
Total corrigé	8	243,556			

*Calculé contre le modèle Y=Moyenne(Y)*

**Annex 12.** Test ad-hoc (Tukey HSD) for net carbon accumulation between the 10<sup>th</sup> and the 15<sup>th</sup> experiment days. Upper table: nano-eukaryotes, lower table: pico-eukaryotes.

Contraste	Difference	Standardized difference	Critical value	Pr > Diff
CHR vs C	-704,872	-4,341	3,068	<b>0,012</b>
CHR vs AC	-500,994	-3,085	3,068	<b>0,049</b>
AC vs C	-203,878	-1,256	3,068	0,467

Contraste	Difference	Standardized difference	Critical value	Pr > Diff
CHR vs C	-10,833	-6,088	3,068	<b>0,002</b>
CHR vs AC	-1,000	-0,562	3,068	0,844
AC vs C	-9,833	-5,526	3,068	<b>0,004</b>

**Annex 13.** RM ANOVA results obtained for microphytoplankton density. Upper table: Chronic, lower table: Acute.

Effects	df	Sq	F	Pr > F
TIME	3	16	6,383	<b>0,005</b>
TREAT	1	16	27,912	< <b>0,0001</b>
TIME*TREAT	3	16	39,200	< <b>0,0001</b>
Effects	df	Sq	F	Pr > F
TIME	3	16	4,521	<b>0,018</b>
TREAT	1	16	72,801	< <b>0,0001</b>
TIME*TREAT	3	16	10,844	<b>0,000</b>

**Annex 14.** RM ANOVA results obtained for microphytoplankton carbon biomasses estimations. Upper table: Chronic, lower table: Acute.

Effects	df	Sq	F	Pr > F
TIME	3	16	3,046	0,059
TREAT	1	16	12,269	<b>0,003</b>
TIME*TREAT	3	16	26,495	< <b>0,0001</b>

Effects	df	Sq	F	Pr > F
TIME	3	16	3,351	<b>0,045</b>
TREAT	1	16	60,907	< <b>0,0001</b>
TIME*TREAT	3	16	10,472	<b>0,000</b>

**Annex 15.** ANOVA results obtained for net carbon accumulation in microphytoplankton from the 6<sup>th</sup> experiment day.

Source	df	Sq	Squares Average	F	Pr > F
Modèle	2	4286400,827	2143200,413	21,760	<b>0,002</b>
Erreur	6	590946,271	98491,045		
Total corrigé	8	4877347,098			

**Annex 16.** Test ad-hoc (Tukey HSD) for net carbon accumulation in microphytoplankton from the 6<sup>th</sup> experiment day.

Contrast	Difference	Standardized difference	Critical value	Pr > Diff
AC vs C	-1656,012	-6,463	3,068	<b>0,002</b>
AC vs CHR	-534,034	-2,084	3,068	0,173
CHR vs C	-1121,977	-4,379	3,068	<b>0,011</b>

**Annex 17.** RM ANOVA results obtained for fucoxanthin concentrations. Upper table: Chronic, lower table: Acute.

Effects	df	Sq	F	Pr > F
TIME	4	20	42,736	<b>&lt; 0,0001</b>
TREAT	1	20	29,293	<b>&lt; 0,0001</b>
TIME*TREAT	4	20	6,695	<b>0,001</b>

Effects	df	Sq	F	Pr > F
TIME	4	20	86,899	<b>&lt; 0,0001</b>
TREAT	1	20	6,221	<b>0,022</b>
TIME*TREAT	4	20	6,194	<b>0,002</b>

**Annex 18.** RM ANOVA results obtained for Chlorophyll *b* concentrations. Upper table: Chronic, lower table: Acute.

Effects	df	Sq	F	Pr > F
TIME	4	20	21,056	<b>&lt; 0,0001</b>
TREAT	1	20	8,916	<b>0,007</b>
TIME*TREAT	4	20	1,435	0,259

Effects	df	Sq	F	Pr > F
TIME	4	20	34,435	<b>&lt; 0,0001</b>
TREAT	1	20	5,477	<b>0,030</b>
TIME*TREAT	4	20	1,105	0,381

**Annex 19.** RM ANOVA results obtained for Chlorophyll *c1* concentrations. Upper table: Chronic, lower table: Acute.

Effects	df	Sq	F	Pr > F
TIME	4	20	59,842	<b>&lt; 0,0001</b>
TREAT	1	20	63,728	<b>&lt; 0,0001</b>
TIME*TREAT	4	20	15,548	<b>&lt; 0,0001</b>
Effects	df	Sq	F	Pr > F
TIME	4	20	170,387	<b>&lt; 0,0001</b>
TREAT	1	20	28,023	<b>&lt; 0,0001</b>
TIME*TREAT	4	20	19,867	<b>&lt; 0,0001</b>

**Annex 20.** RM ANOVA results obtained for Chlorophyll *c2* concentrations. Upper table: Chronic, lower table: Acute.

Effects	df	Sq	F	Pr > F
TIME	4	20	62,328	<b>&lt; 0,0001</b>
TREAT	1	20	30,017	<b>&lt; 0,0001</b>
TIME*TREAT	4	20	6,542	<b>0,002</b>
Effects	df	Sq	F	Pr > F
TIME	4	20	165,440	<b>&lt; 0,0001</b>
TREAT	1	20	10,231	<b>0,005</b>
TIME*TREAT	4	20	7,523	<b>0,001</b>

**Annex 21.** RM ANOVA results obtained for neoxanthin concentrations. Upper table: Chronic, lower table: Acute.

Effects	df	Sq	F	Pr > F
TIME	4	20	115,423	<b>&lt; 0,0001</b>
TREAT	1	20	23,276	<b>0,000</b>
TIME*TREAT	4	20	10,523	<b>&lt; 0,0001</b>
Effects	df	Sq	F	Pr > F
TIME	4	20	115,477	<b>&lt; 0,0001</b>
TREAT	1	20	16,340	<b>0,001</b>
TIME*TREAT	4	20	7,743	<b>0,001</b>

**Annex 22.** RM ANOVA results obtained for Violaxanthin concentrations. Upper table: Chronic, lower table: Acute.

Effects	df	Sq	F	Pr > F
TIME	4	20	46,595	<b>&lt; 0,0001</b>
TREAT	1	20	2,878	0,105
TIME*TREAT	4	20	6,914	<b>0,001</b>
Effects	df	Sq	F	Pr > F
TIME	4	20	32,547	<b>&lt; 0,0001</b>
TREAT	1	20	0,555	0,465
TIME*TREAT	4	20	2,855	0,051

**Annex 23.** RM ANOVA results obtained for MGDVP concentrations. Upper table: Chronic, lower table: Acute.

Effects	df	Sq	F	Pr > F
TIME	4	20	18,571	<b>&lt; 0,0001</b>
TREAT	1	20	4,945	<b>0,038</b>
TIME*TREAT	4	20	0,464	0,761
Effects	df	Sq	F	Pr > F
TIME	4	20	19,250	<b>&lt; 0,0001</b>
TREAT	1	20	1,402	0,250
TIME*TREAT	4	20	0,330	0,855

**Annex 24.** RM ANOVA results obtained for Alloxanthin concentrations. Upper table: Chronic, lower table: Acute.

Effects	df	Sq	F	Pr > F
TIME	4	20	57,473	<b>&lt; 0,0001</b>
TREAT	1	20	2,098	0,163
TIME*TREAT	4	20	0,787	0,547
Effects	df	Sq	F	Pr > F
TIME	4	20	38,783	<b>&lt; 0,0001</b>
TREAT	1	20	2,970	0,100
TIME*TREAT	4	20	0,271	0,893

**Annex 25.** RM ANOVA results obtained for Prasinoxanthin concentrations. Upper table: Chronic, lower table: Acute.

Effects	df	Sq	F	Pr > F
TIME	4	20	16,491	<b>&lt; 0,0001</b>
TREAT	1	20	43,926	<b>&lt; 0,0001</b>
TIME*TREAT	4	20	19,187	<b>&lt; 0,0001</b>
Effects	df	Sq	F	Pr > F
TIME	4	20	36,249	<b>&lt; 0,0001</b>
TREAT	1	20	32,627	<b>&lt; 0,0001</b>
TIME*TREAT	4	20	13,787	<b>&lt; 0,0001</b>

**Annex 26.** RM ANOVA results obtained for zeaxanthin concentrations. Upper table: Chronic, lower table: Acute.

Effects	df	Sq	F	Pr > F
TIME	4	20	23,766	<b>&lt; 0,0001</b>
TREAT	1	20	17,223	<b>0,000</b>
TIME*TREAT	4	20	6,106	<b>0,002</b>
Effects	df	Sq	F	Pr > F
TIME	4	20	61,607	<b>&lt; 0,0001</b>
TREAT	1	20	47,020	<b>&lt; 0,0001</b>
TIME*TREAT	4	20	19,851	<b>&lt; 0,0001</b>

**Annex 27.** RM ANOVA results obtained for the  $Fv/Fm$  parameter measured by FRRF. Upper table: Chronic, lower table: Acute.

Effects	df	Sq	F	Pr > F
TIME	15	64	7,438	<b>&lt; 0,0001</b>
TREAT	1	64	0,435	0,512
TIME*TREAT	15	64	3,237	<b>0,001</b>
<hr/>				
Effects	df	Sq	F	Pr > F
TIME	15	64	13,026	<b>&lt; 0,0001</b>
TREAT	1	64	2,354	0,130
TIME*TREAT	15	64	4,913	<b>&lt; 0,0001</b>

---